Jagiellonian University
Marian Smoluchowski Institute of Physics
Condensed Matter Theory Department

Properties of molecules and nanoscopic systems from a combined exact diagonalization - *ab initio* approach

Edward M. Görlich

Ph. D. Thesis under the supervision of

Prof. dr hab. Józef Spałek

Kraków, July 2004

Uniwersytet Jagielloński
Instytut Fizyki im. Mariana Smoluchowskiego
Zakład Teorii Materii Skondensowanej

Własności molekuł oraz wybranych układów nanoskopowych w metodzie ścisłej diagonalizacji połączonej z podejściem *ab initio*

Edward M. Görlich

Rozprawa doktorska

Promotor:
Prof. dr hab. Józef Spałek

Kraków, lipiec 2004

Abstract

In this Thesis we implement the recently introduced novel method of determining the correlated electronic states. The method combines the exact diagonalization of the Hamiltonian in the Fock space with the optimization of the single particle basis in the Hilbert space. It is called EDABI (**E**xact **D**iagonalization - **AB I***nitio* approach). In this method all the configurations of N interacting electrons in the Fock space are accounted for *rigorously* within an assumed *subspace* of Hilbert space of single-particle states for given system. The single-particle orbitals forming the subspace (and defining the field operators) are adjusted in the ground state of those correlated systems. We exploit and discuss major features of the method and relate it to the existing methods such as the multiconfigurational interaction (MCI-SCF) method used in quantum chemistry. We apply first the EDABI method to small systems such as the light atoms and ions, to test the subsequent starting basis choice. Next, we implement the method for the description of simple molecules and molecular ions. The calculations are performed using the hydrogenic-like wave-function basis and include virtually *all* non-relativistic electron-electron interactions. The effect of crystalline field and of the spin-orbit interaction are also introduced to the Hamiltonian of interacting 3d electrons in small clusters. The values of the crystal-field splitting are calculated with the adjusted 3d wave functions.

Streszczenie

W niniejszej rozprawie doktorskiej ukazujemy niedawno wprowadzoną metodę wyznaczania stanów skorelowanych elektronów. Metoda ta łączy ścisłą diagonalizację Hamiltonianu w przestrzenii Focka z optymalizacją bazy jednocząstkowej w przestrzenii Hilberta. Proponujemy dla tej metody nazwę EDABI (**E**xact **D**iagonalization - **AB I***nitio* approach). W metodzie tej wszystkie konfiguracje N oddziaływujących cząstek są uwzględniane w sposób ścisły wewnątrz założonej podprzestrzenii przestrzenii Hilberta stanów jednocząstkowych dla danego układu. Orbitale jednocząstkowe wyznaczające tą podprzestrzeń (i zarazem definiujące operatory pola) są dostosowywane w stanie podstawowym oddziaływującego układu. Ukazujemy i rozważamy najwazniejsze cechy tej metody i odnosimy ją do istniejących metod takich, jak metoda wielokonfiguracyjnego oddziaływania (MCI-SCF) wykorzystywana w chemi kwantowej. Stosujemy metodę EDABI do małych układów takich, jak lekkie atomy i jony, w celu ukazania sposobu doboru bazy jednocząstkowej. Następnie, używamy metodę do opisu prostych molekuł i jonów molekularnych. Obliczenia są przeprowadzane z wykorzystaniem bazy wodoropodobnych funkcji falowych i zawierają *wszystkie* nierelatywistyczne oddziaływania elektronowe. Wpływ pola krystalicznego i oddziaływania spin-orbita jest wprowadzany do Hamiltonianu oddziaływujących elektronów 3d w małych klastrach. Wartości rozszczepienia spin-orbita są wyliczane dla zoptymalizowanych funkji falowych 3d.

Podziękowanie (Acknowledgements)

Niniejszym pragnę wyrazić głęboką wdzięczność promotorowi tej pracy prof. dr hab. Józefowi Spałkowi za wymyślenie metody postępowania (EDABI) oraz wiele dyskusji. Dobrze wskazane cele, silna zachęta i czujny nadzór umożliwiły skończenie tej rozprawy.
Niniejsza praca była wspierana przez Komitet Badań Naukowych (KBN) w grantach 2 P03B 050 23 oraz 1 P03B 015 26 (promotorski). Pragnę również podziękować Fundacji na Rzecz Nauki Polskiej (FNP) za specjalne stypendium ufundowane w ramach subsydium profesorskiego przyznanego na lata 2003-6 prof. J. Spałkowi.

Contents

Chapter 1

Introduction

One of the most important aims of quantum physics is to determine electronic states in different microscopic systems and devices. Those properties are needed to describe the nature of the ground state and the excited states, as well as the electronic transport properties. In the context of atomic physics, the Hartree-Fock approximation is regarded as a starting point, as it provides the standard *hydrogenic-like* hierarchy of the single-particle energy levels and terms [1]. In the solid-state physics, on the other hand, the methods based on the ideas of periodic potential and of the Bloch function form a basis, into which the correlation and the exchange effective potentials are built into to obtain a quantitative description of the *band structure* and other properties [2]. These two approaches are successful for many systems, some of them even quantitatively [3]. It is absolutely astonishing, that an effectively single-particle approach, which neglects the many-body corrections, can be so effective for many molecular or solid-state systems. It works particularly well for three dimensional systems far away from the *Mott-Hubbard localization*, i.e. for systems of high density, where the local correlation effects are screened out.

The situation changes when we try to describe low-dimensional and/or *strongly correlated systems*. In those situations not only the local correlations can play a dominant role, but also the nature of the resultant quantum liquid may deviate from the Landau Fermi-liquid behavior. In such situation other methods of approach should be applied, which allow explicitly for a mixing of different (and renormalized) single-particle configurations. The EDABI[1] method is one of them and as such should be tested on the simplest quantum systems. The main purpose of the present Thesis is to provide such tests.

To state it briefly, the difference between the EDABI approach and the

[1] the acronym stands for **E**xact **D**iagonalization combined with an **Ab I**nitio approach.

currently used LDA+U [4] or LDA+DMFT [5] methods is associated with the circumstance that the former method treats exactly the electronic correlations, albeit so far in model situations. In effect, one can trace the evolution of the system in a systematic manner as a function of the interatomic distances.

1.1 The EDABI method as applied to the nanoscopic systems

The nanoscopic systems are the systems close to the atomic systems, but with specific many-body properties. This nontrivial feature of those systems has already been shown explicitly on the example of nanoscopic chains and ladders [6]. Here our aim is different. Namely, we start from few-electron atoms and build up more complicated structures of atomic (nanometer) size. This provides us with a method of addressing in an exact manner the properties of those systems by enriching theoretical models with the number of states defining the field operator and thus the second quantized Hamiltonian. The EDABI approach helped us to realize that the theoretical models of correlated electrons are defined by selecting the *subspace of relevant dynamic processes*. This is the only approximation made for the systems considered. This feature of our approach calls for reexamination of some of the many-body text-book examples of correlated systems. This is one of the principal aims of this Thesis. In the separate work [7] we study extended clusters and rings. The two works [7, 6] and the present one form a coherent picture of the EDABI method at the model- and formalism- building stage. The future research should concentrate on its application to concrete systems (cf. also Chapter 6 of the present Thesis).

1.2 Aim and scope of the Thesis

As we already said above, the purpose of this Thesis is to discuss a formal basis of the EDABI method, as well as to test it on the simplest atomic, molecular, and nanocluster systems. The method used is a combination of a *direct* exact diagonalization of a microscopic Hamiltonian in the Fock space combined with a *variational* optimization of the orthogonalized single-particle wave functions contained in the microscopic parameters of second quantized models of these systems. We discuss, in particular the obvious circumstance that *all* the parameterized many-body models of correlated electrons amount to selecting a truncated Hilbert subspace of the states regarded a priori as

the only relevant to the dynamics of the system at hand. Here we optimize the error in selecting such a subspace by minimizing the ground state energy with respect to subspace basis of wave functions. The physical examples considered in the Thesis allow starting from the hydrogenic-like atomic wave functions of variable size, which in turn adjust themselves in the resultant correlated state of the entire system. The self-adjusted (renormalized) wave equation for those wave functions is proposed, but its solution presents to us a formidable task to be solved directly. We also discuss the difference between our method of approach and other methods: the Hartree-Fock (HF) and the multiconfigurational-interaction method (MCI) used frequently in quantum chemistry.

Turning to the main results of the Thesis, in Chapter 3 we consider simple atoms and ions (H^-, He, He^-, Li, Be^+) composed of s and p starting orbitals only. Were we show the convergence of the methods with enlarging the single-particle basis in the Hilbert space. These calculations could be extended by incorporating the $n = 3$ staring atomic wave function. This has not been done, as some excellent variational calculations of the ground-state energy have been performed containing up to 2000 Gaussian functions with as many variational parameters! Our method provides relatively fast convergence of the results.

In Chapter 4 we consider the simplest many-site cases: H_2 and H_2^- systems. We introduce there the *many-body covalency* and the *mobile orbitals*, i.e. the starting atomic orbitals centered at points shifted by a distance from their parent nuclei positions. The most of the results in the Fock space are analytic and therefore, the results there provide a lucid illustration of the method. The calculations there can be extended in a straightforward manner by enlarging the atomic basis set (though they may become quite cumbersome).

In Chapter 5 we consider a practical example involving 3d wave functions namely, evaluate the crystal-field levels for $3d^1$ and $3d^2$ systems in an octahedral environment. We calculate the electronic states and observe a quantum transformation of the ground state as a function of interionic distance.

Throughout the Thesis we demonstrate complementarity of the 2^{nd} quantization (particle) language with the 1^st quantization (wave mechanics of single particle states, adjusted in the correlated many-particle state). The proposed *self-adjusted wave equation* for such a state has a fundamental character.

The Appendices A-I provide mathematical details needed when solving problems with the help of EDABI method.

Chapter 2

The EDABI method

In this chapter we present the formal features of the method we employ in the following chapters. First, we discuss the principal properties of second-quantization representation of many-particle states.

2.1 The formalism in the second-quantization form and the self-adjusted wave equation

In the general case, a non-relativistic system of N interacting particles can be described by the following Hamiltonian

$$H = \sum_i H_1(\mathbf{r}_i) + \frac{1}{2}\sum_{i,j} H_2(\mathbf{r}_i, \mathbf{r}_j). \tag{2.1}$$

It contains single-particle terms such as the kinetic and potential energies, as well as the two body interparticle interactions. The latter are considered to be symmetric, so the fraction one half in front of the second term cancels out the double counting of pairs (i, j) in the sum. In the simplest version one neglects the relativistic corrections such as the spin-orbit interaction. The interactions involving more than two particles are not included in it. Eq. (2.1) provides the standard expression for the Hamiltonian in the Schrödinger (position) representation. The summations over the indices i, j cover a range equinumerous to the number N of electrons in the system. As a stationary solution of the above Hamiltonian we obtain the N-particle wave function $\Psi(\mathbf{r}_1, \ldots, \mathbf{r}_N)$.

The EDABI method we apply is based on the second-quantization formalism [8, 9]. We will discuss here indistinguishable fermions, which obey then the Pauli exclusion principle. Thus, their wave function has to be anti-

symmetric with respect to the particle-coordinate transpositions [1]. In effect, it can be decomposed in a basis of Slater determinants

$$\Psi(\mathbf{r}_1,\ldots,\mathbf{r}_N) = \sum_{\mathbf{k}_1,\ldots,\mathbf{k}_N} A_{\mathbf{k}_1,\ldots,\mathbf{k}_N} \Phi_{\mathbf{k}_1,\ldots,\mathbf{k}_N}(\mathbf{r}_1,\ldots,\mathbf{r}_N). \tag{2.2}$$

The determinants $\Phi_{\mathbf{k}_1,\ldots,\mathbf{k}_N}(\mathbf{r}_1,\ldots,\mathbf{r}_N)$ will consist of products of the single-particle wave functions $\{w_{\mathbf{k}_i}(\mathbf{r})\}_{i=1\ldots N}$. Each of the indices $\mathbf{k}_i$ describes a complete set of quantum numbers. This expansion is generally exact, since any function $\Psi(\mathbf{r}_1,\ldots,\mathbf{r}_N) \in L^2$, i.e. square integrable, can be expanded in an N-dimensional Fourier series, with a basis in the form of a product of single variable functions. The decomposition (2.2) is the basic assumption valid for any N-particle wave function, together with its normalizability. It is required that the basis functions we expand the wave function into, fulfil several conditions. First, they have to form a complete basis set in a quantum-mechanical sense. It is also convenient to have them orthogonalized and normalized. The selection of the basis functions is going to be discussed in detail later on in Section 3.1. The Slater determinants merely keep track of the antisymmetry. On the other hand, the vectors $\mathbf{r}_i$ may be, and in fact usually are multidimensional. In most cases, they parameterize a point in a 3-dimensional space.

Now, we substitute the description of the system by the set of numbers $\{n_i\}$ of particles in a given state $\mathbf{k}_i$ instead of the set of quantum numbers $\{\mathbf{k}_i\} \equiv \{i\}$. The number of possible states $\mathbf{k}_i$ does not have to be finite. Naturally, the number of particles is fixed, i.e. $\sum_i n_i = N$. The new representation, characterized by the set $\{n_i\}$, is called the *occupation number representation.* It has the advantage of being a countable set. This is true for a countable set $\{\mathbf{k}_i\}$ and, as long the quantum numbers $\mathbf{k}_i$ are quantized, it is fulfilled. One has to introduce some operators enabling operations on the vectors in the new representation. They are the *creation* $a_i^\dagger$ and the *annihilation* a_i operators, which respectively add or remove a particle in the i-th single-particle state described by the corresponding wave function $w_{\mathbf{k}_i}(\mathbf{r})$. Usually, we describe electrons in this manner, so in what follows, the name electron and particle will be used interchangeably. The creation and annihilation operators do not necessary create real particles. An electron creation or destruction at the real-space point $\mathbf{r}$ is described by the respective two-component field

[1] The spin variables can be treated as either coordinates or quantum numbers. Actually, the meaning of a coordinate and a quantum number is here the same and the main purpose is to fix the focus on certain aspects of the system described.

operators

$$\hat{\Psi}^{\dagger}(\mathbf{r}) = \sum_i w_i^{\star}(\mathbf{r}) \begin{pmatrix} a_{i\uparrow}^{\dagger} \\ a_{i\downarrow}^{\dagger} \end{pmatrix} \equiv \sum_i w_i^{\star}(\mathbf{r}) a_i^{\dagger},$$

$$\hat{\Psi}(\mathbf{r}) = \sum_i w_i(\mathbf{r}) \begin{pmatrix} a_{i\uparrow} \\ a_{i\downarrow} \end{pmatrix} \equiv \sum_i w_i(\mathbf{r}) a_i. \tag{2.3}$$

One may ask how does the Hamiltonian (2.1) look like in the new representation? Using the operators (2.3) it is of the form [8, 9]

$$\hat{H} = \int d^3\mathbf{r} \hat{\Psi}^{\dagger}(\mathbf{r}) H_1(\mathbf{r}) \hat{\Psi}(\mathbf{r}) +$$

$$\frac{1}{2} \int d^3r d^3r' \hat{\Psi}^{\dagger}(\mathbf{r}) \hat{\Psi}^{\dagger}(\mathbf{r}') H_2(\mathbf{r}, \mathbf{r}') \hat{\Psi}(\mathbf{r}') \hat{\Psi}(\mathbf{r}). \tag{2.4}$$

This form is *equivalent* to the form (2.1) if the number of particles is conserved. This representation has the advantage over (2.1) in the sense that it contains only either one or two spatial coordinates, $\mathbf{r}$ and $\mathbf{r}'$. If the two body interactions are independent of the two particles absolute positions separately, we can write that $H_2(\mathbf{r}, \mathbf{r}') = H_2(|\mathbf{r} - \mathbf{r}'|)$. It is usually the case, as it can be seen on the example of the Coulomb interaction. One can clearly identify the direct correspondence of one- and two- electron operators in Hamiltonians (2.1) and (2.4). A one-electron operator for the whole system has in the first-quantization (position representation) the form

$$O_1 = \sum_i o_1(\mathbf{r}_i), \tag{2.5}$$

where $o_1(\mathbf{r}_i)$ is its correspondant for a single particle. The corresponding two-electron operator characterizing the whole system is defined as

$$O_2 = \sum_{ij} o_2(\mathbf{r}_i, \mathbf{r}_j). \tag{2.6}$$

The changeover to the second-quantization representation of these operators can be written in the form of the following transformation

$$O_1 \rightarrow \hat{O}_1 = \int d^3\mathbf{r} \hat{\Psi}^{\dagger}(\mathbf{r}) o_1(\mathbf{r}) \hat{\Psi}(\mathbf{r}) \tag{2.7}$$

and, respectively, for the two-particle operators

$$O_2 \rightarrow \hat{O}_2 = \int \int d^3\mathbf{r} d^3\mathbf{r}' \hat{\Psi}^{\dagger}(\mathbf{r}) \hat{\Psi}^{\dagger}(\mathbf{r}') o_2(\mathbf{r}, \mathbf{r}') \hat{\Psi}(\mathbf{r}') \hat{\Psi}(\mathbf{r}). \tag{2.8}$$

The above prescriptions hold not only for the Hamiltonian terms, in our case $o_1 = H_1$ and $o_2 = H_2$, but for any operators satisfying the definitions (2.5) and (2.6). Actually, one can extend it for an any-particle-number operator. As the actual calculations are carried out using a well-defined wave-function basis and the corresponding to it set of creation and annihilation operators, it is handy to reevaluate the above expressions in these categories, i.e. rewrite (2.5) in the form

$$\hat{O}_1 = \sum_{ij} \underbrace{\int w^{\star}_{\mathbf{k}_i}(\mathbf{r}) o_1(\mathbf{r}) w_{\mathbf{k}_j}(\mathbf{r}) d^3\mathbf{r}}_{<i|o_1|j>} a^{\dagger}_{\mathbf{k}_i} a_{\mathbf{k}_j}, \tag{2.9}$$

and, respectively, for the two-particle operators the Eq. (2.6) in the form

$$\hat{O}_2 = \sum_{ijkl} \underbrace{\int\int w^{\star}_{\mathbf{k}_i}(\mathbf{r}) w^{\star}_{\mathbf{k}_j}(\mathbf{r}') o_2(\mathbf{r},\mathbf{r}') w_{\mathbf{k}_k}(\mathbf{r}) w_{\mathbf{k}_l}(\mathbf{r}') d^3\mathbf{r} d^3\mathbf{r}'}_{<ij|o_2|kl>} a^{\dagger}_{\mathbf{k}_i} a^{\dagger}_{\mathbf{k}_j} a_{\mathbf{k}_l} a_{\mathbf{k}_k}. \tag{2.10}$$

One should note an essential fact. Namely, the operators o_1 and o_2 act on a single or two electrons located at points $\mathbf{r}$ and $\mathbf{r}'$. The second quantized operators $\hat{O}_1$ and $\hat{O}_2$ do act on *every* single electron or pair of electrons in the system. In other words, the operators in the first-quantization representation act locally, whereas their second-quantized counterparts act globally. It is caused by the summation in the definitions (2.5) and (2.6) and this is the way one should understand single- or two- particle operators acting on N particle system. In the present situation, the set of quantum numbers $\mathbf{k}$ consists barely of the wave function index, defining the shape of the wave function, and the spin quantum number which may take the values $\uparrow$ or $\downarrow$. Applying the formulas (2.9) and (2.10)) to the Hamiltonian (2.1) we obtain

$$H = \sum_{ij\sigma} t_{ij} a^{\dagger}_{i\sigma} a_{j\sigma} + \frac{1}{2} \sum_{ijkl\sigma_1\sigma_2} V_{ijkl} a^{\dagger}_{i\sigma_1} a^{\dagger}_{j\sigma_2} a_{l\sigma_2} a_{k\sigma_1}, \tag{2.11}$$

with the *microscopic parameters* defined by

$$t_{ij} \equiv < w_i|H_1|w_j > = \int d^3\mathbf{r} w^{\star}_i(\mathbf{r}) H_1(\mathbf{r}) w_j(\mathbf{r}), \tag{2.12}$$

and

$$V_{ijkl} \equiv < w_i w_j|H_2|w_k w_l > = \int d^3\mathbf{r} d^3\mathbf{r}' w^{\star}_i(\mathbf{r}) w^{\star}_j(\mathbf{r}') H_2(|\mathbf{r}-\mathbf{r}'|) w_k(\mathbf{r}) w_l(\mathbf{r}'). \tag{2.13}$$

The parameters relate the Hamiltonian to the properties of the real-world system. We assume the spin invariance of the Hamiltonian, i.e. assume for both H_1 and H_2 that $[H, \hat{S}_z] = [H, \hat{S}^2] = 0$, where $\hat{S}^2$ and $\hat{S}_z$ are the total-spin $\hat{\mathbf{S}}$ characteristics. It is true for the Coulomb interaction. But in the general case, e.g. if we start to consider relativistic effects like the spin-orbit coupling, this is not obeyed. Anyhow, the spin conservation does not matter for the method implementation, but merely simplifies the argument, as it reduces the number of spin variable summations. We may keep the whole set of quantum numbers $\{\mathbf{k}_i\}$ without separating it into the spin and the orbital parts. The distinction will be made later, namely in Section 5.2.

We have thus related the Hamiltonian in the multiparticle Hilbert space to that in the Fock space. By solving it, one obtains the states in the occupation-number representation of the Fock space. To complete the solution it is necessary to trace back the Fock state to the original Schrödinger (position) representation. This problem also relates the many-body problem to the single-particle wave-function determination. In the wave mechanics of interacting particles, only the N-particle wave function holds the information about the state of the system. In the Fock space we determine the state by evaluating the microconfigurations consisting of occupations of each of the single particle states, which are characterized by the single particle wave functions, which in turn appear explicitly in the expressions for the microscopic parameters. The N-particle state $|\Phi_0>$ in the Fock space can be defined by combining the expansion (2.2) and definition (2.3) in the following manner [10, 11]

$$|\Phi_0\rangle = \frac{1}{\sqrt{N!}} \int d^3\mathbf{r}_1 \dots \mathbf{r}_N \Psi_0(\mathbf{r_1}, \dots, \mathbf{r_N}) \hat{\Psi}^\dagger(\mathbf{r_1}) \dots \hat{\Psi}^\dagger(\mathbf{r_N}) |0\rangle, \qquad (2.14)$$

where $|0\rangle$ is the vacuum state in the Fock space. The index "0" means the ground state, but the expression is true for any state $\Psi(\mathbf{r}_1 \dots \mathbf{r}_N)$ and $|\Phi>$. One can see that the value of many-particle wave function $\Psi_0(\mathbf{r}_1 \dots \mathbf{r}_N)$ determines the weight for N electrons created at point $\{\mathbf{r}_1 \dots \mathbf{r}_N\}$. On the other hand, we obtain these weights expressed via $\Psi_0(\mathbf{r}_1 \dots \mathbf{r}_N)$ by determining the expectation value between the vacuum and the $|\Phi_0>$ states after annihilating the electrons at those locations. Explicitly, we have the inverse relation [12]

$$\Psi_0(\mathbf{r_1}, \dots, \mathbf{r_N}) = \frac{1}{\sqrt{N!}} \langle 0 | \hat{\Psi}(\mathbf{r_1}) \dots \hat{\Psi}(\mathbf{r_N}) | \Phi_0 \rangle. \qquad (2.15)$$

The last two formulas determine once more the formal equivalence of the states in the Fock and the Hilbert spaces.

With the help of the second-quantization representation we have separated above the single- and many- particle aspects of the N-body problem.

The first-quantization aspects are confined (hidden) in the expressions for the microscopic parameters t_{ij} and V_{ijkl} of the Hamiltonian (2.11). The second-quantization aspect is accounted for by the diagonalization procedure of the Hamiltonian in the occupation-number representation. This diagonalization of (2.11) in the Fock space amounts to determining $E_G =< \Psi_0|H|\Psi_0 >$ as a function of the set of microscopic parameters t_{ij} and V_{ijkl}, which are dependent on the basis single particle wave functions, in a functional manner. That is why we may treat $E_G \equiv E_G\{w_i(\mathbf{r})\}$ still as a functional of $\{w_i(\mathbf{r})\}$. The ground state of a system corresponds to the lowest energy so we may reach it by finding the minimum of E_G by optimizing it with respect to the basis $\{w_i(\mathbf{r})\}$. In effect, we can propose the renormalized (self-adjusted) wave equation, which takes the form of Euler equation for $E_G\{w_i(\mathbf{r})\}$ with the condition N=const and $< w_i|w_j >= \delta_{ij}$ [13] [2]. Namely,

$$\frac{\delta E_G}{\delta w_i^\star(\mathbf{r})} - \nabla \cdot \frac{\delta E_G}{\delta(\nabla w_i^\star(\mathbf{r}))} - \sum_{j \geq i,\sigma} (\lambda_{ij} - \mu) w_j(\mathbf{r}) < a_{i\sigma}^\dagger a_{j\sigma} >= 0 \qquad (2.16)$$

where λ_{ij} and the chemical potential μ play the role of the Lagrange multipliers imposing the orthogonality constraint and that preserving the number of particles in the system respectively. As said in the footnote, if the orbitals are orthogonal from the beginning then $\lambda_{ij} \equiv 0$. If, additionally, we work with the formalism with the fixed particle number, then also one puts $\mu = 0$, and Eq. (2.16) reduces to the system of the Euler equations for the functions $\{w_i(\mathbf{r})\}$. This wave equation is extremely difficult to solve directly, so we will resort here to choosing the starting basis, which will be optimized subsequently, as discussed next. In the simplest case, e.g. in the Hartree-Fock approximation, this equation reduces to the well-known Hartree-Fock wave equation.

2.2 The method

The procedure described in the previous Subsection does not introduce any approximation as long as the basis $\{w_i(\mathbf{r})\}$ is complete in the quantum-mechanical sense. For practical reasons, it is impossible to work with an infinite basis set, which is introduced by demanding its completeness. That is why we have to introduce approximation. Namely, we *restrict the basis*

[2] The first condition is important when we work in a concrete problem with *grand canonical ensemble* formulation in the occupation-number representation. The second condition reflects the nonorthonormal basis taken to define the field operators (2.3). In the latter case the (anti)commutation relations for the creation and annihilation operators are nonstandard [26]; see also Section 3.1

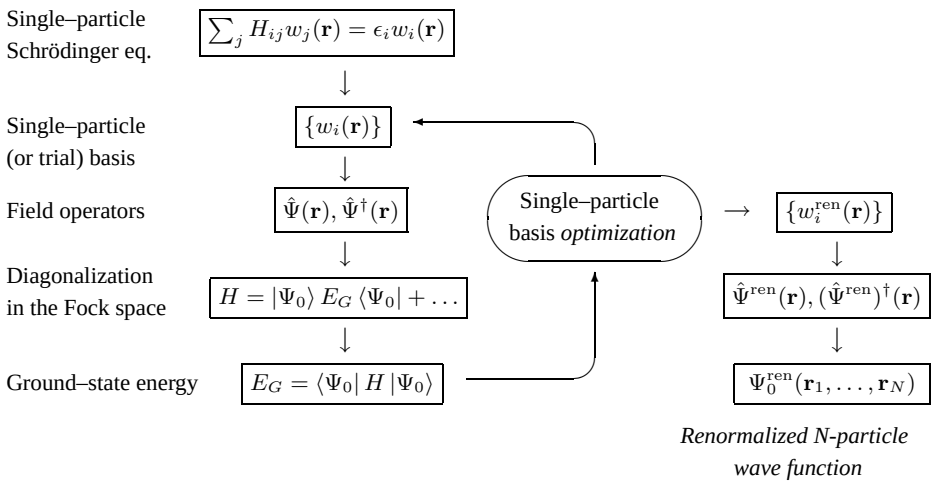

Figure 2.1. The schematic flowchart of the EDABI method.

size to a finite number of functions This is the only essential approximation we make. Such procedure allows for a reduction of the number of parameters $\{t_{ij}\}$ and $\{V_{ijkl}\}$ making the problem tractable. Also, it makes a matrix diagonalization executable as the dimension matrix representation of the Hamiltonian (2.11) increases exponentially with the number of functions in the basis. There are some cases, where we do not need the matrix representation [16] but in general, this step is unavoidable. The reduction limits the accuracy of the system description in the sense that some, possibly highly excited virtual excitations, are not taken into account. Also, the selection of the states to be discarded, must be carried out carefully. To reduce the inaccuracy of this selection, one might choose to adjust the remaining basis functions. Instead of a set of fixed single particle wave functions $\{w_i(\mathbf{r})\}$ being the solution of a concrete single-particle problem, we take a set of wave functions belonging to the same class $\{w_i(\mathbf{r};\alpha_i)\}$, characterized by an adjustable parameter α_i. The α_i choice depends on the specific physics of the problem at hand, as it is discussed in Section 3.1. The first step in the EDABI method is the selection of the reduced basis set classes as shown in Fig. 2.1. Now we can construct the field operators $\hat{\Psi}(\mathbf{r})$ as defined in (2.3), except that the summation runs now over the restricted basis set. The field operators selected in this manner can also be used for determination of the model Hamiltonian (2.11) in the occupation-number representation. The parameters $\{t_{ij}\}$ and $\{V_{ijkl}\}$ are determined likewise, by the selected wave functions.

The choice of the restricted basis represents an *essential* step. Namely, we can talk about the *model solution*, not about a *complete solution*. The neglected states (and the corresponding dynamical processes) may be irrel-

evant to the physics of the problem, but must be mentioned at the start. A minor subsequent approximation made at this point may sometimes influence the accuracy of the results. Namely, having obtained the parameters(at last their starting values) we carry out the diagonalization of the Hamiltonian. The diagonalization method is not set by the specifications of the EDABI method. Obviously, the solution of the problem in the second-quantization representation means solving the Heisenberg equation for the field operator

$$\imath\hbar\frac{\partial\hat{\Psi}}{\partial t} = [\hat{\Psi}, \hat{H}]. \tag{2.17}$$

This is not feasible in any physically relevant situation.

There are many other ways to proceed with the diagonalization and most of them, but not all, have the matrix representation of the Hamiltonian in common. Usually one obtains some or all of the eigenenergies. The eigenvalues depend, *in fact*, on the parameters $\{\alpha_i\}$. As a final step, we minimize the ground state energy E_G with respect to $\{\alpha_i\}$ and determine the *physical* ground state. In some cases, the eigenenergies are obtained as explicit expressions of parameters α_i. In such situations, we can directly minimize the lowest of them and obtain the ground state energy, as well as the renormalized values $\alpha_i \equiv \alpha_i^{opt}$. Nevertheless, if it is not possible to obtain explicit expressions, but only their numerical values for the starting set of values $\{\alpha_i\}$, we can reduce the ground state energy iteratively getting the optimal values at the procedure end. The resultant renormalized parameters α_i^{opt} allow for the selection of renormalized basis set $\{w_i^{opt}(\mathbf{r})\}$ from the initial class of wave functions $\{w_i(\mathbf{r})\}$. One has to underline, we substitute the optimal values of $\alpha_i = \alpha_i^o pt$ obtained for the ground state to characterize *all* the calculated states. This, in turn, makes the construction of the renormalized field operators $\hat{\Psi}(\mathbf{r})$ and $\hat{\Psi}^\dagger(\mathbf{r})$ possible. According to Eq. (2.15), we can obtain the interacting many particle wave function from them. This completes the solution within the method of examining a system of correlated electrons.

Summarizing, the EDABI method consists of the basis reduction, impact of which is then easied out by allowing the retained basis set functions to be self-adjusted to the many-particle (correlated) ground state. The flowchart of the EDABI procedure is schematically summarized in Fig. 2.1.

To make the approach explicit we can write down the scheme described above in form of equations. Namely, the field operator $\hat{\Psi}(\mathbf{r})$ defined by Eq. (2.3) in terms of the sum over a complete basis $\{w_i(\mathbf{r})\}$ contains an infinite number of single-particle states. We represent the field operator by a finite

number M of wave functions $\{w_i(\mathbf{r})\}$. Explicitly,

$$\hat{\Psi}(\mathbf{r}) \equiv \sum_{i=1}^{\infty} w_i(\mathbf{r}) a_i \simeq \sum_{i=1}^{M} w_i(\mathbf{r}) a_i, \tag{2.18}$$

with i representing a complete set of quantum numbers and M being a finite fixed number. We can then express the approximate N-particle wave function in the following manner

$$\Psi_\alpha(\mathbf{r_1}, \ldots \mathbf{r_n}) \simeq \frac{1}{\sqrt{N!}} \sum_{i_1,\ldots,i_N=1}^{M} \langle 0|a_{i_N} \ldots a_{i_1}|\Phi_N\rangle w_{i_1}(\mathbf{r_1}) \ldots w_{i_N}(\mathbf{r_N}). \tag{2.19}$$

There is a constraint imposed on the basis reduction, namely we have the condition $N \leq M$. Otherwise, due to the Pauli principle, it would not be possible to accommodate all the N electrons in the system. Actually, the functions $\{w_i(\mathbf{r})\}$ may include not only spatial degrees of freedom but also, for example, the spin degrees. Recognizing, that within the occupation-number space spanned on the states $\{|i_k\rangle\}_{k=1\ldots M}$, we have the N-particle state in the Fock space of the form

$$|\Phi_N\rangle = \frac{1}{\sqrt{N!}} \sum_{j_1,\ldots,j_N=1}^{M} C_{j_1\ldots j_N} a_{j_1}^\dagger \ldots a_{j_N}^\dagger |0\rangle, \tag{2.20}$$

where $C_{j_1\ldots j_N}$ represents the expansion coefficients, which are determined from a diagonalization procedure. Substituting the Eq. (2.20) to (2.19) we obtain

$$\Psi_\alpha(\mathbf{r_1}, \ldots, \mathbf{r_N}) = \frac{1}{N!} \sum_{i_1,\ldots,i_N=1}^{M} \sum_{j_1,\ldots,j_N=1}^{M} \langle 0|a_{i_1} \ldots a_{i_N} a_{j_1}^\dagger \ldots a_{j_N}^\dagger|0\rangle C_{j_1\ldots j_N} w_{i_1}(\mathbf{r_1}) \ldots w_{i_N}(\mathbf{r_N}). \tag{2.21}$$

The expression provides $N!$ nonzero terms, each with the factor $(-1)^P$, where P represents the sign of the permutation of quantum numbers $(j_1 \ldots j_N)$ with respect to $(i_1 \ldots i_N)$. In other words, we can write that

$$\Psi_\alpha(\mathbf{r_1}, \ldots, \mathbf{r_N}) = \frac{1}{N!} \sum_{i_1,\ldots,i_N=1}^{M} C_{i_1\ldots i_N}(A, S)[w_{i_1}(\mathbf{r_1}) \ldots w_{i_N}(\mathbf{r_N})]. \tag{2.22}$$

We have the same expansion coefficients for both $|\Phi_N\rangle$ and $\Psi_\alpha(\mathbf{r_1}, \ldots, \mathbf{r_N})$! Therefore, the above expression represents the multiconfigurational interacting wave function of N particles distributed among M states, with the

corresponding weights $C_{i_1 \ldots i_N}$ for each configuration, and (A, S) represent respectively the antisymmetrization (Slater determinant) or the symmetrization (simple product $w_{i_1}(\mathbf{r_1}) \ldots w_{i_N}(\mathbf{r_N})$) expressions for the fermions and bosons, respectively.

2.3 Relation to other methods

An important aspect of the discussion of our novel method is the comparison with those existing already. As the framework of the EDABI method is quite general, there are some limiting situations, in which it coincides with the existing approaches. One of them is the multiconfigurational-interaction (MCI-SCF)[3] method.

2.3.1 Difference with multiconfigurational-interaction approach

By looking at Eq. (2.22), one might get the impression that the EDABI and the MCI methods are *identical*. Both of them minimize the ground state energy by finding some optimal multiparticle wave function for a finite basis set $\{w_i\}$ selected from the start. Whereas the MCI method used in quantum chemistry [14, 15], bases on the variational optimization of both the coefficients $C_{i_1 \ldots i_N}$ and the basis $\{w_i(\mathbf{r})\}$, here the coefficients C are determined from an exact diagonalization in the Fock space, spanned on M states in the Hilbert space. Also, the functions $\{w_i(\mathbf{r})\}$ obey a self-consistent wave equation (SWE). The derivation of SWE supplements thus the MCI approach.

The differences between the EDABI and the MCI methods, both of which belong to the class of multi-determinant expansion of N-particle wave function, can be summarized under the following headings:

i) **Historical.** MCI evolved from variational methods of quantum physics and chemistry to include the electronic correlations and hence, to obtain a better value of E_G, by starting from many-particle Schrödinger equation. EDABI represents a procedure of calculating single-particle wave function starting from parameterized models of strongly correlated electrons. So the starting points of the methods are rather complementary than identical.

[3] "SCF" is the shortcut for self-consistent field.

ii) **Technical.** In MCI, we optimize simultaneously the coefficient expressing the weights of different determinants (representing different microconfigurations), as well as the parameters of the trial single-particle basis. In EDABI, we diagonalize the Hamiltonian expressed in the Fock space (with the help of either analytic or numerical methods), combined with a simultaneous optimization of the orbital size in the resultant ground state. As a result, we obtain not only the ground state, but also excited states, which may be used to determine dynamical properties of the system and thus exemplifies an essential extension of MCI [18]. The diagonalization procedure is not set. We may use some numerical diagonalization procedures such as the Lanczos method[20]. So, we may use some subsequent approximations at this point to tackle larger problems. In the flow of calculation the Hamiltonian is expressed in a second quantized form. The role of different terms can be then seen in the formalism. So, we may successively refine our model by exposing only the major physical processes, but still keeping the connection with real systems, i.e. not restricting ourselves to a parameterized model situation. For example, the density matrix renormalization group or quantum Monte-Carlo methods may be used as well (such work is planned for the future).

iii) **Essential.** In the case of analytically solvable models, EDABI leads formally to the explicit form of the renormalized wave equation, which represents a *nonlinear Schrödinger equation of nonlocal type*. This circumstance opens up a new direction of studies in *mathematical quantum physics*. Additionally, it allows for a direct determination of dynamical correlation functions, transport properties, etc. in the convenient, second-quantization, language. In this case we may be able to solve some infinite systems, e.g. one dimensional Hubbard model [12]. As a byproduct, we obtain the values of the microscopic parameters.

2.3.2 Hartree-Fock approximation: He atom example

The Hartree-Fock approximation fits also into the scheme of the EDABI method. In this approximation, we find the best single Slater determinant, which minimizes the ground state energy. It is equivalent to solving the problem of an electron moving in the averaged field of all other electrons. As the matter of fact, all electronic correlations are disregarded in this mean field approach, since it can be equivalently expressed by starting from the following approximation of a product of a pair of operators A and B in the

Hamiltonian, namely

$$(A- < A >)(B- < B >) \simeq 0 \tag{2.23}$$

$$\Updownarrow$$

$$AB = A < B > +B < A > - < A >< B > . \tag{2.24}$$

Exactly the same result can be obtained in the EDABI method by taking just the lowest possible number of basis functions, namely as many as there are electrons in the system. In this case we can skip the diagonalization process as we have only one many-electron state. So, we just minimize its energy. The results obtained in this framework are the same as those provided by the Hartree-Fock approximation.

We illustrate the Hartree-Fock approach on the example of the He atom. To do this, we start by selecting as $\{w_i(\mathbf{r})\}$ just two 1s-like states for the He atom $\Psi_\sigma(\mathbf{r}) = (\alpha^3/\pi)^{1/2}\exp(-\alpha r)\chi_\sigma$, where α is the effective inverse radius of the states. In other words, the simplest trial field operator is of the form

$$\hat{\Psi}(\mathbf{r}) = \Psi_\uparrow(\mathbf{r})a_\uparrow + \Psi_\downarrow(\mathbf{r})a_\downarrow, \tag{2.25}$$

where a_σ is the annihilation operator of particle in the state $\Psi_\sigma(\mathbf{r})$. The Hamiltonian in the second quantization for this two-element basis has then the form

$$H = \epsilon_a(n_\uparrow + n_\downarrow) + Un_\uparrow n_\downarrow, \tag{2.26}$$

where $n_\uparrow = a_\uparrow^\dagger a_\uparrow$, whereas

$$\epsilon_a = \langle \Psi_\sigma | H_1 | \Psi_\sigma \rangle, \tag{2.27}$$

and

$$U = \langle \Psi_\sigma \Psi_{\overline{\sigma}} | V | \Psi_\sigma \Psi_{\overline{\sigma}} \rangle, \tag{2.28}$$

are the matrix elements of the single-particle part defined as

$$H_1 = -\frac{\hbar^2}{2m}\nabla_1^2 - \frac{\hbar^2}{2m}\nabla_2^2 - \frac{2e^2}{\kappa_0 r_1} - \frac{2e^2}{\kappa_0 r_2} \stackrel{a.u.}{\equiv} -\nabla_1^2 - \nabla_2^2 - \frac{4}{r_1} - \frac{4}{r_2} \tag{2.29}$$

and of the Coulomb interaction between electrons

$$V = \frac{e^2}{\kappa_0|\mathbf{r_1} - \mathbf{r_2}|} \stackrel{a.u.}{\equiv} \frac{2}{|\mathbf{r_1} - \mathbf{r_2}|}, \tag{2.30}$$

with the corresponding definitions in atomic units (a.u.) after the second equality sign. The only eigenvalue of (2.26) is obtained for the state $a_\uparrow^\dagger a_\downarrow^\dagger|0>$ and is $E = 2\epsilon_a + U$. This total energy is then minimized with respect to α

to obtain the well-known variational estimate [27] of both α and the ground state energy E_G. However, we may look at the problem differently. As the field operator can be defined for an arbitrary basis, we may regard the eigenvalue E as a functional of $\Psi_\sigma(\mathbf{r})$, since the functions are under the integral expressions. Therefore, the true wave function is obtained from the Euler equation for the functional under the proviso that the wave function is normalized. This means that we minimize the functional

$$E\{\Psi_\sigma(\mathbf{r})\} = \sum_\sigma \int d^3r \Psi^*_\sigma(\mathbf{r}) H_1(\mathbf{r}) \Psi_\sigma(\mathbf{r}) + \frac{1}{2} \sum_\sigma \int d^3r d^3r' |\Psi_\sigma(\mathbf{r})|^2 V_{12}(\mathbf{r}-\mathbf{r}') |\Psi_{\overline{\sigma}}(\mathbf{r})|^2. \tag{2.31}$$

In effect, the Euler Eq. (2.16) take the form of the unrestricted Hartree-Fock equations for $\Psi_\sigma(\mathbf{r})$, namely

$$\left(\nabla^2 - \frac{2e^2}{\kappa_0 r}\right) \Psi_\sigma(\mathbf{r}) + \Psi_\sigma(\mathbf{r}) \int d^2r' \frac{e^2}{\kappa_0 |\mathbf{r}-\mathbf{r}'|} |\Psi_{\overline{\sigma}}(\mathbf{r}')|^2 = \lambda \Psi_\sigma(\mathbf{r}), \tag{2.32}$$

where λ reflects the imposed normalization function in the same manner, as in original Schrödinger formulation of the wave equation [28]. If we would have taken two spin-orbitals instead of two orbitals we would obtain the restricted Hartree-Fock equation. Thus we can see that taking in the simplest case just two spin orbitals we obtain either well-known variational estimate [27] for α and E_G for He atom: $\alpha = 27/(16a_0)$ and $E_G = -5.695Ry$, where $a_0 \simeq 0.53$Å is the 1s Bohr orbit radius. The energies present in this case are shown in Fig. 2.2.

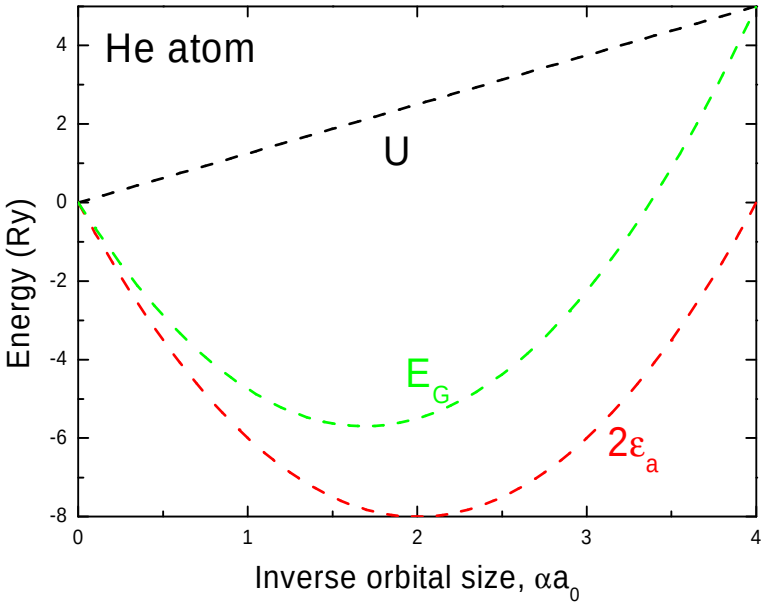

Figure 2.2. The interplay between the atomic energy ϵ_a (dotted line) and interaction energy U (dashed line) resulting in the ground state energy E_G (solid line) as a function of the inverse orbital size α.

Chapter 3

Light atoms and ions: a test of EDABI method

3.1 Selection of the single-particle basis

The EDABI method described in Chapter 2 leaves several important decisions to be made when implementing it in concrete cases. One of the most important is the choice of the starting single-particle basis.

If the basis chosen were complete, then we would not have any approximation. The transition to the second-quantization formalism would be exact and the problem solved rigorously for an arbitrary complete basis $\{w_i(\mathbf{r})\}$ provided we would be able to calculate in that basis the microscopic parameters explicitly. The choice is arbitrary in this case, but usually we are not able to perform any calculations due to complexity problems as stated before. So we have to leave only some orbitals. It is to be decided which single-particle orbitals are to be left, and which should be ignored. As it is an approximation, the result of the calculations may and does depend on the choice we do. As said earlier, this approximation represents one of the most *fundamental* features when constructing the models. Our method allows for construction of theoretical models *without* parameters, but requires a degree of ingenuity when selecting the basis.

The neglected states usually represent highly excited (and thus negligible) states in the system. They are supposed to be almost unoccupied and so their contribution negligible. Obviously, due to the interactions the identity of the single particles may become blurred if the interaction is stronger than the difference in energy for such single-particle states.

What other mathematical properties should the reduced basis set expose? It is very convenient to perform all the calculations using an orthonormalized

basis set. What happens if it is not the case[26]? The occupation number of a given single particle state i is governed by the creation and annihilation operators a_i and $a_i^\dagger$, whereas the existence of an electron in at real space coordinate $\mathbf{r}$ is altered by the field operators $\hat{\Psi}(\mathbf{r})$ and $\hat{\Psi}^\dagger(\mathbf{r})$. Due to Pauli principle the fermionic wave function has to be antisymmetric. Hence the field operators should have the following anticommutation relations

$$\left\{\hat{\Psi}^\dagger(\mathbf{r}), \hat{\Psi}(\mathbf{r}')\right\} = \delta(\mathbf{r}-\mathbf{r}'), \tag{3.1}$$

where $\{A, B\} \equiv AB + BA$. In addition to that, if both operators are conjugated or not, then they anticommute. One could expect the creation and the annihilation operators to behave in a similar manner. Such commutation relations let the particles in single particle states behave like real fermions. Also, simple commutation rules imply a smaller number of terms in the actual calculations involving them. A pair of creation and annihilation operators acting on an N-particle state gives

$$\begin{aligned} a_j a_i^\dagger |w_1 \dots w_N> &= a_j |w_i, w_1 \dots w_N> = \\ &< w_j|w_i> |w_1 \dots w_N> + \sum_{k=1}^{N} (-1)^k < w_j|w_k> |w_i, w_1 \dots \not{w}_k \dots w_N>, \end{aligned} \tag{3.2}$$

where $\not{w}_k$ shows that the particle described by w_k is not longer present in the many-particle state. In the inverted order, we have

$$\begin{aligned} a_i^\dagger a_j |w_1 \dots w_N> &= \\ &\sum_{k=1}^{N} (-1)^k < w_j|w_k> a_i^\dagger |w_1 \dots \not{w}_k \dots w_N> = \\ &\sum_{k=1}^{N} (-1)^k < w_j|w_k> |w_i, w_1 \dots \not{w}_k \dots w_N> . \end{aligned} \tag{3.3}$$

The sum of above Eqs. (3.2) and (3.3) gives us the wanted commutator

$$\left\{a_i^\dagger, a_j\right\} = < w_i|w_j> = \int d^3\mathbf{r} w_i(\mathbf{r})^\star w_j(\mathbf{r}) = S_{ij}. \tag{3.4}$$

The integral is the overlap integral between the orbitals w_i and w_j. In the same manner, we can obtain the results for two creation or two annihilation operators namely $\{a_i, a_j\} = \{a_i^\dagger, a_j^\dagger\} = 0$. So, the fermionic anticommutation rules are preserved only for orthonormal basis sets, where $S_{ij} \equiv \delta_{ij}$.

If the single particle basis is not normalized then the particles count cannot be determined using the usual number of particles operator $a^\dagger a$. If $\{a_i^\dagger, a_i\} =< w_i|w_i >= S_{ii}$ then

$$< w_i|a_i^\dagger a_i|w_i >=< w_i|S_{ii} - a_i a_i^\dagger|w_i >= S_{ii} < w_i|w_i >= S_{ii}^2$$

what is equal to one only if $S_{ii} = 1$. Note that the value of $S_i i$ is nonnegative, because the overlap integral involves only one orbital, hence S_{ii} cannot be equal to -1.

Another problem do discuss is the connection between the completeness of the single particle basis and the anticommutation relations for the field operators. Expanding the anticommutator according to definition (2.3), we obtain

$$\left\{\hat{\Psi}^\dagger(\mathbf{r}), \hat{\Psi}(\mathbf{r}')\right\} = \sum_{ij} w_i^\star(\mathbf{r}) w_j(\mathbf{r}') \left\{a_i^\dagger, a_j\right\} = \sum_{ij} w_i^\star(\mathbf{r}) w_i(\mathbf{r}') S_{ij} = \sum_i w_i^\star(\mathbf{r}) w_i(\mathbf{r}'), \tag{3.5}$$

where the third equality implies an orthonormal basis set. The resultant expression can be identified as equivalent to the definition of the completeness of a set $\{w_i(\mathbf{r})\}$

$$\sum_i w_i^\star(\mathbf{r}) w_i(\mathbf{r}') = \delta(\mathbf{r} - \mathbf{r}'). \tag{3.6}$$

So if the basis is not complete, we do not have the correct commutation rules for the field operators defined by Eq. (3.5) (the same is true for an infinite but nonorthogonal basis). Because we work with a finite basis, we may approximate these rules only in a limited region of space. That is why it is important to choose the basis functions to cover well the area, where we expect an ample abundance of electrons.

For the light atoms and ions discussed in this Section it is the vicinity of the nuclei, where we expect the electrons prevail, at least as long as we are interested in their bound states. If the selected starting wave functions coincide with the states of the interacting system, then the approximation works very well. The first choice to determine the class of basis function is to start with a solvable subset of the system. In the case of atoms and ions, we might drop first the interaction between electrons. This is only the starting moment of selecting the initial class of wave functions. We thus obtain a single particle Schrödinger equation describing an electron in the Coulomb field of the nucleus. As the solution we obtain the well known hydrogenic-like wave functions.

As mentioned before, we would like to optimize them later to account better the interactions. So, we have to decide in which way to vary them. One might expect that due to the repulsive Coulomb interactions, the orbitals

can be either expanded on, to allow the electrons to be further away from each other, or to the contrary, to be squeezed in, to take the advantage of the nucleus attraction. In the simplest and physically appealing approach, the radial size of the orbitals may be varied. On the other hand, the total angular momentum of the electrons in the atom should be invariant under the electron-electron interactions, so we may try to retain the angular dependence in its original form, as it does not change drastically under the interaction (the spin-orbit interaction is regarded as small on this energy scale). The size change of different orbitals does not necessary have to be related to each other. Every single orbital can have a free parameter instead of its Bohr radius na_0. The class of hydrogenic-like wave functions is thus defined by the radial parts of the form

$$\begin{aligned} R_{1s}(r;\alpha) &= 2\alpha^{3/2}\exp(-\alpha r), \\ R_{2s}(r;\alpha) &= 2\alpha^{3/2}(1-\alpha r)\exp(-\alpha r), \\ R_{2p}(r;\alpha) &= \tfrac{2}{\sqrt{3}}\alpha^{5/2} r\exp(-\alpha r). \end{aligned} \tag{3.7}$$

The complete wave functions are obtained by multiplying the radial parts by the standard spherical dependence represented by spherical harmonics Y_{lm},i.e.[1]

$$\begin{aligned} \phi_{1s}(r,\theta,\phi;\alpha_1) &= R_{1s}(r;\alpha_1)Y_{00}(\theta,\phi), \\ \phi_{2s}(r,\theta,\phi;\alpha_2) &= R_{2s}(r;\alpha_2)Y_{00}(\theta,\phi), \\ \phi_{2p0,\pm1}(r,\theta,\phi;\alpha_{3,4,5}) &= R_{2p}(r;\alpha_{3,4,5})Y_{10,\pm1}(\theta,\phi). \end{aligned} \tag{3.8}$$

The above functions form a group of wave functions dependent on the parameters α_i, which has the dimension of inverse length. For the hydrogen atom, this parameter has a fixed value 1 for 1s state (atomic units) and 1/2 for the remaining hydrogenic-like states (2s and 2p 0,$\pm$1)[2]. This parameter corresponds to the size of the orbital. Their inverse is the Bohr-radius for each orbital. One can calculate the expectation value of the distance of the electron from the nuclei, which is

$$< \phi_i|r|\phi_i >= \int d^3\mathbf{r}|\phi_i(\mathbf{r};\alpha)|^2 r = \begin{cases} \frac{3}{2\alpha} & \text{for 1s states} \\ \frac{3}{\alpha} & \text{for 2p 0,}\pm1\text{ states.} \end{cases} \tag{3.9}$$

We shall see that the optimized Bohr-radii are not exactly equal to those values.

[1]For the definitions and conventions, see Appendix A.

[2]The Table 3.1 shows the results obtained in Section 3.4 in terms of the Bohr-radii, which are the inverse of α_i parameters.

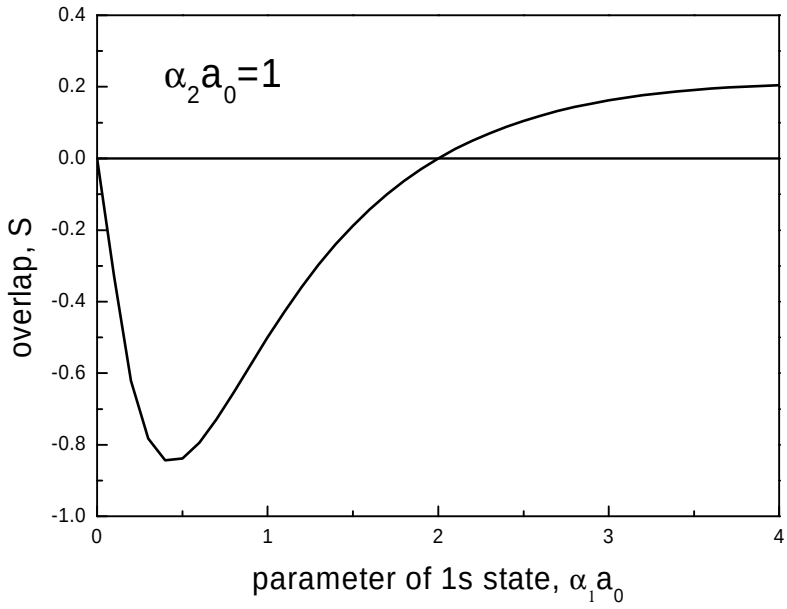

Figure 3.1. Overlap integral between normalized 1s and 2s hydrogenic-like wave functions. The size parameter for the 2s state is kept fixed at the value $\alpha_2 = 1$.

The selected functions are normalized, but they are not orthogonal for an arbitrary value of the parameters α. They are the solutions of the Hamiltonian of an electron in the Coulomb potential of the nucleus. And thus if they have different energies, they are orthogonal only for a single value of the parameter. We do not change the angular dependence of the wave functions, but only the radial part. So only the functions corresponding to the same spherical harmonics may be nonorthogonal. In our case, with the starting basis (3.8), these are only the 1s and the 2s states. One can calculate the overlap integral for these states and obtain that

$$S =< \phi_{1s}|\phi_{2s} >= \int d^3\mathbf{r}\phi^{\star}_{1s}(\mathbf{r};\alpha_1)\phi_{2s}(\mathbf{r};\alpha_2) = \frac{8\sqrt{\alpha_1^3}\,(\alpha_1 - 2\,\alpha_2)\,\sqrt{\alpha_2^3}}{(\alpha_1+\alpha_2)^4}. \tag{3.10}$$

Only for the values of α_1 and α_2 satisfying the equality $\alpha_1 = 2\alpha_2$ the above overlap integral is equal to zero. This line in the (α_1,α_2) plane corresponds to a different strength of the Coulomb attraction of the nucleus. Fig. 3.1 shows

this dependence vs. α_1 for a fixed value of $\alpha_2 = 1$. When the size of 1s orbital is smaller ($\alpha_1 > 2$), then the sign of the overlap is positive. It is negative in the opposite case. The limit $\alpha_1 \to 0$ means an infinite orbital size and can be regarded as the free-electron limit for the given state. Because we optimize the parameters and require that the basis wave functions are orthogonal for any set of values of the parameters α_i we have to introduce a procedure, that guarantees this. The orthonormal set of basis wave functions can be called the set of Wannier functions w_i. The straightforward way to achieve it is by mixing these two nonorthogonal orbitals. The orthogonality relation to all other basis functions is preserved by the nontrivial angular dependence of the corresponding wave functions.

We have two functions ϕ_1 and ϕ_2 satisfying relations

$$< \phi_{1s}|\phi_{1s} >=< \phi_{2s}|\phi_{2s} >= 1; \;\; < \phi_{1s}|\phi_{2s} >= S, \tag{3.11}$$

and we would like to obtain the orthogonalized functions w_1 and w_2, which satisfy

$$< w_1|w_1 >=< w_2|w_2 >= 1; \;\; < w_1|w_2 >= 0. \tag{3.12}$$

Such a transformation is not unique. Namely, we may choose the following form

$$\begin{cases} w_1(r,\theta,\phi;\alpha_1,\alpha_2) = \beta\phi_{1s}(r,\theta,\phi;\alpha_1) + \gamma\phi_{2s}(r,\theta,\phi;\alpha_2), \\ w_2(r,\theta,\phi;\alpha_1,\alpha_2) = \gamma\phi_{1s}(r,\theta,\phi;\alpha_1) + \beta\phi_{2s}(r,\theta,\phi;\alpha_2). \end{cases} \tag{3.13}$$

It is an ansatz and a special case of a general method, the *Löwdin method*, described in Appendix B. As the solution of (3.11) and (3.12) we obtain in this case

$$\begin{cases} \beta = \frac{\sqrt{1-S}+\sqrt{1+S}}{2\sqrt{1-S^2}}, \\ \gamma = \frac{\sqrt{1-S}-\sqrt{1+S}}{2\sqrt{1-S^2}}. \end{cases} \tag{3.14}$$

The mixing coefficients β and γ are displayed in Fig. 3.2 as a function of α_1. The choice of the mixing in form (3.13) has the advantage of preserving the major aspects of the shape of the wave functions, such as the number of nodes, as is shown in Fig. 3.3. This is useful because we may still identify the properties of the Wannier functions as similar to the original atomic functions. Most importantly, the orthogonalized functions w_1 and w_2 reduce to the atomic orbitals ϕ_1 and ϕ_2 in the atomic limit $\alpha_2 = 2\alpha_1$.

As mentioned before, the finite basis choice makes its completeness condition basis break down. The severity of this breakdown can be accounted for in terms of its definition $\sum_i w_i^\star(\mathbf{r}) w_i(\mathbf{r}') = \delta(\mathbf{r}-\mathbf{r}')$. We can calculate the sum on the left to see, to what extent it does approximate the three-dimensional Dirac delta function $\delta(\mathbf{r}-\mathbf{r}')$. To visualize this approach, it is advisable to

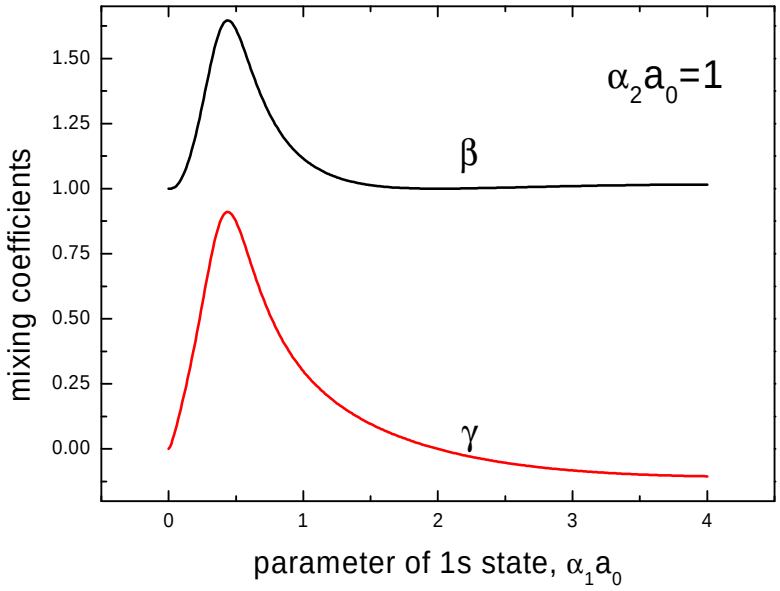

Figure 3.2. Mixing coefficients β and γ as a function of the inverse 1s-orbital size α_1. The inverse 2s-orbital size is fixed at $\alpha_2 = 1$. The area where the orthogonalization procedure is necessary, can be seen. Both limits $\alpha_1 \to 0$ and $\alpha_1 \to \infty$, do not require it.

reduce the number of components to be able to display the value on a plot. We define the function

$$C(r, r') = \frac{1}{4\pi} \int_0^{\pi} \int_0^{2\pi} d\phi d\theta \sum_i w_i^{\star}(r, \theta, \phi) w_i(r', \theta, \phi), \tag{3.15}$$

in which we are averaging of the completeness condition over the angles θ and ϕ. It is plotted in Fig. 3.4 for the atomic basis selected. For a complete basis we should obtain a δ-like peak along the line $r = r'$. The height of the peak measures the representation of a given region by the basis. For the ideal case the height is obviously infinite and equal along the whole line. The relative width of the peak shows the spatial resolution of the selected basis in the radial direction. It can be seen that the area close to nucleus is best represented in the basis. These functions decay exponentially in the large r limit.

The choice of the hydrogenic-like wave functions has also some disadvan-

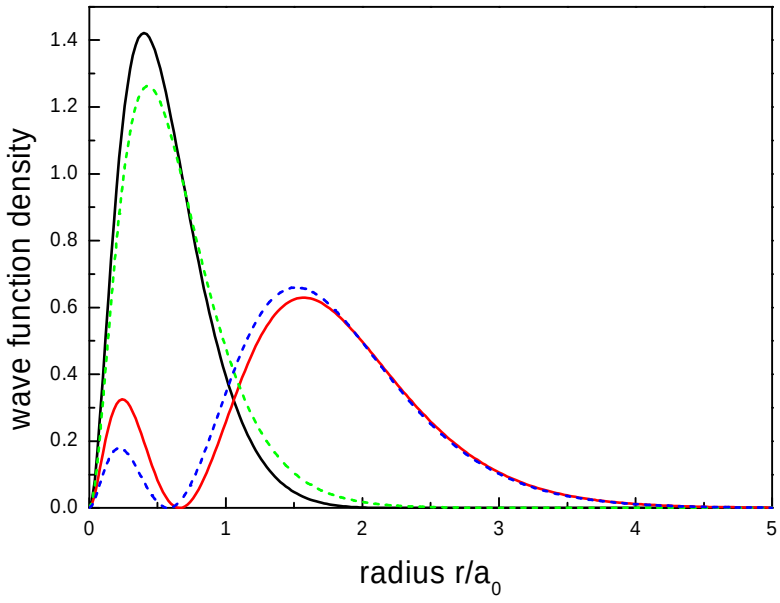

Figure 3.3. The atomic 1s and 2s orbitals (dashed lines) vs. the corresponding orthogonalized (Wannier) orbitals (solid lines). The size of both atomic and Wannier orbitals is adjusted on example of the He atom, by carrying out the complete EDABI procedure. A larger localization of the Wannier orbitals around the nucleus is seen.

tages. They are somewhat difficult to handle in actual calculations, because the integrals involving them are difficult or even, in many cases, impossible to be calculated analytically. Such integrals appear in the microscopic parameters t_{ij} and V_{ijkl} as expressed by Eqs. (2.12) and (2.13).

Another possibility is to use the Gaussian type orbitals [21, 22, 23, 24] of the form

$$\psi(\mathbf{r}) = \left(\frac{2\Gamma^2}{\pi}\right)^{3/4} e^{-\Gamma^2\mathbf{r}^2},$$

for the starting basis set. It was done in [6]. From the point of view of the calculations themselves it is much easier to proceed. They have much nicer integral properties and the process of determining the microscopic parameters does not present a principal difficulty [25]. This allows for an automatical extension of the calculations to larger systems. However, the Gaussian functions are the solution of the harmonic-oscillator problem. Matching them, by

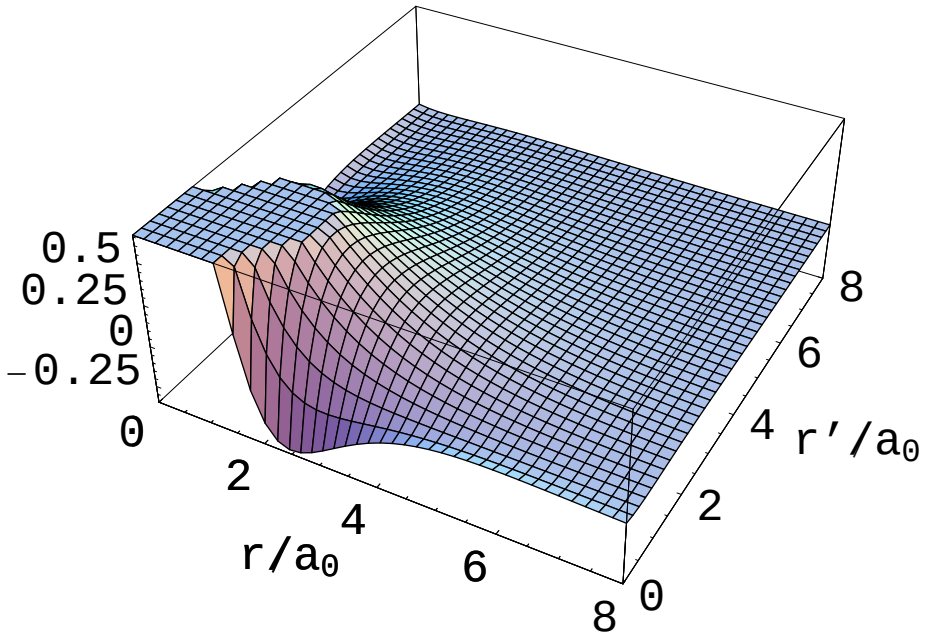

Figure 3.4. The function $C(r, r')$ of Eq. (3.15) characterizing the completeness condition (3.6), averaged over the angles θ and ϕ of the wave functions for 1s, 2s, and 2p 0,$\pm$1 orbitals. The plateau seen around the origin is caused by an artificial cutoff to accommodate spike nature of the dependence. All the functions used in calculation have the same value $\alpha_{1...5} = 1$. The change of this parameter scales the plot, without changing its shape.

minimizing the single electron energy of a linear combination of Gaussian functions, for electron moving in the Coulomb potential, can be regarded as a mathematical, rather than physical, approximation. Because the harmonic oscillator potential is unbounded with the increasing distance, these wave functions are damped exponentially with r squared, so we may also miss long-range correlations. The *Slater orbitals* are a better approximation of the single particle functions in atomic systems than the Gaussian functions. Because of this we have selected the Slater orbitals in the remaining part of this Thesis.

3.2 Calculation of the microscopic parameters

The choice of the class of the basis functions is the first step. Next we have to express explicitly the Hamiltonian (2.11) in order to diagonalize it. So we need to tackle the problem of calculating the one-electron (2.12) and two-electron parameters(2.13). The calculations can be performed in the atomic basis. Because we want to work with orthonormal Wannier functions, we have to transform the parameters from atomic to the Wannier representation.

3.2.1 One-electron parameters

Our model describes electrons of charge $-e$ moving in the field originating from the nucleus with charge Ze. The charge of the nucleus does not have to be set in advance as we want to calculate several different atoms and ions. The single particle part of the Hamiltonian (2.1) consists of the kinetic term and the nuclear Coulomb term, which reads in atomic units

$$H_1(\mathbf{r}) = -\nabla^2 - \frac{2Z}{|\mathbf{r}|}. \tag{3.16}$$

The Hamiltonian is expressed in atomic units, i.e. the distance is measured in the units of Bohr radius a_0, the charge in units of electronic charge e and the energy in Rydberg Ry. We want to determine the expression for the hopping integral in the atomic (≡primed) representation

$$t'_{ij} \equiv \int d^3\mathbf{r}\phi_i^\star(\mathbf{r})H_1(\mathbf{r})\phi_j(\mathbf{r}). \tag{3.17}$$

According to origin of our basis the atomic functions $\{\phi_i\}$selected are the solutions to this Hamiltonian. As stated before only the $\phi_1 \equiv \phi_{1s}$ and $\phi_2 \equiv \phi_{2s}$ are not orthogonal. Because of this fact all off-diagonal terms in the atomic (primed) representation of t'_{ij}, except of t'_{12}, are zero. So we have only 6 nonequivalent nonzero terms left out from the total of 15. We may also note that the states ϕ_2 and $\phi_{3,4,5} \equiv \phi_{2p_{0,+1,-1}}$ correspond to the same energy eigenvalue of the Hamiltonian. So, the form of $t'_{11} \ldots t'_{55}$ is identical. We only have to insert different parameters $\alpha_2 \ldots \alpha_5$. This observation reduces further the number of different integrals to calculate to 3. All orbitals are centered around the same origin. The evaluation of these integrals is straightforward in the spherical coordinates. The nonzero elements of t'_{ij} are

$$\begin{aligned} \varepsilon'_1 \equiv t'_{11} &= (\alpha_1 - 2Z)\alpha_1 \\ \varepsilon'_{2,3,4,5} \equiv t'_{22,33,44,55} &= (\alpha_{2,3,4,5} - Z)\alpha_{2,3,4,5} \end{aligned}$$

$$t'_{12} = \frac{8\,(\alpha_1\,\alpha_2)^{\frac{3}{2}}\;(\alpha_1\alpha_2(2\alpha_1-\alpha_2)+Z(\alpha_2^2-\alpha_1^2))}{(\alpha_1+\alpha_2)^4} \tag{3.18}$$

Having obtained the result in the atomic basis, we have to transform it to the orthogonalized basis according to Eqs. (3.13) and (3.14). Because $t_{ij} =< w_i|H_1|w_j >$ and the decomposition (3.13), the corresponding expressions transformed to the atomic basis have the following form

$$\begin{aligned}\varepsilon_1 &= \beta^2\varepsilon'_1 + \gamma^2\varepsilon'_2 + 2\beta\gamma t'_{12}\\ \varepsilon_2 &= \gamma^2\varepsilon'_1 + \beta^2\varepsilon'_2 + 2\beta\gamma t'_{12}\\ t_{12} &= \left(\beta^2+\gamma^2\right)t'_{12} + \beta\gamma\left(\varepsilon'_1+\varepsilon'_2\right)\end{aligned} \tag{3.19}$$

Such a change of basis introduces thus a substantial change in the values of these parameters as is shown in Fig. 3.5 for the nucleus charge $Z = 2$, where the dashed line represents the results in the atomic basis and the solid line is for the orthogonalized basis. In this plot only the value of α_1 corresponding to the 1s orbital is changing while $\alpha_2 a_0 = 1$ for the 2s orbital which corresponds to the case of nuclear charge 2. For the hydrogenic-like limit $\alpha_1 a_0 = 2$, $\alpha_2 a_0 = 1$ the orthogonalized functions become identical to the atomic functions. Then, the atomic and Wannier parameters are equal in this limit. Due to the angular dependence of the 2p 0 states, they do not mix with each other and with s states. Their atomic energy is equal to the atomic energy for the 2s state at the same value of parameter α. Note that the sign of the hopping parameter t_{12} does not necessary have to be the same as that of $t'_1 2$. On the other hand, the sign of this parameter does not really matter for a two level system since the eigenvalues of its Hamiltonian

$$H = \begin{pmatrix} \varepsilon_1 & t_{12} \\ t_{12} & \varepsilon_2 \end{pmatrix}$$

have the form

$$\epsilon_\pm = \frac{\varepsilon_1+\varepsilon_2}{2} \pm \sqrt{\left(\frac{\varepsilon_1-\varepsilon_2}{2}\right)^2 + t_{12}^2},$$

which is obviously independent from the sign of t.

3.2.2 Two-electron parameters

The two-particle parameters are defined by Eq. (2.13). The Hamiltonian operator has the form of the Coulomb repulsive interaction

$$H_2(\mathbf{r},\mathbf{r}') = H_2(|\mathbf{r}-\mathbf{r}'|) = \frac{2}{|\mathbf{r}-\mathbf{r}'|}. \tag{3.20}$$

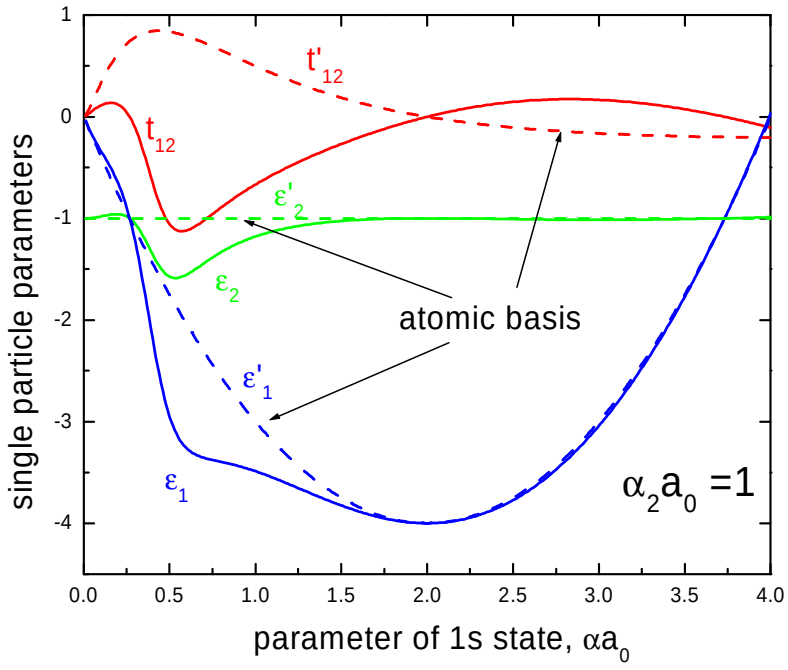

Figure 3.5. The single particle parameters of the 1s and 2s orbitals. The charge of the nucleus is $Z = 2$. Dashed line represents the results in the atomic basis. Solid line is for the Wannier basis. All parameters except of the 1s α are fixed at the value 1. t_{12} - red line, ε_1 - blue line, ε_2 - green line.

We want to determine first the values of parameters in the atomic (primed) representation

$$V'_{ijkl} \equiv \int d^3\mathbf{r} d^3\mathbf{r}' \phi_i^\star(\mathbf{r}) \phi_j^\star(\mathbf{r}') \frac{2}{|\mathbf{r} - \mathbf{r}'|} \phi_k(\mathbf{r}) \phi_l(\mathbf{r}'), \tag{3.21}$$

where the atomic functions $\phi_i(\mathbf{r})$ are of the form (3.8). All these functions are centered around a common origin (nucleus position for the atoms). The common origin allows for an analytic evaluation of all integrals (3.21). The difficult part is the expression for the inverse relative distance of electrons

$$\frac{1}{|\mathbf{r} - \mathbf{r}'|} = \frac{1}{\sqrt{(r_x - r'_x)^2 + (r_y - r'_y)^2 + (r_z - r'_z)^2}}.$$

This expression in not likely integrable in Cartesian coordinates. So we have to use spherical polar coordinates and the multipole expansion (C.3)of

$1/|\mathbf{r}-\mathbf{r}'|$ appropriate to those coordinates, which is more closely described in Appendix C,

$$\frac{1}{|\mathbf{r}-\mathbf{r}'|} = \sum_{s=0}^{\infty}\sum_{m=-s}^{s} \frac{(s-|m|)!}{(s+|m|)!}\frac{r_<^s}{r_>^{s+1}} P_s^{|m|}(\cos\theta) P_s^{|m|}(\cos\theta') e^{\imath m(\phi-\phi')}. \quad (3.22)$$

Here the corresponding coordinates of the points $\mathbf{r}$ and $\mathbf{r}'$ are (r,θ,ϕ) and (r',θ',ϕ') respectively, where r and r' are the distances from the origin, θ is the polar angle from the z-axis with $0 \le \theta \le \pi$ and ϕ is the azimuthal angle in the xy-plane from the x-axis with $0 \le \phi \le 2\pi$ [3]. $r_<$ and $r_>$ are respectively the minimum and the maximum of the two distances r and r'. The functions $P_k^m(\cos\theta)$ are the associated Legendre functions. Inserting Eqs. (3.8) and (3.22) into (3.21) we obtain

$$\begin{aligned} V'_{ijkl} = \int d^3\mathbf{r}\phi_i^\star(\mathbf{r})\phi_k(\mathbf{r}) \int dr' R_j(r')R_l(r') \times \\ \times \sum_{s=0}^{\infty}\sum_{m=-s}^{s} \frac{(s-|m|)!}{(s+|m|)!}\frac{r_<^s}{r_>^{s+1}} P_s^{|m|}(\cos\theta) \times \\ \times \int d\theta' \underbrace{d\phi' P_s^{|m|}(\cos\theta') e^{\imath m(\phi-\phi')} Y_j^\star(\theta',\phi') Y_l(\theta',\phi')}_{(\star)}. \end{aligned} \quad (3.23)$$

The spherical harmonics behave like $Y(\theta,\phi)_{lm} \sim e^{\imath m\phi}$. Hence the integration over ϕ' of the part $(\star)$ in Eq. (3.23) leads to a substantial reduction of the sum over m, since $\int_0^{2\pi} \exp(\imath m\phi')d\phi' = 2\pi\delta_{m0}$. Namely, $(\star)$ is nonzero only for $m = m_j - m_l$. On the other hand, the integration over the azimuthal angle ϕ of the first electron leads to a further constraint on Eq. (3.23) for the value $m = m_k - m_i$. If we combine this we obtain the following relation $m_i + m_j = m_k + m_l$, which means that the total z-component of angular momentum of electrons created in states i and j has to be equal to that of electrons annihilated in states k and l, so this component is conserved by the electron-electron interaction. Expressing spherical harmonics in terms of associated Legendre functions (A.5) we may rewrite Eq. (3.23) as

$$\begin{aligned} V'_{ijkl} = C\delta_{m_i+m_j,m_k+m_l} \int dr dr' r^2 r'^2 R_i(r)R_k(r)R_j(r')R_l(r') \times \\ \times \sum_{s\ge|m|} \frac{(s-|m|)!}{(s+|m|)!}\frac{r_<^s}{r_>^{s+1}} \int d\theta \sin\theta P_s^{|m|}(\cos\theta) P_i^{m_i}(\cos\theta) P_k^{m_k}(\cos\theta) \times \end{aligned}$$

[3] Unfortunately, the convention in which the symbols θ and ϕ are reversed is frequently used, especially in mathematics, leading to unnecessary confusion.

$$\times \int d\theta' \sin\theta' P_s^{|m|}(\cos\theta') P_j^{m_j}(\cos\theta') P_l^{m_l}(\cos\theta'), \tag{3.24}$$

where the preceding normalization factor $C = 4\pi^2 \beta_{im_i} \beta_{jm_j} \beta_{km_k} \beta_{lm_l}$ and β_{im_i} are defined by (A.6). The integrations over the polar angles θ and θ' of both electrons result in the total angular momentum conservation rules as the integrals of type

$$I_{ijk} \equiv \int dx P_i^{m_i}(x) P_j^{m_j}(x) P_k^{m_k}(x)$$

are nonzero only if two of the parameters can be added in a vector-like manner to construct the third one. After carrying out the angular integration, we can expand the radial part of the integration according to

$$\int_0^\infty dr \int_0^\infty dr' f(r_<, r_>) = \int_0^\infty dr \left(\int_0^r dr' f(r', r) + \int_r^\infty dr' r(r, r') \right). \tag{3.25}$$

As the final result we obtain that $V'_{ijkl} = f(\alpha_i, \alpha_j, \alpha_k, \alpha_l)$, where f is a rational function of its parameters.

The selected by us earlier minimal atomic basis consists of five orbitals. So, the number permutations of four indices in parameters defined by Eq. (3.21) is $5^4 = 625$. The number of relevant integrals is not as large. Most of them vanish because of the total angular momentum and the z-component of the angular momentum conservation rules discussed in the previous paragraph, which reduces the number of nonzero and independent values. The number of independent values of the two-particle interaction parameters is also reduced because of the symmetries exhibited by Eq. (3.21). Firstly, the particles are indistinguishable. Hence, the integration variables $\mathbf{r}$ and $\mathbf{r}'$ can be swapped without changing the value calculated: $\{i, k\} \leftrightarrow \{j, l\}$. The next fact is caused by the z-component of the angular momentum constraint. Note that the operator (3.20) takes real values only. The only complex terms in (3.21) are then $\exp(\imath m\phi)$ functions of the azimuthal dependence of the spherical harmonics. But, the integration cancels out all the contributions, in which the total ϕ dependence is different from the ϕ' dependence. In this case, the integral has to be real. So, we may conjugate it and obtain the same real value whereas the indices change by definition

$$\left(V'_{ijkl}\right)^\star = \left(\int d^3\mathbf{r} d^3\mathbf{r}' \phi_i^\star(\mathbf{r}) \phi_j^\star(\mathbf{r}') \frac{2}{|\mathbf{r} - \mathbf{r}'|} \phi_k(\mathbf{r}) \phi_l(\mathbf{r}') \right)^\star =$$

$$= \int d^3\mathbf{r} d^3\mathbf{r}' \phi_i(\mathbf{r}) \phi_j(\mathbf{r}') \frac{2}{|\mathbf{r} - \mathbf{r}'|} \phi_k^\star(\mathbf{r}) \phi_l^\star(\mathbf{r}') = V'_{klij},$$

like $\{i,j\} \leftrightarrow \{k,l\}$. Combining the above two permutations we may construct all the nonequivalent sequences of indices in the following way. First, we construct all possible pairs of two indices corresponding to the same particle such that the first index is not greater then the second, which is possible because of the second property. The number of such pairs is equal to the sum

$$\sum_{i}^{n}\sum_{j\geq i}^{n} 1 = \sum_{i}^{n}(n-i) = \frac{n(n-i)}{2}, \tag{3.26}$$

where n is the number of different elements put in ordered pairs. In due course of this calculation we obtain 15 different pairs from initial 5 orbitals, which in turn are paired again to build ordered pairs of pairs. This reduces the initial number of integrals 625 to the value 120 calculated from (3.26). After performing the actual calculation there are only 24 nonzero values left. They are listed in Appendix D.
The next step is the transformation from the basis of atomic wave functions to the Wannier basis. Just like for the single particle states the transformation is defined by the Eqs. (3.13) and (3.14). They transform as

$$V_{ijkl} = \sum_{i'j'k'l'} V'_{i'j'k'l'} \prod_{z=\{i,j,k,l\}} \left(\delta_{zz'} + \beta(\delta_{z1}\delta_{z'1} + \delta_{z2}\delta_{z'2}) + \gamma(\delta_{z1}\delta_{z'2} + \delta_{z2}\delta_{z'1})\right). \tag{3.27}$$

Their explicit expressions will not be listed here.

3.3 Construction of Hamiltonian matrix and role of symmetries

Having all the parameters required to express fully the second-quantized Hamiltonian (2.11), we may try to diagonalize it. Unfortunately, there is no analytic solution in the general case. We do not impose any further constraints on the one- and the two- electron parameters calculated in Section 3.2. To be able to diagonalize it we have to use a "brute force" method. Namely we select a fixed number of electrons. We do know the number of electrons for each atom and ion. They are 2 electrons for He, and H^- and 3 for Li, Be^+, and He^- respectively. Then we construct all the possible configurations of electrons distributed among the five Wannier states used in the calculations. Each Wannier function introduces two spin states. The number of configurations can be calculated as

$$\Omega = \binom{2M}{N} = \frac{(2M)!}{N!(N-2M)!}, \tag{3.28}$$

where M is the number of Wannier states and N is the number of electrons. The number of multiparticle states is in our case 45 for 2 electrons and 120 for 3 electrons. Note that the number of multiparticle states has its minimum for an empty or completely filled system and reaches the maximum value for the half-filled case, i.e. for $N = M$. For the case of more than half-filled system, the number of multiparticle states for a given number of holes N_h in the filled state is equal to the number of states for $N = N_h$ electrons for $N \leq M$.

Each two- or three- particle state can be expressed by the creation operators

$$|I> \equiv |ij> = a_i^\dagger a_j^\dagger |0> \quad \text{or} \quad |I> \equiv |ijk> = a_i^\dagger a_j^\dagger a_k^\dagger |0> . \tag{3.29}$$

The multiparticle states are numbered from one to Ω (which is either 45 or 120 for $N = 2$ and 3,respectively). The simplest way to generate consecutive states is to iterate over the indices i, j and if applicable k, restricting the variation range of them to

$$i = 1 \ldots 2M \quad j = i + 1 \ldots 2M \quad k = j + 1 \ldots 2M \tag{3.30}$$

to avoid the generation of states differing only by a phase. The Hamiltonian (2.11) links every pair consisting of a multiparticle state $|I>$ and a conjugated multiparticle state $<J|$, to build the matrix element of the Hamiltonian matrix

$$H_{IJ} = <J|H|I> = f(\alpha_1, \ldots, \alpha_5).$$

Such a matrix consists of analytic functions of parameters $\alpha_1 \ldots \alpha_5$. These functions are expressed merely through sums, differences, multiplications, divisions, and square roots, but may be quite lengthy. After constructing the Hamiltonian matrix we simultaneously have to diagonalize it and minimize the obtained lowest eigenvalue with respect to the $\alpha_1 \ldots \alpha_5$ parameters. The complexity of the matrix plays crucial role in simplifying this process. For the states generated as combinations of operators for 2 electrons, the elements which may be nonzero for some values of parameters are shown in Fig. 3.6. One may see that the matrix is not very complicated but it turns out that it may be further simplified by regarding the symmetries of the system. This feature will be even more important for larger systems.

How may we classify the states to obtain a simplified Hamiltonian matrix? The Hamiltonian (2.11) commutes both with the z-component and squared spin operator, i.e.

$$[H, S_z] = [H, \mathbf{S}^2] = 0.$$

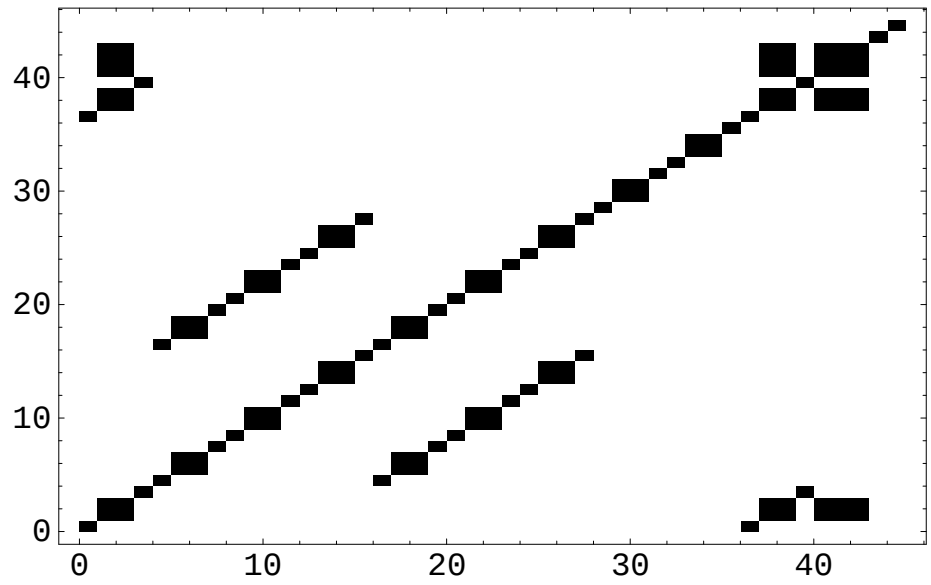

Figure 3.6. General structure of nonzero elements of the Hamiltonian matrix for the 2-electron situation with the multiparticle states generated as ordered combinations of the 10 operators casted on numbers, e.g. $a^\dagger_{1s\uparrow} \to 1$ $a^\dagger_{1s\downarrow} \to 2$ ... $a^\dagger_{2p-1\downarrow} \to 10$. The larger size boxes correspond to 2×2 blocks and the smaller are individual elements. There are also four 2×3 boxes and one 3×3 box. Note that the largest block effectively has the size 7×7.

So any selected values of these operators stay invariant under the action of the Hamiltonian, i.e. the diagonalization does not mix states with different values of these observables. In the graphical representation of the matrix, the Hamiltonian matrix constructed on such states is block diagonal. Hence, it is easier to diagonalize. Firstly one notices that two electrons may be located either on the same orbital or on two different orbitals. In the first case, due to the Pauli principle the electrons have to have opposite spins. In this case, we know that their total spin is equal to zero. There are five such states, one for each basis orbital. In the case of two electrons located on different orbitals each of them may have an arbitrary value of spin z component. Two electrons can build together a state with total spin either $S = 0$ or $S = 1$. In the latter case, the z-component takes values $-1, 0$ and 1. The class diagram of the ordered multiparticle states is displayed in Fig. 3.7. There is another question as to how to find the states, which fit in this scheme, automatically. The mono-orbital states can be simply labelled, but the bi-orbital states have to determined. The connections between the two orbital states are shown in Fig. 3.8. Each pair of orbitals has such structure.

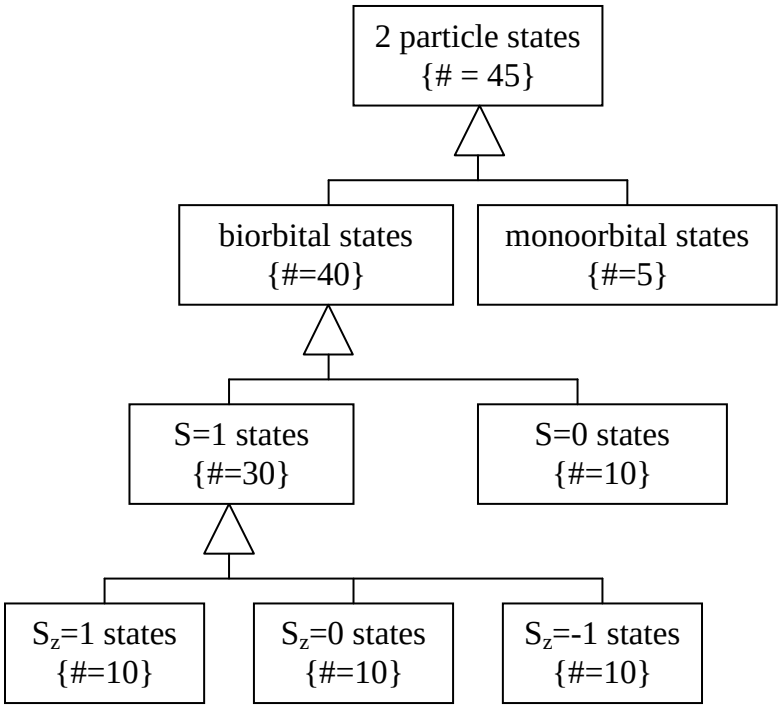

Figure 3.7. Classes of the ordered multiparticle states. The number of states composing each class is displayed.

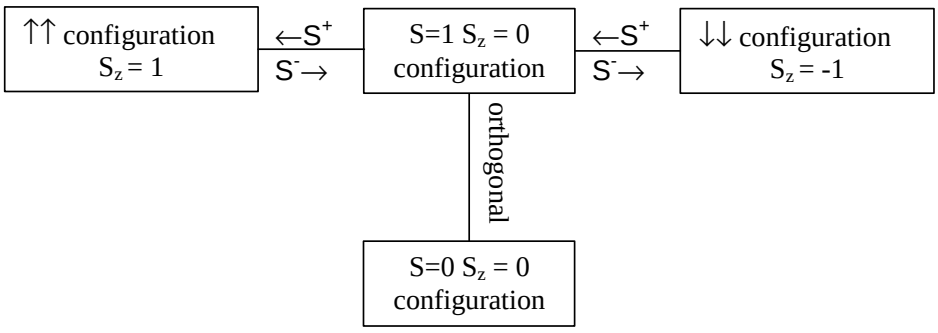

Figure 3.8. Connections between different multiparticle states with two different orbitals. Each orbital pair has a similar structure.

There are 10 nonequivalent pairs for 5 orbitals, since all other pairs differ only by a phase. So we see, that there are 10 possible states in each class, giving the total of 40 bi-orbital states. Which, after the addition of mono-orbital states, reproduce the total number of 45 multiparticle configurations, calculated in (3.28). The procedure of navigating along the possible connections in Graph 3.8 is equivalent to finding the Clebsh-Gordan coefficients [1, 29] when adding two angular momenta. The $S^{\pm}$ operators are of the form

$$S^{+} = \sum_{i=1}^{M} a_{i\uparrow}^{\dagger} a_{i\downarrow}$$

$$S^{-} = \sum_{i=1}^{M} a_{i\downarrow}^{\dagger} a_{i\uparrow}. \tag{3.31}$$

The initial state can be chosen as a state with either two spins up or two spins down. The second and third state is obtained from it by applying the $S^{\pm}$ operators. The fourth state, completing the subspace, is obtained using the orthogonality condition. In our case, it merely corresponds to change of sign between two terms building the $S = 1$, $S_z = 0$ state, providing thus $S = 0$, $S_z = 0$ state. The change to the states found in this way simplifies the Hamiltonian matrix in a substantial manner, as shown in Fig. 3.9. The size of the largest block is 5×5. It is spanned on the states

$$\begin{aligned} |A> &= \frac{1}{\sqrt{2}}(a_{4\uparrow}^{\dagger} a_{5\downarrow}^{\dagger} + a_{5\uparrow}^{\dagger} a_{4\downarrow}^{\dagger})|0> \\ |B> &= \frac{1}{\sqrt{2}}(a_{1\uparrow}^{\dagger} a_{2\downarrow}^{\dagger} + a_{2\uparrow}^{\dagger} a_{1\downarrow}^{\dagger})|0> \\ |C> &= a_{1\uparrow}^{\dagger} a_{1\downarrow}^{\dagger}|0> \\ |D> &= a_{2\uparrow}^{\dagger} a_{2\downarrow}^{\dagger}|0> \\ |E> &= a_{3\uparrow}^{\dagger} a_{3\downarrow}^{\dagger}|0> . \end{aligned} \tag{3.32}$$

The states of the set $\{|A>, |B>, |C>, |D>, |E>\}$ involve in its construction all five orbitals. As turns out in the following calculations it cannot be reduced further based solely on the symmetry considerations. The size of the largest block allows for an analytic solution for the eigenenergies, as there exist analytic formulas for the roots of polynomials up to the fifth order.

The basis in the Fock space for a two-electron system can be used as a starting point for simplifying the Hamiltonian matrix for the three electron system, size of which is 120×120. If we generate the basis in the Fock space iterating the states (3.29) in the range (3.30) we obtain very simple states

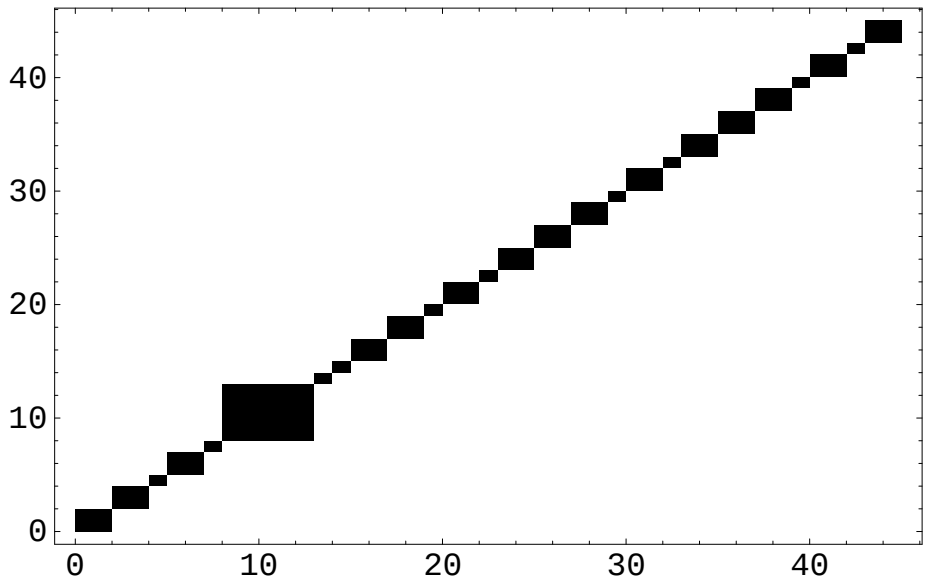

Figure 3.9. The nonzero elements of the Hamiltonian matrix for the 2 electrons case with states generated in a way explained in the main text, which simplifies the Hamiltonian matrix to the block irreducible form. The largest block is 5×5, the remaining are 2×2 and 1×1.

but the Hamiltonian matrix will not be very diagonal. The nonzero elements of the Hamiltonian matrix for three electrons are exhibited in Fig. 3.10. To obtain the basis of multiparticle states in the Fock space, we expand the existing basis for two electrons by adding the third. There are three major situations:

i) We start with the five mono-orbital states. We add to them a third electron. Due to the Pauli principle, it cannot be located on the same orbital as the initial two. So there are four orbitals left to place the new electron, which spin can have any value. So, we get $4 * 2 = 8$ new three particle states from a single one mono-orbital two-particle state. These procedure is done with all orbitals in this class so that we finally obtain $5 * 4 * 2 = 40$ states. An important fact to note is that we have already got *all states* with two electrons on the same orbital. Adding a second electron on some orbital in a bi-orbital state can only lead to one of the states obtained from a mono-orbital state. So, all multiparticle states discussed subsequently have to consist of electrons on three different orbitals. Since the mono-orbital states always have $S = S_z = 0$, the resultant 3 particle state belongs to the subspace $S = 1/2$ and $S_z = \pm 1/2$;

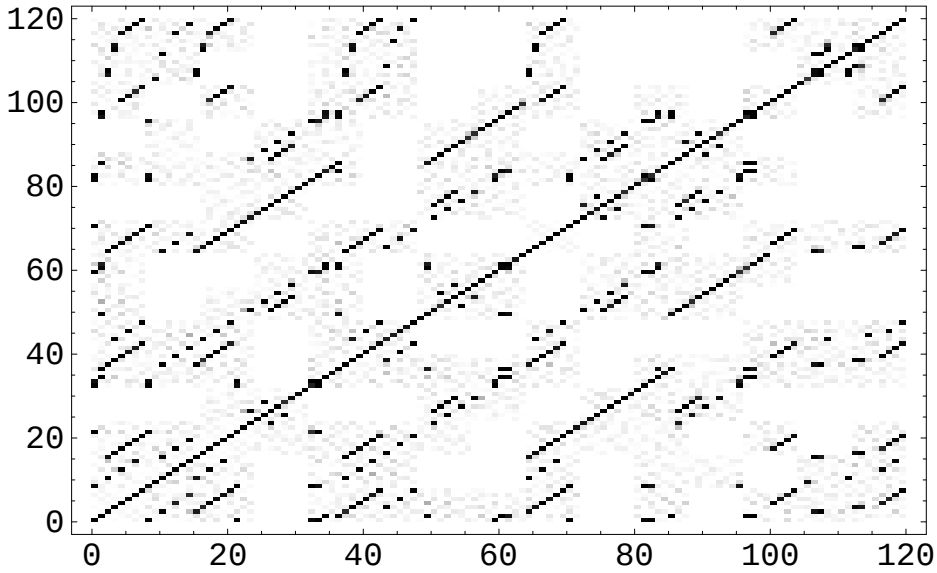

Figure 3.10. The nonzero elements of the Hamiltonian matrix for 3-electrons situation, with states generated as ordered combinations of the 10 operators casted on numbers, e.g. $a^{\dagger}_{1s\uparrow} \rightarrow 1\ a^{\dagger}_{1s\downarrow} \rightarrow 2\ \ldots\ a^{\dagger}_{2p-1\downarrow} \rightarrow 10$

ii) We add an electron to the existing $S = 1$ state. It has to be located on a third orbital, because states constructed out of two kinds of orbitals have already been depleted in the previous case. According to Fig. 3.8 there are three classes of states with $S = 1$ for two electrons. The new electron can be in two states, i.e. it can either have spin up or spin down. One has also to note that there are $\binom{5}{3} = 10$ nonequivalent choices of three orbitals out of five. So, in this way, we get $3{*}2{*}10 = 60$ states. We get the total spin either $S = 3/2$ or $S = 1/2$. In the former case we have a quartet with possible projections on z-axis: $-3/2, -1/2, 1/2, 3/2$. In the latter case, we have only the two middle values. In each of these three particle subclasses there are 10 multiparticle states;

iii) Finally, we can add third electron to the $S = 0$ two electron state. We can count the states analogously, as above. We have only one class of bi-orbital two-particle states with $S = 0$. So, because of the two possible states of electron we get $1 * 2 * 10 = 20$ three-particle states.

We can sum up the state count obtained in the three situations and obtain the total number of 120 multiparticle states, which agrees with the number obtained from iteration (3.30). The nonzero elements of the Hamiltonian matrix, calculated from the states generated in the above described way, are

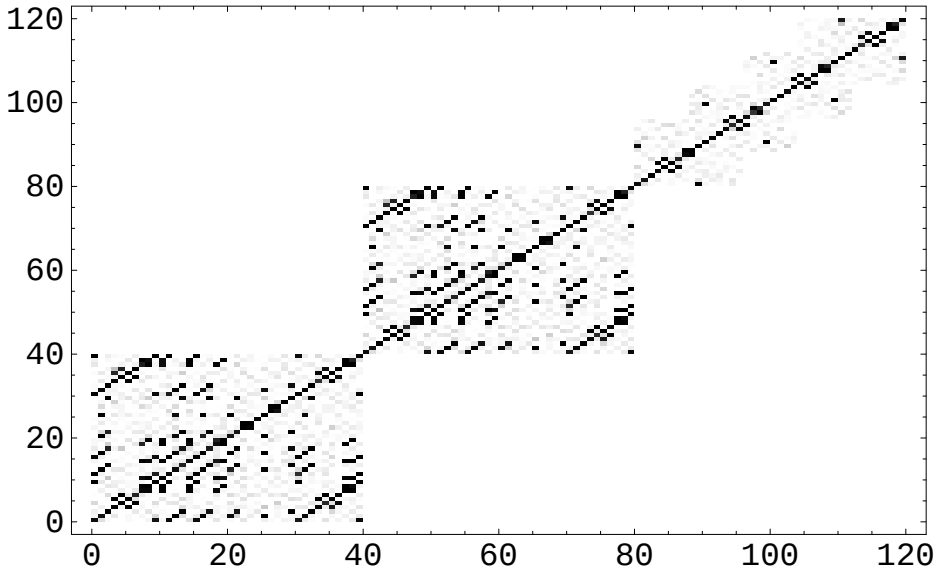

Figure 3.11. Nonzero elements of the Hamiltonian matrix for the 3 electrons in the block representation, with the multiparticle states generated in the way originating from the 2-particle-basis generated earlier. The largest effective block is 8×8.

depicted in Fig. 3.11. Blocks corresponding to different values of S and S_z can be seen. The states are not sorted but even inside the blocks they are decoupled into subblocks. The largest block of mutually dependent states has the size 8×8. Hence the eigenvalues can be looked up independently in different blocks. It does not allow for an analytic solution, but the matrix of such size can be easily and very rapidly diagonalized numerically, without resorting to any of the advanced methods. This is essential, as the optimization of a function depending on many parameters $\alpha_1, \ldots, \alpha_5$ requires repeated calculation of the function's values, each involving full diagonalization. The further decoupling of subblocks within the block with given values of spin is a manifestation of orthogonality of different orbitals. It was not assumed in advance, but the procedure of ordering the multiparticle states also separates, to some extent, the spaces with given values of the total angular momentum. An alternative and fully formal method of generating the multiparticle basis would consist of simultaneous generating a series of states with fixed values of S, S_z, L, L_z, using the ladder operators $S^{\pm}$ and $L^{\pm}$. But it turns to be not necessary, as the simpler method introduced by us here provides also satisfying results.

Table 3.1. Optimized Bohr-orbit radii $a_i = \alpha_i^{-1}$ of 1s, 2s, and 2p orbits (in units of a_0), the overlap S between renormalized 1s and 2s states, and the ground state energy for the lightest atoms and ions (with five Slater orbitals taken into account). For comparison, the experimental values of energy taken from [30], are displayed. The reference energy for H^- ion is taken from [34, 36]

	a_{1s}	a_{2s}	a_{2p}	S	E_G (Ry)	E_G^{exp} (Ry)
H	1	2	2	0	-1	-0.999466555
H^-	0.9696	1.6485	1.017	-0.1	-1.0487	-1.0556
He	0.4274	0.5731	0.4068	-0.272	-5.79404	-5.804791
He^-	1.831	1.1416	0.4354	-0.781	-5.10058	
Li	0.3725	1.066	0.2521	0.15	-14.8334	-14.95803
Be^+	0.2708	0.683	0.1829	0.109	-28.5286	-28.65154651

3.4 Results for He, H^-, Li, Be^+, and He^-

By diagonalizing the corresponding Hamiltonian matrices and subsequently, minimizing the lowest eigenvalue with respect to the parameters α_i - the radial extension of wave functions, we obtain the results presented in Table 3.1. There is only one parameter value a_{2p} for all 2p states as the values a_{2pm} are all equal within the numerical accuracy $\sim 10^{-6}$. This fact reflects the spherical symmetry of our potential. For example, the ground state energy of He is $E_G = -5.794$ Ry, which is close to the accepted experimental value [30] -5.8074, given the simplicity of our approach. Further improvement is feasible by either enriching the basis by including the $n = 3$ states or by resorting to a large Gaussian basis, with many parameters, which allows for very accurate variational estimates[31, 32, 33].

For the H^- ion we also obtain correct results. They agree with other calculations of the ground-state energy [34, 35, 36]. We get correctly the single bound state [37] for this system.

We can represent the ground state multi-particle wave function in the Fock space in the form (2.20) as follows: for He atom

$$\begin{aligned}|\Psi_0^{He}> = (&-0.799211 a^+_{1s\downarrow}a^+_{1s\uparrow} + 0.411751 a^+_{1s\downarrow}a^+_{2s\uparrow} - 0.411751 a^+_{1s\uparrow}a^+_{1s\downarrow} \\ &-0.135451 a^+_{2s\downarrow}a^+_{2s\uparrow} + 0.0357708 a^+_{2p0\downarrow}a^+_{2p0\uparrow} + 0.0357641 a^+_{2p1\downarrow}a^+_{2p-1\uparrow} \\ &-0.0357641 a^+_{2p1\uparrow}a^+_{2p-1\downarrow})|0>,\end{aligned} \tag{3.33}$$

and the one of the two spin $S = \frac{1}{2}$ degenerate Li ground states, e.g. with $S^z = +1/2$

$$|\Psi_0^{Li}> = (0.99749 a^+_{1s\downarrow} a^+_{1s\uparrow} a^+_{2s\uparrow} - 0.057024 a^+_{1s\uparrow} a^+_{2s\downarrow} a^+_{2s\uparrow} + 0.003959 a^+_{1s\uparrow} a^+_{2p0\downarrow} a^+_{2p0\uparrow} + 0.003959 a^+_{1s\uparrow} a^+_{2p1\downarrow} a^+_{2p-1\uparrow} - 0.003959 a^+_{1s\uparrow} a^+_{2p1\uparrow} a^+_{2p-1\downarrow} - 0.023783 a^+_{2s\uparrow} a^+_{2p0\downarrow} a^+_{2p0\uparrow} - 0.023781 a^+_{2s\uparrow} a^+_{2p1\downarrow} a^+_{2p-1\uparrow} + 0.023781 a^+_{2s\uparrow} a^+_{2p1\uparrow} a^+_{2p-1\downarrow})|0> . \tag{3.34}$$

The above expressions use the orthogonalized basis for the creation operators, which provides us standard anticommutation relations for a and $a^\dagger$ operators Note that we have a substantial admixture of the excited-singlet state (1s↑2s↓ and 1s↓2s↑) to the simple hydrogenic-like configuration of He (1s↓1s↑). One could also transform these two expressions to the representation with the electron creation operators $\tilde{a}^\dagger$ in initial atomic states,i.e.

$$|\Psi_0^{He}> = (-0.82274 \tilde{a}^\dagger_{1s\downarrow} \tilde{a}^\dagger_{1s\uparrow} + 0.309636 \tilde{a}^\dagger_{1s\downarrow} \tilde{a}^\dagger_{2s\uparrow} - 0.404512 \tilde{a}^\dagger_{1s\uparrow} \tilde{a}^\dagger_{2s\downarrow} - 0.021729 \tilde{a}^\dagger_{2s\downarrow} \tilde{a}^\dagger_{2s\uparrow} + 0.0357708 \tilde{a}^\dagger_{2p0\downarrow} \tilde{a}^\dagger_{2p0\uparrow} + 0.0357641 \tilde{a}^\dagger_{2p1\downarrow} \tilde{a}^\dagger_{2p-1\uparrow} - 0.0357641 \tilde{a}^\dagger_{2p1\uparrow} \tilde{a}^\dagger_{2p-1\downarrow})|0>, \tag{3.35}$$

and for the Li atom

$$|\Psi_0^{Li}> = (1.01321 \tilde{a}^\dagger_{1s\downarrow} \tilde{a}^\dagger_{1s\uparrow} \tilde{a}^\dagger_{2s\uparrow} + 0.018639 \tilde{a}^\dagger_{1s\uparrow} \tilde{a}^\dagger_{2s\downarrow} \tilde{a}^\dagger_{2s\uparrow} + 0.005804 \tilde{a}^\dagger_{1s\uparrow} \tilde{a}^\dagger_{2p0\downarrow} \tilde{a}^\dagger_{2p0\uparrow} + 0.005804 \tilde{a}^\dagger_{1s\uparrow} \tilde{a}^\dagger_{2p1\downarrow} \tilde{a}^\dagger_{2p-1\uparrow} - 0.0058034 \tilde{a}^\dagger_{1s\uparrow} \tilde{a}^\dagger_{2p1\uparrow} \tilde{a}^\dagger_{2p-1\downarrow} - 0.024289 \tilde{a}^\dagger_{2s\uparrow} \tilde{a}^\dagger_{2p0\downarrow} \tilde{a}^\dagger_{2p0\uparrow} - 0.024286 \tilde{a}^\dagger_{2s\uparrow} \tilde{a}^\dagger_{2p1\downarrow} \tilde{a}^\dagger_{2p-1\uparrow} + 0.024286 \tilde{a}^\dagger_{2s\uparrow} \tilde{a}^\dagger_{2p1\uparrow} \tilde{a}^\dagger_{2p-1\downarrow})|0> . \tag{3.36}$$

The complete set of energies and multiparticle states for the He atom is displayed in Appendix E. One may notice that the coefficients in front of the $\tilde{a}$ operators do not even square sum to the proper probability normalization, which should be 1. This is not a mistake and is caused by the nonorthogonality of the basis discussed in Section 3.1. We see that the probability of encountering the configuration $1s^2$ in He is less than 2/3, whereas the corresponding configuration $1s^2 2s$ for Li almost coincides with that for the hydrogenic-like picture. The reason for the difference is due to the circumstance that the overlap integral $S =< 1s|2s >$ between $1s$ and $2s$ states in the former case is large and the virtual transitions $1s \rightleftharpoons 2s$ do not involve a substantial change in the Coulomb energy. Those wave functions can be used to evaluate any ground-state characteristic by calculating $< \Psi_G|\hat{O}|\Psi_G >$ for $\hat{O}$ represented in the 2nd quantized form. For example, the dipole moment

operator is $\hat{\mathbf{d}} = e\int d^3r\hat{\Psi}^\dagger(\mathbf{r})\mathbf{x}\hat{\Psi}(\mathbf{r})$, etc. In this manner, a nonrelativistic quantum field theory of atomic states can be formulated

Another feature of our approach is connected with the determination of the microscopic parameters V_{ijkl} in our Hamiltonian, since their knowledge is crucial for the atomic-cluster calculations, as well as for the determination of physical properties of extended systems as a function of the lattice parameter. Namely, we can rewrite Hamiltonian (2.11) for the case of single atom in a longer form, but with parameters, that is easier to interpret and that appears often in various models, namely

$$H = \sum_{i\sigma}\epsilon_i n_{i\sigma} + t\sum_{\sigma}\left(a^\dagger_{2\sigma}a_{1\sigma} + a^\dagger_{1\sigma}a_{2\sigma}\right) + \sum_{i=1}^{5}U_i n_{i\uparrow}n_{i\downarrow} + \frac{1}{2}\sum_{i\neq j}K_{ij}n_i n_j$$

$$-\frac{1}{2}\sum_{i\neq j}J_{ij}\left(\mathbf{S_i}\cdot\mathbf{S_j} - \frac{1}{2}n_i n_j\right) + \sum_{i\neq j}J_{ij}a^\dagger_{i\uparrow}a^\dagger_{i\downarrow}a_{j\downarrow}a_{j\uparrow} + \sum_{i\neq j\sigma}V_{ij}n_{i\bar{\sigma}}a^\dagger_{i\sigma}a_{j\sigma}. \quad (3.37)$$

t is the hopping integral between 1s and 2s states, U_i are the intraorbital Coulomb interactions, K_{ij} are their interorbital correspondants, V_{ij} is the so-called correlated-hopping integral, and J_{ij} is the direct exchange integral, for states i and $j = 1,\ldots,5$. The principal parameters defined above for the atoms and selected ions are provided in Table 3.2. From this formulation, the following interpretation can be drawn. The calculated energy difference ΔE for He between the ground state singlet and the first excited triplet is $-2.3707 - (-5.794) \simeq 3.423Ry$ (the singlet $1s\uparrow 2s\downarrow$ is still 1 Ry higher). The corresponding energy of the repulsive Coulomb interaction for electrons in the $1s^2$ configuration is $U_1 = 3.278$, the value comparable to ΔE. Additionally, the repulsive interorbital Coulomb interaction in $1s\uparrow 2s\downarrow$ state is $K_{12} \approx 1.5Ry$, a substantially lower value. The relative energetics tells us why we have a substantial admixture of the excited $1s\uparrow 2s\downarrow$ state to the singlet $1s^2$. In other words, a substantial Coulomb interaction ruins hydrogenic-like scheme, although the actual values could be still more realistic by enriching further the trial basis with $n = 3$ states.

If we compare the energies of the excited states obtained in this calculation with the experimental results [30] one can cleanly see vast discrepancies. The observed excited-energy levels are not very well reproduced. Merely their qualitative properties are similar. The reason for such a behavior is the optimization of the basis with respect to the ground state energy *only*. The orbitals take a shape most convenient with respect to this quantity. So, for the excited multiparticle states the decomposition into single-electron orbitals may be not correct any longer. The experimental spectra, on which the level determination is based, are obtained by the absorbtion or the emission of photons. The state of electron when this process is taking place, is

Table 3.2. Microscopic parameters (in Ry) of the selected atoms and ions. All quantities are calculated for the orthogonalized atomic states. t is the 1s-2s hopping magnitude, U_i is the intraorbital Coulomb interaction (i=1s(1), 2s(2), 2p m=0(3), and 2p m=±1(p)), whereas K_{ij} and J_{ij} are the interorbital Coulomb and exchange interaction parameters, respectively.

	t	U_1	U_2	U_3	U_p	K_{12}	K_{13}	K_{23}	J_{12}	J_{13}
H^-	0.057	1.333	0.369	0.77	0.728	0.519	0.878	0.457	0.061	0.138
He	1.186	3.278	1.086	1.924	1.821	1.527	2.192	1.289	0.212	0.348
He^-	-1.1414	1.232	0.764	1.798	1.701	0.929	1.421	1.041	0.269	0.28
Li	-0.654	3.267	0.533	3.105	2.938	0.749	3.021	0.743	0.06	0.606
Be^+	-0.929	4.509	0.869	4.279	4.049	1.191	4.168	1.175	0.105	0.837

definitely not stationary, so the information about the ground state wave function, such like the optimal parameters α_i, may get lost in this process. The only assumption we can make about the excited multiparticle states is their orthogonality to the ground state. The orthogonality in the Fock space is of course assured by the process of diagonalization. But, in general case, the single particle orbitals do not have to be of the same shape for the excited states. We keep their shape and this is an *additional assumption* about these states. To improve the accuracy, one would have to perform an additional optimization of the energy in the subspaces with all states, with lower energy than the state actually determined, excluded. The orthogonality condition would lead to a number of subsequent constraints on the α optimization parameters, making thus in most cases, the procedure unavailable from the practical point of view. Sometimes this is nonetheless possible, as will be shown in Section 5.1, but it is not the case for the model and the basis selected here.

How does the size of the single particle basis affect the results? For the sake of comparison, the same calculations were also performed using a simpler basis. The case of the simplest possible basis consisting only of $1s$ states is already contained in Section 2.3.2 giving for He atom: $\alpha = 27/(16a_0)$ and $E_G = -5.695Ry$, where $a_0 \simeq 0.53$Å. The next richer basis consists of the $1s$ and $2s$ states. It allows for an estimation of the influence of the size of the single particle basis on the accuracy of the calculations. This reduced basis calculations make also a visualization of the ground state energy as a function of the optimization parameters α_i possible, as we only have two such parameters. The ground state energy in this case is shown in Fig. 3.12 for the He atom and in Fig. 3.13 for the H^- ion. One can see from these pictures, that the ground state energy depends strongly on the optimization

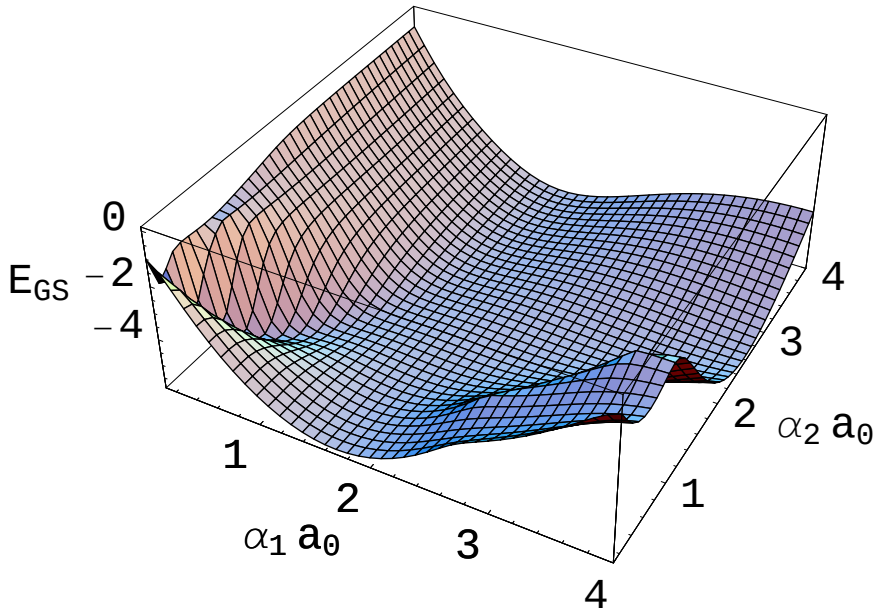

Figure 3.12. The ground state energy of the He atom as a function of inverse atomic orbital size α_1 for 1s and α_2 for 2s, respectively. One can clearly see that the optimization of this parameters does matter for the energy.

parameters. We have global minima in both situations. Another thing to note is the similarity of the two plots. If one takes into account the rescaling of the axes, caused by the change of the nuclear charge by the factor of two between hydrogen ion and the helium atom, one can observe that the general shape of valleys in both plots is similar. This expresses the affinity of the systems.

The number of multiparticle states for two orbitals is $\binom{4}{2} = 6$, which split up into three spin- singlets and one triplet. The maximal number of electrons, which can be accommodated by this smaller basis is 4. But the case with more than half filling can be mapped onto the case with less than half filled system, so the calculations are shown only for up to 2 electrons, i.e. the H, He atoms and the H^- ion. The results of this calculations are shown in Table 3.3. We see the obvious fact that the basis enlargement improves the accuracy. For He atom the relative error to the "exact" value is 1.89% for one orbital, .86% for two orbitals and .19% for five orbitals in the basis set. We also know that for an infinite basis we would reach the exact value, which differs from the experimental because we also made some approximations on the Hamiltonian, i.e. it is non relativistic. It is clearly seen for the

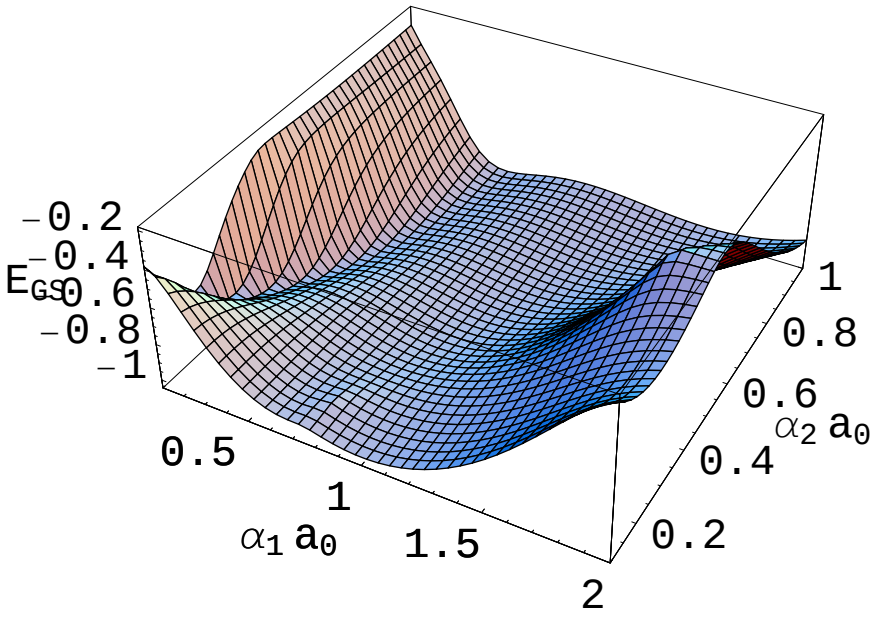

Figure 3.13. Same as Fig. 3.12 for H^- ion.

case of hydrogen in Table 3.1 where the ground state energy is not exactly equal to unity. For weaker bound systems like H^-, the improvement due to basis enrichment is relatively larger. Also, the size of the various basis orbitals change, but in this case it cannot be compared to the experiment. The orbital size of the 2p states may be a little bit uncommon, but these states contribute a relatively small amount to the ground state, so the probability of encountering electrons, for the systems considered, on these orbitals, is almost negligible.

One can also look at the role of optimization on the accuracy of the approach. In Table 3.4 we compare the ground state energy and the microscopic parameters for the He atom and H^- ion for the situation with and without optimization of the parameters α_i. Only 1s and 2s orbitals were taken into account. On the example of helium can be seen that the ground energy value for *one* optimized orbital basis set is lower than that for *two* not optimized orbitals basis. The microscopic parameters are of the same order, and the changes are more essential for two-particle interaction parameters. It is because we have four wave functions in the corresponding integrals, so the difference in α_i parameters is counted twice. This Table shows the importance of the optimization procedure for establishing the electronic structure.

Table 3.3. Optimized Bohr-orbit radii $a_i = \alpha_i^{-1}$ of 1s and 2s Slater orbitals, in units of a_0, the ground state energy for the lightest atoms and ions with only two orbitals. The energy and the parameter difference when compared with five-orbital situation (see Table 3.1) is also shown.

	a_{1s}	a_{2s}	E_G (Ry)	$\Delta a_{1s}[10^{-3}]$	$\Delta a_{2s}[10^{-3}]$	$\Delta E_G(Ry)$
H	1	2	-1	0	0	0
H^-	0.9805	1.7699	-1.0245	10.79	121.42	0.02424
He	0.4287	0.5788	-5.7549	1.3184	5.62	0.03911

Table 3.4. Microscopic parameters (in Ry) of the selected atoms and ions. All quantities are calculated for the orthogonalized atomic states. The basis consists of 1s and 2s states only. t is the 1s-2s hopping magnitude, ϵ_i is the atomic energy, U_i is the intraorbital Coulomb interaction, whereas K and J are the interorbital Coulomb and exchange interaction parameters. The lower part of the Table shows the values displayed above and calculated without the optimization of parameters α_i. The hydrogenic-like values $\alpha_1 = 2$ and $\alpha_2 = 1$ were taken then. The last column shows the ground state energies.

	t	ϵ_1	ϵ_2	U_1	U_2	K	J	E_G
H^-	0.0336	-0.9983	-0.243	1.3	0.3422	0.48	0.0539	-1.02446
He	1.149	-3.6466	-0.0987	3.2589	1.0744	1.5109	0.209	-5.75493
H^-_{noopt}	0	-1	-0.25	1.25	0.3	0.4198	0.0439	-1.02174
He_{noopt}	0	-4	-1	2.5	0.6016	0.8396	0.0878	-5.662

Chapter 4

Simple molecules and molecular ions

The next, more complicated, system is a biatomic molecule or a molecular ion [41]. The simplest in this category are the hydrogen molecule H_2 and ion H_2^-, where respectively two or three electrons are shared by two nuclei. Such system introduces an additional external parameter, the distance between the nuclei. In addition to the ground state energy, also this parameter can be compared with experiment. It exposes the major advantage of the EDABI method namely, the introduction of real world parameters into the model calculations.

As in the case of atoms, we have to choose again the initial class of wave functions to define our Fock space. Following an argument similar to the atomic case in Section 3.1 we choose the orthogonalized atomic functions [1] centered on two sites.

The model of the H_2 and H_2^- molecules system is depicted schematically in Fig. 4.1. The real space parameters: the bond length R and the atomic orbital size $1/\alpha$ are shown. In the center of each of the atoms, there is a nucleus with charge $Z = 1$. Because we have two centers, we may locate the atomic orbitals on both of them. In the simplest case we may restrict ourselves to the 1s orbitals only. In this way we get space for up to four electrons. The location of more then a single 1s orbital on each nucleus is possible, but it increases essentially analytical difficulties in the microscopic-parameter calculations. The parameter α controlling the size of the orbitals has been set equal on both of them.

The 1s atomic orbitals located on each of the two centers of distance R apart are not orthogonal. Let us set the origin of the coordinate system on

[1] They are identical to the functions used in Chapter 3 defined by Eq. (3.8)

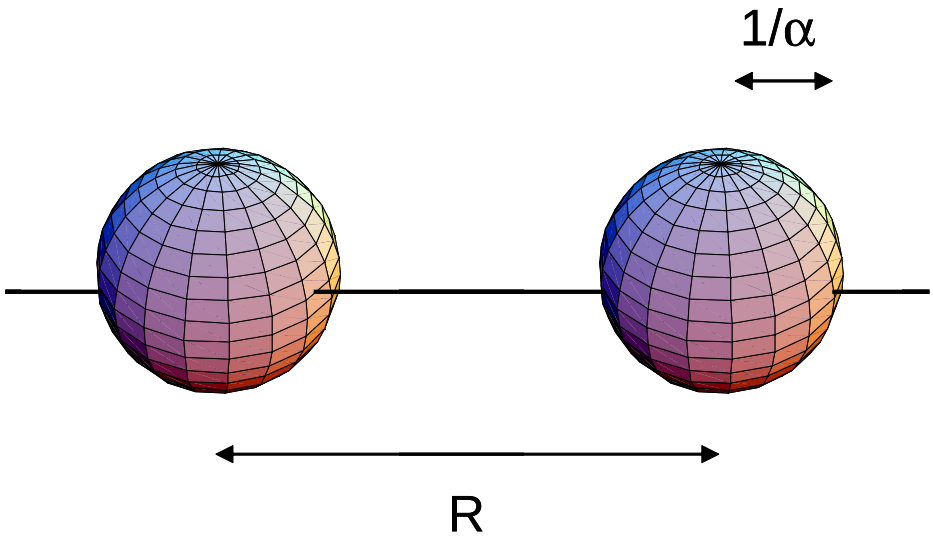

Figure 4.1. Model of the H_2 and H_2^- molecules with real space parameters: the bond length R and the orbital size $1/\alpha$. The orbital size is just guide for the eye, as the atomic function does not really have a sharp border.

the line connecting both nuclei, half way between them. The atomic wave functions are of the following form

$$\phi_1(\mathbf{r};\alpha) = \sqrt{\frac{\alpha^3}{\pi}}\exp(-\alpha|\mathbf{r}-\mathbf{R}/2|) \quad \phi_2(\mathbf{r};\alpha) = \sqrt{\frac{\alpha^3}{\pi}}\exp(-\alpha|\mathbf{r}+\mathbf{R}/2|), \quad (4.1)$$

where $\mathbf{R}$ is a vector of length R along the axis of the molecule. They have to be orthogonalized by mixing the wave functions located according to the procedure already described in Section 3.1. We will calculate the microscopic parameters in atomic functions and then transform them to the orthogonalized Wannier basis. The mixing coefficients expressed in Eqs. (3.13) and (3.14) depend on the overlap integral S. The shape of atomic and Wannier functions is shown in Fig. 4.2. One can notice that the orthogonalized Wannier functions have a node, hence they cannot be the ground state functions for the single atom case. This is because the overlap is removed by changing the sign of one function in the area, where the second is located.

4.1 Parameters

The parameters needed to formulate the Hamiltonian in this case have to be calculated [42]. They can be divided in two classes: the one- and the two-

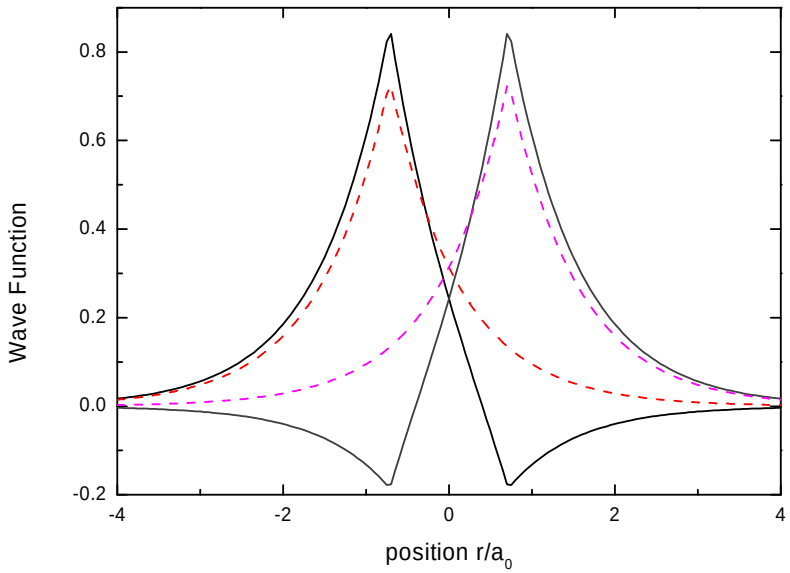

Figure 4.2. The wave function along the molecule axis. The orthogonalized Wannier functions(solid line) and the original atomic 1s wave functions (dashed line) are shown for comparison.

electron microscopic parameters. Unlike it was in the case of atoms, the resultant expressions for parameters depend not only on α but also on the interatomic distance R.

The single electron parameters have to represent the introduction of two atomic sites into our model. The form of the single-electron part of Hamiltonian in the Schrödinger representation has to be extended. Namely, we have to add to the Eq. (3.16) a term representing the influence of the second nucleus

$$H_1(\mathbf{r}) = -\nabla^2 - \frac{2Z}{|\mathbf{r}-\mathbf{r}_1|} - \frac{2Z}{|\mathbf{r}-\mathbf{r}_2|}, \tag{4.2}$$

where $\mathbf{r}_1 = \mathbf{R}/2$ and $\mathbf{r}_2 = -\mathbf{R}/2$ are the displacements of respectively the first and the second nuclei from the origin. Because we have two orbitals, there are two kinds of microscopic single particle parameters defined by Eq. (2.12). The basis functions are centered on two different atoms. Both centers are equivalent, hence there is only one α. That is why it is enough to calculate two single electron parameters instead of four.

The atomic energy $\varepsilon' \equiv t'_{11} = t'_{22}$ represents the energy of an electron

located on a center. It differs from that calculated for an atom by the contribution of the second nucleus

$$\varepsilon' = (\alpha - 2Z)\alpha + \underbrace{\int d^3\mathbf{r}\phi_1(\mathbf{r};\alpha)^\star \frac{-2Z}{|\mathbf{r}-\mathbf{R}/2|}\phi_1(\mathbf{r};\alpha)}_{2^{nd}\ nucleus\ contribution}. \tag{4.3}$$

The calculation of this additional contribution has to be done in spheroidal coordinates [43, 44][2]. When expressed in these, coordinates it can be directly evaluated and is of the form

$$-2Z\int_0^{2\pi} d\phi \int_1^\infty d\lambda \int_{-1}^1 d\mu \frac{\alpha^3}{\pi} e^{-\alpha R(\lambda+\mu)} \frac{2}{\lambda-\mu}\frac{R^3}{8}(\lambda^2-\mu^2) = \\ = Z\alpha\left(e^{-2\alpha R}\left(2+\frac{2}{\alpha R}\right) - \frac{2}{\alpha R}\right), \tag{4.4}$$

providing also the complete expression for atomic energy in the molecular system, which is

$$\varepsilon' = \alpha^2 + 2Z\alpha\left(e^{-2\alpha R}\left(1+\frac{1}{\alpha R}\right) - \frac{1}{\alpha R} + 1\right). \tag{4.5}$$

If the basis functions of the microscopic parameter being evaluated are located on two different centers, the parameter is the so called "hopping", $t' \equiv t'_{12} = t'_{21}$. Its value represents the change in energy of an electron moving between the nuclei, i.e. the kinetic energy of the electron. This case is completely different from that of the single atom, and we cannot reuse the former expressions for the parameters here. The easiest way to calculate them is to employ again the prolate spheroidal coordinates. The second and the third term in Eq. (4.2), lead the terms of the form

$$\int d^3\mathbf{r}\phi_1(\mathbf{r};\alpha)^\star \frac{-2Z}{|\mathbf{r}\pm\mathbf{R}/2|}\phi_2(\mathbf{r};\alpha), \tag{4.6}$$

which are equivalent. They can be directly evaluated, since

$$-2Z\int_0^{2\pi} d\phi \int_1^\infty d\lambda \int_{-1}^1 d\mu \frac{\alpha^3}{\pi} e^{-\alpha R\lambda} \frac{2}{\lambda\pm\mu}\frac{R^3}{8}(\lambda^2-\mu^2) = \\ = -2Z\alpha e^{-2\alpha R}(1+\alpha R). \tag{4.7}$$

The first term in Eq. (4.2) requires the calculation of the expectation value of the Laplacian and can also be directly evaluated, namely

$$\int d^3\mathbf{r}\phi_1(\mathbf{r};\alpha)(-\nabla^2)\phi_2(\mathbf{r};\alpha) = \frac{1}{3}\alpha^2 e^{-\alpha R}\left(-\alpha^2R^2 + 3\alpha R + 3\right). \tag{4.8}$$

[2] See Appendix F for details.

The final expression for the hopping integral is

$$t' = \alpha^2 \frac{1}{3} e^{-\alpha R} \left(-\alpha^2 R^2 + 3\alpha R + 3\right) - 4Z\alpha e^{-2\alpha R} \left(1 + \alpha R\right). \tag{4.9}$$

The last parameter in the group of single electron integrals is the overlap integral S required to obtain the orthogonalized Wannier functions, which is

$$S = \int d^3\mathbf{r} \phi_1(\mathbf{r};\alpha)\phi_2(\mathbf{r};\alpha) = e^{-\alpha R}\left(1 + \alpha R + \frac{1}{3}\alpha^2 R^2\right). \tag{4.10}$$

It is important to examine the asymptotic behavior of the parameters for small as well as for large values of R. For $R = 0$ our system turns into an atom with nucleus charge $2Z$. On the other hand for $R \to \infty$ electrons are located on well separated nodes. They interact much weaker and we expect to recover the atomic limit. The hopping on an infinite distance should be impossible, so we expect it to vanish then. Explicitly, the limits are

$$\begin{aligned} \lim_{R\to 0} \varepsilon' &= \alpha^2 - 4\alpha Z = \lim_{R\to 0} t' \\ \lim_{R\to \infty} \varepsilon' &= \alpha^2 - 2\alpha Z \\ \lim_{R\to \infty} t' &= 0. \end{aligned} \tag{4.11}$$

They confirm the correctness of the basis-function choice. The R dependence of the atomic microscopic parameters is shown in Fig. 4.3.

The second class of microscopic parameters are the two electron parameters. Because we have the symmetry of exchanging the integration variables and the two sites are equivalent, there are only four two electron parameters. A short classification of them is listed in Table 4.1. The usually largest of the two electron interactions is the intraatomic Coulomb interaction U'. It is the energy penalty for locating two electrons with opposite spin on the same orbital. Of course, since on both centers there is the same 1s wave function, it does not matter which functions, ϕ_1 or ϕ_2 we use in the calculation. Similarly the interatomic Coulomb interaction K' represents the interaction between two electrons located on different centers. The last two parameters do not represent a classical contribution. The third parameter V' is the so-called correlated-hopping or hybrid integral. It can be interpreted as a hopping in the presence of another electron. Here again, it does not matter from the resultant expression whether ϕ_1 appears thrice and ϕ_2 once in the integral or it is the opposite case. The last one is the direct exchange integral J'. It differs from the intersite Coulomb interaction, since each integration variable connects an orbital centered on one site with an orbital centered on neighboring site.

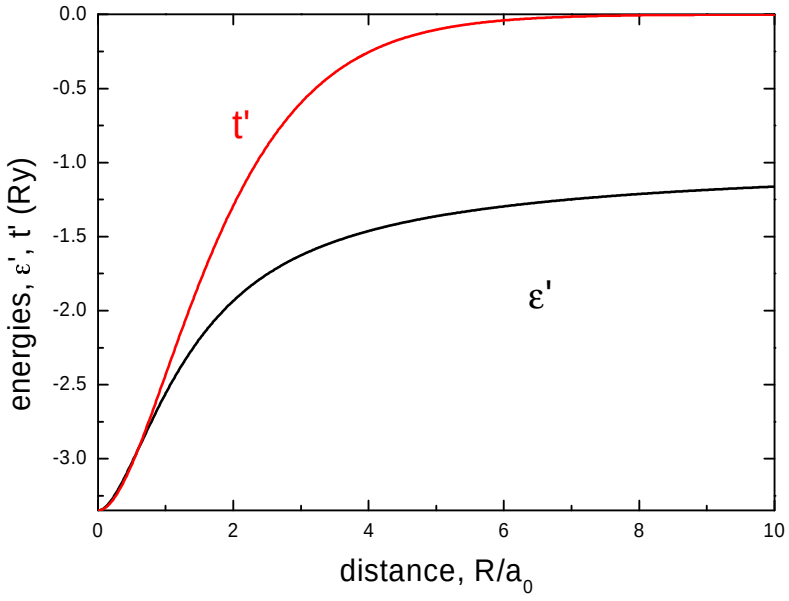

Figure 4.3. Single-electron microscopic parameters, calculated in the atomic basis, as a function of interatomic distance R. The values are in Ry.

Table 4.1. Classification of microscopic parameters for two centers with identical orbitals located on each. The definition of each parameter is done according to Eqs. (2.12) and (2.13). Only a single of the equivalent expressions is listed.

name	symbol	definition
hopping	t'	$< \phi_1 \vert H_1 \vert \phi_2 >$
atomic energy	ε'	$< \phi_1 \vert H_1 \vert \phi_2 >$
overlap	S	$< \phi_1 \vert \phi_1 >$
intraatomic Coulomb	U'	$< \phi_1\phi_1 \vert H_2 \vert \phi_1\phi_1 >$
interatomic exchange	J'	$< \phi_1\phi_1 \vert H_2 \vert \phi_2\phi_2 >$
interatomic Coulomb	K'	$< \phi_1\phi_2 \vert H_2 \vert \phi_1\phi_2 >$
correlated hopping (hybrid)	V'	$< \phi_1\phi_1 \vert H_2 \vert \phi_1\phi_2 >$

The calculation of first three parameters U', K' and V' has in common the integration over the first variable $\mathbf{r}$. Let us define

$$I(\mathbf{r}';\alpha) = \int d^3\mathbf{r}\phi_1^2(\mathbf{r};\alpha)\frac{2}{|\mathbf{r}-\mathbf{r}'|}. \tag{4.12}$$

All three parameters can be expressed with help of I in the following way

$$\begin{aligned} U' &= \int d^3\mathbf{r}' I(\mathbf{r}';\alpha)\phi_1^2(\mathbf{r}';\alpha) \\ K' &= \int d^3\mathbf{r}' I(\mathbf{r}';\alpha)\phi_2^2(\mathbf{r}';\alpha) \\ V' &= \int d^3\mathbf{r}' I(\mathbf{r}';\alpha)\phi_1(\mathbf{r}';\alpha)\phi_2(\mathbf{r}';\alpha) \end{aligned} \tag{4.13}$$

The calculation of $I(\mathbf{r}';\alpha)$ is not very complicated. We may use the inverse distance expansion in spherical coordinates (C.3). We attach the origin of the usual spherical coordinate system (r,θ,ϕ) to the first nuclei. The wave functions defined by Eq. (4.1) have a very simple angular dependence. So, the integration over the angles θ and ϕ provides zero for all terms in (C.3) except one, namely, that with $l=0$ and $m=0$. Then, in turn identity (3.25) may be used to enable the integration over r to yield

$$I(\mathbf{r}';\alpha) = \frac{2}{r'}\left(1 - e^{-2\alpha r'}(1+\alpha r')\right). \tag{4.14}$$

In what follows we must remember, that since we have used the spherical coordinates originating at the first nuclei, r' denotes the distance of point $\mathbf{r}'$ from *this* origin.

The intraorbital Coulomb parameter U' is obtained simply by inserting (4.1) and (4.14) into (4.13) and carrying on the integration using spherical coordinates. The integrals over ϕ', θ' yield immediately the factor of 4π. The integration over r' is straightforward and as the final result we have

$$U' = \frac{5\alpha}{4}. \tag{4.15}$$

It is equal to the atomic result exhibited in Appendix D, as this two-electron integral includes wave functions located on only one nucleus.

In the cases of calculating K' and V' we have to utilize spheroidal coordinates, since at least one of the wave functions appearing in the formulas, is located on center not at the origin of the spherical coordinate system used in calculation of I in Eq. (4.14). We insert the expression for I into the second and third expressions in Eq. (4.13) and transform the obtained formulas into

spheroidal coordinates. The integration over ϕ' is straightforward as it does not appear in the integrand. The resultant integrals can be cast into product of a functions of λ and of μ, and each of the resulting integrands is a polynomial multiplied by an exponential of sum or difference of λ and μ. It can be calculated by elementary methods, which yield

$$\begin{aligned} K' &= -\frac{e^{-2\alpha R}}{12R}\left(4\alpha^3R^3+18\alpha^2R^2+33\alpha R+24\right)+\frac{2}{R}, \\ V' &= \frac{1}{8R}\left(e^{-\alpha R}(16\alpha^2R^2+2\alpha R+5)-e^{-3\alpha R}(2\alpha R+5)\right). \end{aligned} \quad (4.16)$$

These expressions are different than their atomic correspondants, but we can examine their asymptotics. The large and small R limits of K' are respectively

$$\begin{aligned} \lim_{R\to\infty} K' &\stackrel{l.t.}{=} \frac{2}{R} \\ \lim_{R\to 0} K' &= \frac{5\alpha}{4}, \end{aligned} \quad (4.17)$$

where l.t. is for leading term, as the proper value of the limit is zero. The first line shows the correct classical expression for the long-range interaction, where the electrons on orbitals can be treated as point charges. The second line reproduces the result for U', as $R = 0$ means the two electrons are located on the same orbital. Analogously, the corresponding limits for the hybrid integral are

$$\begin{aligned} \lim_{R\to\infty} V' &\stackrel{l.t.}{=} \exp(-\alpha R) \\ \lim_{R\to 0} V' &= \frac{5\alpha}{4}. \end{aligned} \quad (4.18)$$

The first formula shows the exponential decay of the two-orbital overlap. The second expression reproduces the intraatomic Coulomb interaction for the same reason as for the parameter K'.

The exchange integral J' cannot be computed in the same manner. There is no use in expression for I since both integration variables, $\mathbf{r}$ and $\mathbf{r}'$, connect wave functions centered on different atoms. We need instead an intermediate expression

$$I'(\mathbf{r}';\alpha) \equiv \int d^3\mathbf{r}\phi_1(\mathbf{r};\alpha)\phi_2(\mathbf{r};\alpha)\frac{2}{|\mathbf{r}-\mathbf{r}'|}, \quad (4.19)$$

which contains two different orbital, hence it has to be calculated in spheroidal coordinates. But in this case the expansion (3.22) cannot be used. Instead,

we have to employ an analogous expansion in spheroidal coordinates, which is also called the Neumann expansion,

$$\frac{1}{|\mathbf{r}-\mathbf{r}'|} = \frac{2}{R}\sum_{s=0}^{\infty}\sum_{m=-s}^{s}(-1)^m(2s+1)\left(\frac{(s-|m|)!}{(s+|m|)!}\right)^2 P_s^{|m|}(\lambda_<)Q_s^{|m|}(\lambda_>)P_s^{|m|}(\mu)P_s^{|m|}(\mu')e^{im(\phi-\phi')}, \tag{4.20}$$

where $\lambda_<$ and $\lambda_>$ are respectively the lesser and greater of λ and λ'. $P_s^{|m|}$ are the associated Legendre functions as in Eq. (3.22) and $Q_s^{|m|}$ are the associated Legendre functions of the second kind. The Expansion (4.20) is more closely described in Appendix C. Inserting this expansion into Eq. (4.19), together with providing the wave functions ϕ_1 and ϕ_2, expressed in terms of λ, μ, and ϕ, we see, that there is no ϕ dependence of the charge distribution. So, we may compute this part of the integration, reducing one of the summation indices. In effect we obtain that

$$I' = \alpha^3R^2\sum_{s=0}^{\infty}(2s+1)\int_1^{\infty}d\lambda\int_{-1}^{1}d\mu(\lambda^2-\mu^2)\exp(-\alpha R\lambda) P_s(\lambda_<)Q_s(\lambda_>)P_s(\mu)P_s(\mu'). \tag{4.21}$$

The next step is to carry out the integration over μ. This variable occurs in the formula only twice. We may use either the orthogonality property of the Legendre polynomials

$$\int_{-1}^{1}d\mu P_s(\mu)P_{s'}(\mu) = \delta_{ss'}\frac{2}{2s+1}, \tag{4.22}$$

by expressing $\mu^2 = 1/3P_0(\mu)+2/3P_2(\mu)$, or simply switch over to the explicit polynomial expansions. This next integration reduces further the summation over s leaving only two terms: $s = 0$ and $s = 2$. The most problematic is the integration over λ. We use Eq. (3.25). Unfortunately, the Legendre functions of the second kind $Q_s(\lambda)$ contain terms like $\frac{\lambda+1}{\lambda-1}$, ,which result after integration, in nonelementary contributions. The calculation is quite cumbersome. With help of the overlap integral and an auxiliary definition $S' \equiv e^{\alpha R}(1-\alpha R+1/3\alpha^2R^2)$ we have as the result

$$I'(\lambda,\mu,\phi;\alpha) = \frac{2}{R}\left(1-(9/4)(\mu^2-1/3)(\lambda^2-1/3)\right)\left(S\ln\left(\frac{\lambda+1}{\lambda-1}\right) -S'Ei(-\alpha R(\lambda+1))+SEi(-\alpha R(\lambda-1))-\alpha R\exp(-\alpha R\lambda)\right) +\frac{9}{R}9\mu^2-1/3)(e^{-\alpha R\lambda}(-1/6\alpha R-\lambda-1/2\alpha R\lambda^2)+\lambda S). \tag{4.23}$$

The special function appearing here is the exponential integral function

$$Ei(z) = -\int_{-z}^{\infty} \frac{e^{-t}}{t} dt = \gamma_{Euler} + \ln z + \sum_{n=1}^{\infty} \frac{z^n}{nn!}, \tag{4.24}$$

where $\gamma_{Euler} \simeq 0.5772$ is the Euler's constant. The primary use of the expression (4.23) is the calculation of J, but it can also be employed to an alternate calculation of the correlated-hopping integral V to check the consistency of the calculations. Next we have to multiply $I'(\mathbf{r}';\alpha)$ by $\phi_1(\mathbf{r}';\alpha)\phi_2(\mathbf{r}';\alpha)$ and integrate out the variables ϕ', μ' and λ'. After a somewhat lengthy calculation, we get the final expression for the exchange integral of 1s orbitals

$$\begin{aligned} J' = \frac{12}{5R}\left(S^2\gamma_{Euler} + S^2\ln(\alpha R) - 2SS'Ei(-2\alpha R) + S'^2 Ei(-4\alpha R)\right) \\ +\alpha e^{-2\alpha R}\left(5/4 - 23/10\alpha R - 6/5\alpha^2 R^2 - 2/15\alpha^3 R^3\right). \end{aligned} \tag{4.25}$$

Examining the asymptotic properties of the expression one obtains exactly the same behavior like for the correlated-hopping integral V', namely

$$\begin{aligned} \lim_{R\to\infty} J' &\overset{l.t.}{=} \exp(-\alpha R) \\ \lim_{R\to 0} J' &= \frac{5\alpha}{4} = U', \end{aligned} \tag{4.26}$$

for small R we get back the U' value, and for large R an exponential decay, which reflects the long range shape of the 1s wave functions. The R dependence of the two electron microscopic parameters U', K', V', J' is displayed in Fig. 4.4. All these functions are real valued. It should be stressed that *no approximations* were made in the calculation of all the atomic microscopic parameters.

After calculating the microscopic parameters in the atomic basis, one needs to transform them to the corresponding expressions in the orthogonalized Wannier basis. The general shape of the transformation is identical like for atoms in Eqs. (3.13), (3.14). The only difference is that the overlap integral is expressed by another dependence in Eq. (4.10), which depends on the interatomic distance R. The S dependence is shown in Fig. 4.5. The transformation rules for one- and two- electron parameters are even simpler, than respectively, (3.19) and (3.27). In the first case we have only one atomic energy, hence there is also only one value for Wannier parameters. In the formula for two-electron parameters the summation goes only over two orbitals yielding four parameters in the Wannier basis. Unfortunately, for $R \to 0$ the value of the overlap approaches unity, what makes the mixing coefficients

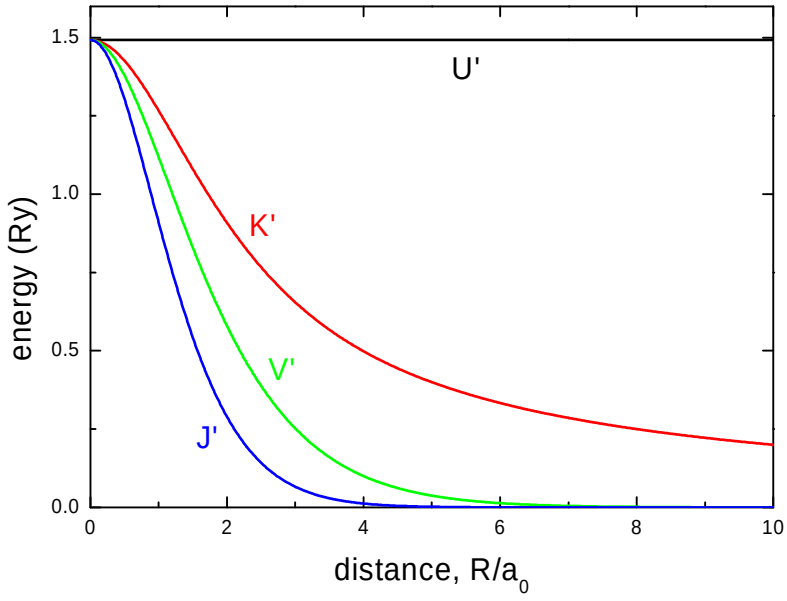

Figure 4.4. Two-electron atomic microscopic parameters as a function of interatomic distance R. The values are in Ry.

diverge. To see the nature of this divergence more clearly it is convenient to rewrite Eq. (3.13) in the following form

$$w_1(\mathbf{r}) = \beta \left(\phi_1(\mathbf{r}) - \left(-\frac{\gamma}{\beta} \right) \phi_2(\mathbf{r}) \right) . \tag{4.27}$$

The second Wannier function is obtained by exchanging the indices $1 \leftrightarrow 2$. Now, β plays the role of the normalization constant, whereas the value 0f $-\frac{\gamma}{\beta}$ tells us how deep the negative kink in $w_1(\mathbf{r})$ should be, at the position of the second nucleus. From Fig. 4.5 we see that $-\frac{\gamma}{\beta} \to 1$, what means it should be equal to the function peak itself. So the normalization β has to diverge at the same level as mixing coefficient $-\frac{\gamma}{\beta}$ approaches unity. These divergencies can make some of the microscopic parameters infinite. Fortunately, as shown in Fig. 4.6 for single electron integrals and in Fig. 4.7 for two electron parameters, it is not true. As long as *all atomic parameters* in a given class *are calculated exactly*, the divergences cancel out. But, if we approximate the atomic parameters, or put them equal zero, the Wannier parameters may diverge. It is not a local effect very near to $R = 0$. In Fig. 4.5 we see that

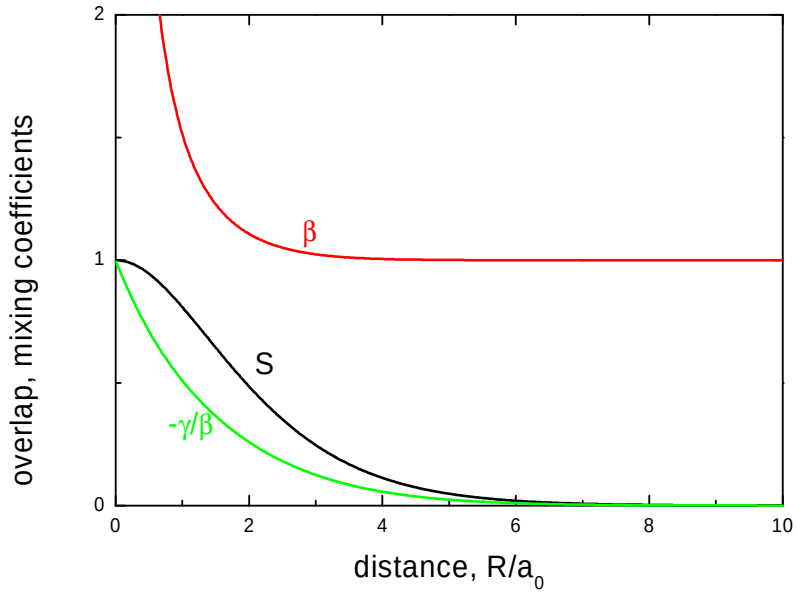

Figure 4.5. The overlap S and the mixing coefficients of atomic into Wannier functions for a molecule consisting of two 1s orbitals. β can be interpreted as the normalization constant, whereas $-\beta/\gamma$ is the amount of the second wave function to be added to the first one to achieve the orthogonality. The parameters diverge with decreasing distance R.

the values of β and γ are starting to rise significantly for $R \simeq a_0$, which is of the order of optimal bond length, obtained later on in the calculations. This is the reason why any approximation at the level of atomic parameters should be controlled. On the other hand, it is relatively safe to put some of the parameters in the Wannier basis as approximately zero. The numerical calculations illustrating this problems are done in Section 4.4 on example of Li_2 molecule. Basing on this assumption one may estimate the atomic parameters of the simplified system [18]. All the Wannier parameters are real valued, as before for the atomic states.

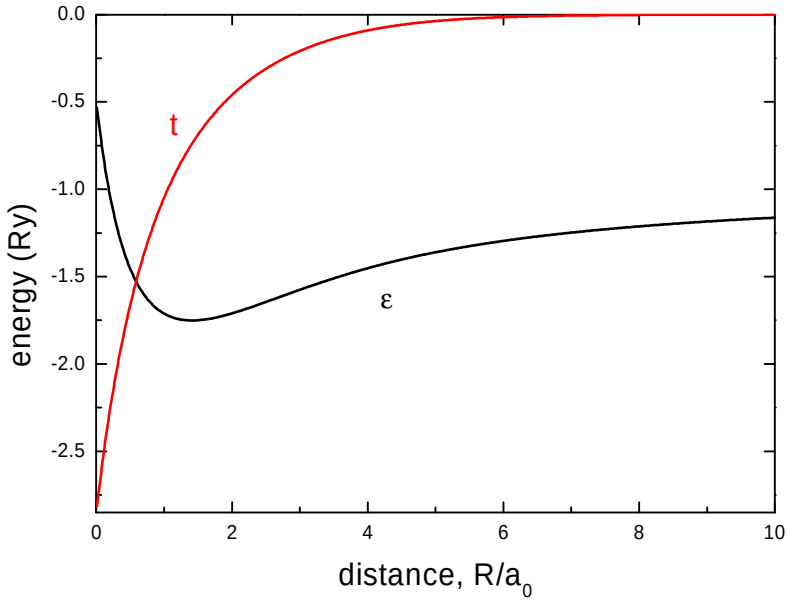

Figure 4.6. Single-electron Wannier microscopic parameters as a function of interatomic distance R. Compare with Fig. 4.3 to see the influence of the orthogonalization.

4.2 Results for H_2, H_2^-

With all the microscopic parameters accounted for, we select now the Fock-space states in a way, which makes the Hamiltonian matrix blockdiagonal. Because we have only two orbitals, there are only $\binom{2*2}{2} = 6$ states for the H_2 molecule and $\binom{2*2}{3} = 4$ states for the H_2^- molecular ion. For the H_2 molecule we may divide all the states into three triplet states

$$\begin{aligned} |1> &= a^\dagger_{1\uparrow} a^\dagger_{2\uparrow} |0>, \\ |2> &= a^\dagger_{1\downarrow} a^\dagger_{2\downarrow} |0>, \\ |3> &= \frac{1}{\sqrt{2}} \left(a^\dagger_{1\uparrow} a^\dagger_{2\downarrow} + a^\dagger_{1\downarrow} a^\dagger_{2\uparrow} \right) |0>, \end{aligned} \tag{4.28}$$

and three singlet states

$$|4> = \frac{1}{\sqrt{2}} \left(a^\dagger_{1\uparrow} a^\dagger_{2\downarrow} - a^\dagger_{1\downarrow} a^\dagger_{2\uparrow} \right) |0>,$$

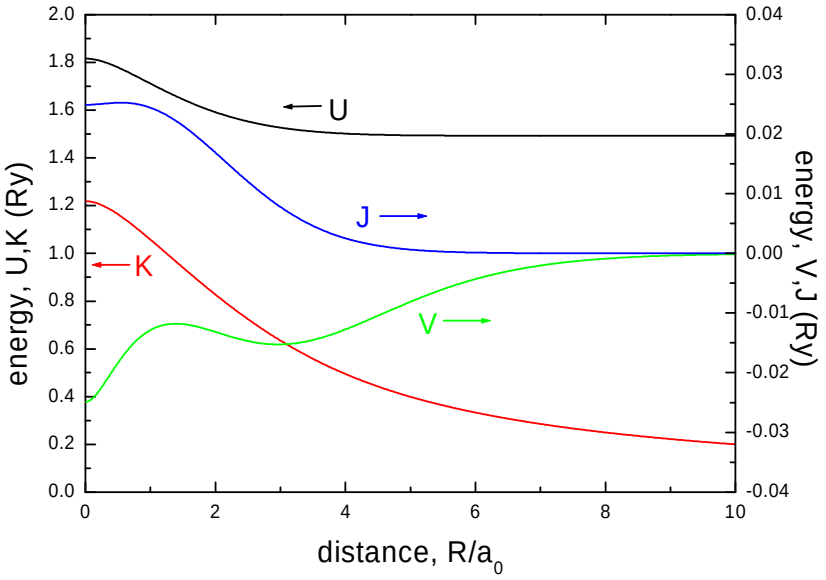

Figure 4.7. Two-electron Wannier microscopic parameters as a function of interatomic distance R. Compare with Fig. 4.4 to see the influence of the orthogonalization. The left axis is for the intraatomic and interatomic Coulomb interactions U and K. The right axis is for the correlated hopping and exchange interactions V and J.

$$|5>=\frac{1}{\sqrt{2}}\left(a^{\dagger}_{1\uparrow}a^{\dagger}_{1\downarrow}+a^{\dagger}_{2\uparrow}a^{\dagger}_{2\downarrow}\right)|0>,$$
$$|6>=\frac{1}{\sqrt{2}}\left(a^{\dagger}_{1\uparrow}a^{\dagger}_{1\downarrow}-a^{\dagger}_{2\uparrow}a^{\dagger}_{2\downarrow}\right)|0>. \qquad (4.29)$$

The Hamiltonian (3.37) can be in this case written as

$$H=\varepsilon(n_{1\uparrow}+n_{1\downarrow}+n_{2\uparrow}+n_{2\downarrow})+t\sum_{\sigma}\left(a^{\dagger}_{1\sigma}a_{2\sigma}+a^{\dagger}_{2\sigma}a_{1\sigma}\right)+U\sum_{i=1}^{2}n_{i\uparrow}n_{i\downarrow}$$
$$-2J\mathbf{S}_1\cdot\mathbf{S}_2+(K+\frac{1}{2}J)(n_{1\uparrow}+n_{1\downarrow})(n_{2\uparrow}+n_{2\downarrow})+J\left(a^{\dagger}_{1\uparrow}a^{\dagger}_{1\downarrow}a_{2\downarrow}a_{2\uparrow}\right)$$
$$+V\sum_{\sigma}(n_{1\sigma}+n_{2\sigma})\left(a^{\dagger}_{1\bar{\sigma}}a_{2\bar{\sigma}}+a^{\dagger}_{2\bar{\sigma}}a_{1\bar{\sigma}}\right) \qquad (4.30)$$

Taking the expectation value of this Hamiltonian we get for the triplet states (4.28), the only nonzero values

$$< I|H|I >= 2\varepsilon + K - J \quad \forall I \in \{1,2,3\}. \tag{4.31}$$

The singlet states (4.29) form a submatrix

$$H_S = \begin{pmatrix} 2\varepsilon + K + J & 2t + 2V & 0 \\ 2t + 2V & 2\varepsilon + U + J & 0 \\ 0 & 0 & 2\varepsilon + U - J \end{pmatrix} \tag{4.32}$$

The eigenvalues can be easily obtained analytically in the form [38]

$$\begin{aligned} E_T &= 2\varepsilon + K - J \\ E_{S1} &= 2\varepsilon + U - J \\ E_{S2} &= 2\varepsilon + \frac{U+K}{2} + J + \frac{1}{2}\sqrt{(K-U)^2 + 16(t+V)^2} \\ E_{GS} \equiv E_{S3} &= 2\varepsilon + \frac{U+K}{2} + J - \frac{1}{2}\sqrt{(K-U)^2 + 16(t+V)^2}, \end{aligned} \tag{4.33}$$

where E_T is the threefold degenerate triplet state and E_{Sx} are the singlet states. E_{S3} has always the lowest energy, thus it is the ground state E_{GS} for any interatomic distance R.

Looking at the absolute value one sees that all the parameters are required. But taking the relative values of the obtained energies, it turns out that the atomic energy has the same contribution to all states 2ε and can be regarded as the reference energy. Similarly, only the difference between the intraatomic and interatomic Coulomb interaction $U - K$ is important, hence the reference level can be set to include one of these values, i.e. the relative energy difference between any two states is a function of $U - K$, not each of them separately.

The corresponding singlet ground state in the Fock space has the form

$$|GS >= \frac{1}{\sqrt{2D(D-U+K)}} \times$$

$$\times \left\{ 4(t+V)\frac{1}{\sqrt{2}}(a^\dagger_{1\uparrow}a^\dagger_{2\downarrow} - a^\dagger_{1\downarrow}a^\dagger_{2\uparrow}) - (D-U+K)\frac{1}{\sqrt{2}}(a^\dagger_{1\uparrow}a^\dagger_{2\downarrow} + a^\dagger_{1\downarrow}a^\dagger_{2\uparrow}) \right\} |0>, \tag{4.34}$$

where

$$D \equiv \left[(U-K)^2 + 16(t+V)^2\right]^{1/2}.$$

The lowest spin-singlet eigenstate has an admixture of the symmetric ionic state $\frac{1}{\sqrt{2}}(a^\dagger_{1\uparrow}a^\dagger_{2\downarrow} + a^\dagger_{1\downarrow}a^\dagger_{2\uparrow})$. Therefore, to see the difference with either the

Hartree-Fock or Heitler-London approach to H_2, we construct the two-particle wave function for the ground state according to the prescription provided by Eq. (2.15), which in this case takes the form

$$\Phi_0(\mathbf{r}_1,\mathbf{r}_2) \equiv \frac{1}{\sqrt{2}} < 0|\hat{\Psi}(\mathbf{r}_1)\hat{\Psi}(\mathbf{r}_2)|G> . \tag{4.35}$$

Taking $\hat{\Psi}(\mathbf{r}) = \sum_{\sigma=\uparrow}^{\downarrow} w_1(\mathbf{r})\chi_\sigma(\mathbf{r})a_{1\sigma}^\dagger + w_2(\mathbf{r})\chi_\sigma(\mathbf{r})a_{2\sigma}^\dagger$, we obtain that

$$\Phi_0(\mathbf{r}_1,\mathbf{r}_2) = \frac{2(t+V)}{\sqrt{2D(D-U+K)}}\Phi_c(\mathbf{r}_1,\mathbf{r}_2) - \frac{1}{2}\sqrt{\frac{D-U+K}{2D}}\Phi_i(\mathbf{r}_1,\mathbf{r}_2), \tag{4.36}$$

where the multiparticle wave function has been separated into two parts of different nature. The covalent part is

$$\Phi_c(\mathbf{r}_1,\mathbf{r}_2) = \left[w_1(\mathbf{r}_1)w_2(\mathbf{r}_2) + w_1(\mathbf{r}_2)w_2(\mathbf{r}_1)\right]\left[\chi_\uparrow(\mathbf{r}_1)\chi_\downarrow(\mathbf{r}_2) - \chi_\downarrow(\mathbf{r}_1)\chi_\uparrow(\mathbf{r}_2)\right], \tag{4.37}$$

whereas the ionic part takes the form

$$\Phi_i(\mathbf{r}_1,\mathbf{r}_2) = \left[w_1(\mathbf{r}_1)w_1(\mathbf{r}_2) + w_2(\mathbf{r}_1)w_2(\mathbf{r}_2)\right]\left[\chi_\uparrow(\mathbf{r}_1)\chi_\downarrow(\mathbf{r}_2) - \chi_\downarrow(\mathbf{r}_1)\chi_\uparrow(\mathbf{r}_2)\right]. \tag{4.38}$$

The ratio of the coefficients before $\Phi_i(\mathbf{r}_1,\mathbf{r}_2)$ and $\Phi_c(\mathbf{r}_1,\mathbf{r}_2)$ can be defined as the *many-body covalency* γ_{mb}. This value should be distinguished from the *single-particle covalency* $-\frac{\gamma}{\beta}$ appearing in the definition (4.27) of the orthogonalized atomic orbital $w_i(\mathbf{r})$. The two quantities are drawn in Fig. 4.8. The many-body covalency γ_{mb} represents a true degree of multiparticle configurational mixing.

For the H_2^- molecular ion we have only 4 multiparticle states in the Fock space

$$\begin{aligned} |1> &= a_{1\uparrow}^\dagger a_{1\downarrow}^\dagger a_{2\uparrow}^\dagger|0>, \\ |2> &= a_{1\uparrow}^\dagger a_{1\downarrow}^\dagger a_{2\downarrow}^\dagger|0>, \\ |3> &= a_{1\uparrow}^\dagger a_{2\uparrow}^\dagger a_{2\downarrow}^\dagger|0>, \\ |4> &= a_{1\downarrow}^\dagger a_{2\uparrow}^\dagger a_{2\downarrow}^\dagger|0> . \end{aligned} \tag{4.39}$$

All these states can be transformed into each other by the symmetries of exchanging the orbitals $1 \leftrightarrow 2$ or the spins $\uparrow\leftrightarrow\downarrow$. The Hamiltonian formulation is identical like for the H_2 molecule (4.30). The Hamiltonian matrix consists of two identical blocks connecting the states $|1>$ with $|3>$, and $|2>$ with $|4>$,i.e.

$$H_{H_2^-} = \begin{pmatrix} 3\varepsilon + U + 2K + J & t - 2V \\ t - 2V & 3\varepsilon + U + 2K + J \end{pmatrix}. \tag{4.40}$$

Table 4.2. Ground-state energy and microscopic parameters (in Ry) for H_2 molecule. The last column represents the kinetic exchange integral characterizing intersite antiferromagnetic exchange

R/a	E_G/N	ϵ_a	t	U	K	V [mRy]	J [mRy]	$\frac{4(t+V)^2}{U-K}$[mRy]
1.0	-1.0937	-1.6555	-1.1719	1.8582	1.1334	-13.5502	26.2545	7755.52
1.5	-1.1472	-1.7528	-0.6784	1.6265	0.9331	-11.6875	21.2529	2747.41
2.0	-1.1177	-1.722	-0.4274	1.4747	0.7925	-11.5774	16.9218	1130.19
2.5	-1.0787	-1.6598	-0.2833	1.3769	0.6887	-12.0544	13.1498	507.209
3.0	-1.0469	-1.5947	-0.1932	1.3171	0.6077	-12.594	9.8153	238.939
3.5	-1.0254	-1.5347	-0.1333	1.2835	0.5414	-12.8122	6.9224	115.143
4.0	-1.0127	-1.4816	-0.0919	1.2663	0.4854	-12.441	4.5736	55.8193
4.5	-1.006	-1.4355	-0.0629	1.2579	0.4377	-11.4414	2.8367	26.9722
5.0	-1.0028	-1.3957	-0.0426	1.2539	0.3970	-9.9894	1.6652	12.9352
5.5	-1.0012	-1.3616	-0.0286	1.2519	0.3623	-8.3378	0.9334	6.1455
6.0	-1.0005	-1.3324	-0.01905	1.251	0.3327	-6.7029	0.5033	2.8902
6.5	-1.00024	-1.3073	-0.0126	1.2505	0.3075	-5.2242	0.2626	1.3452
7.0	-1.0001	-1.2855	-0.0083	1.2503	0.2856	-3.9685	0.1333	0.6197
7.5	-1.00004	-1.2666	-0.0054	1.2501	0.2666	-2.9509	0.066	0.2826
8.0	-1.00002	-1.25	-0.0035	1.25006	0.25	-2.1551	0.032	0.1277
8.5	-1.00001	-1.2353	-0.0023	1.25003	0.2353	-1.5501	0.01523	0.0572
9.0	-1.	-1.2222	-0.0015	1.25001	0.2222	-1.1005	0.0071	0.0254
9.5	-1.	-1.2105	-0.0009	1.25001	0.2105	-0.7725	0.0033	0.0112
10.0	-1.	-1.2	-0.0006	1.25	0.2	-0.5371	0.0015	0.0049

Table 4.3. Same as in Table 4.2 for H_2^- ion. Note That the values for the microscopic parameters V, J, and $\frac{4(t+V)^2}{U-K}$ are in Ry here.

R/a	E_G/N	ϵ_a	t	U	K	V[Ry]	J[Ry]	$\frac{4(t+V)^2}{U-K}[Ry]$
1.0	-0.4591	-1.6607	-0.5869	1.1414	0.7360	-0.0105	0.0163	3.5220
1.5	-0.7659	-1.6647	-0.4285	1.1279	0.6983	-0.0085	0.0161	1.7782
2.0	-0.8813	-1.6259	-0.3083	1.0979	0.6474	-0.0078	0.0150	0.8871
2.5	-0.9264	-1.5737	-0.2221	1.0692	0.5961	-0.0079	0.0133	0.4476
3.0	-0.9423	-1.5204	-0.1603	1.0466	0.5476	-0.0086	0.0113	0.2286
3.5	-0.9460	-1.4704	-0.1154	1.0305	0.5025	-0.0093	0.0091	0.1179
4.0	-0.9450	-1.4252	-0.0826	1.0196	0.4608	-0.0099	0.0071	0.0612
4.5	-0.9426	-1.3848	-0.0585	1.0126	0.4226	-0.0101	0.0052	0.0319
5.0	-0.9402	-1.3491	-0.0410	1.0080	0.3881	-0.0099	0.0037	0.0167
5.5	-0.9384	-1.3176	-0.0284	1.0051	0.3573	-0.0093	0.0025	0.0088
6.0	-0.9373	-1.2901	-0.0194	1.0032	0.3300	-0.0085	0.0017	0.0046
6.5	-0.9365	-1.2621	-0.0130	0.9905	0.3058	-0.0075	0.0011	0.0025
7.0	-0.9363	-1.2402	-0.0086	0.9876	0.2847	-0.0065	0.0007	0.0013
7.5	-0.9365	-1.2211	-0.0056	0.9856	0.2662	-0.0055	0.0004	0.0007
8.0	-0.9367	-1.2044	-0.0036	0.9844	0.2498	-0.0046	0.0003	0.0004
8.5	-0.9372	-1.1897	-0.0022	0.9839	0.2352	-0.0037	0.0002	0.0002
9.0	-0.9376	-1.1768	-0.0013	0.9839	0.2222	-0.0030	0.00009	0.00010
9.5	-0.9380	-1.1653	-0.0008	0.9842	0.2105	-0.0024	0.00005	0.00005
10.0	-0.9384	-1.1549	-0.0004	0.9848	0.2000	-0.0018	0.00003	0.00003

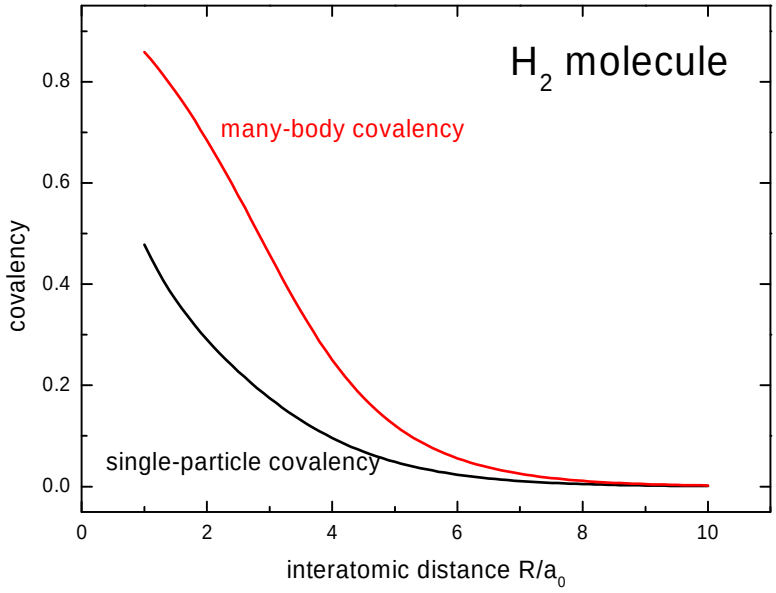

Figure 4.8. The single-particle (γ) and many-body (γ_{mb}) covalency factors for the H_2 wave functions. For details see main text.

The eigenvalues of this Hamiltonian are

$$E_{\pm} = 3\varepsilon + U + 2K + J \pm (t - 2V) \tag{4.41}$$

Each energy is twofold degenerate with respect to spin $\sigma = \uparrow, \downarrow$. Depending on the sign of the value $t - 2V$, the ground state in the Fock space is either a symmetric or an antisymmetric combination of the initial states $|1>$ and $|3>$[3]. As it turns out later during the optimization process, the symmetric combination is energetically favorable for small R, whereas the antisymmetric for larger R.

Because analytic formulas for the ground state energy are available in both , H_2 and H_2^- cases, we can just minimize these values with respect to α and R. The electronic Hamiltonian contains only electron-electron and electron-nuclei interactions. Thus, the obtained ground state energy is the electronic energy E_G^{el} only. To complete the description one has to include an additional contribution of the ion-ion interaction. We treat it classically, as

[3]Because of the degeneracy we may as well talk about $|2>$ and $|4>$

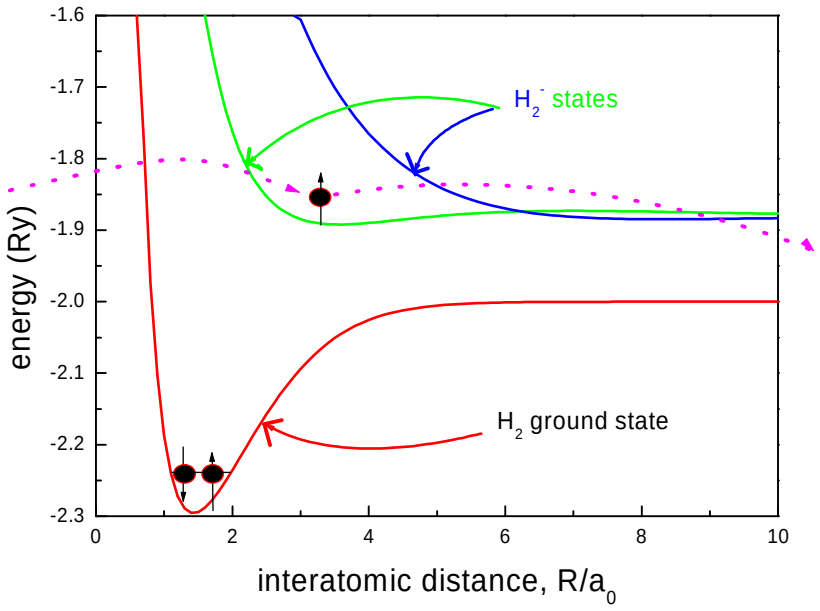

Figure 4.9. The level scheme of the H_2 ground state and the lowest H_2^- states as a function of the interatomic distance R. The hopping electron illustrates the relevance of H_2^- ionic configuration when measuring tunnelling conductivity of H_2 system.

the Coulomb interaction of two point charges lying at the bond distance R from each other. Hence, the full ground-state energy is

$$E_G(R,\alpha) = E_G^{el}(R,\alpha) + \frac{2Z^2}{R}, \tag{4.42}$$

where $Z = 1$ for hydrogen. The results are shown in Table 4.4. The "reference" values for energy are the best variational estimates [39]. Instead of minimizing both R and α simultaneously we can compute the optimal α for a given R. In this way we get the R dependence of the ground state energy and the orbital size. These values are plotted in Figs. 4.9 and 4.10. There are three curves on each plot vs. R, since there are two different ground states for H_2^-. For H_2 the optimal α goes with $R \to \infty$ to the atomic value for H atom, because we have then two separated atoms. For H_2^- we get in this

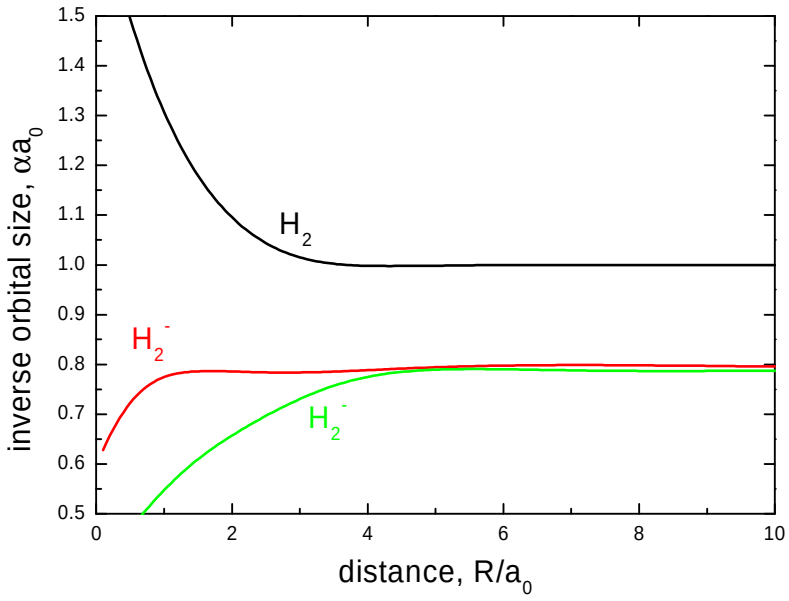

Figure 4.10. Optimal value of the variational α parameter as a function of distance R. For large R we see the atomic limit $\alpha = 1$, which is the value for a hydrogen atom.

limit an intermediate value between the H^- and H parameters[4], as we have then two electrons on one atom and a single on the second.

In Table 4.2 we list the energies and the values of the microscopic parameters for H_2 system with optimized orbitals, whereas in Table 4.3 the same is provided for H_2^- molecular ion. Parenthetically, one should note a drastic difference for the so-called *correlated hopping* matrix element V in the two situations. The same holds true for the direct exchange integral J (ferromagnetic). This exchange integral is always decisively smaller than that for the antiferromagnetic kinetic exchange, $J_{kex} = 4(t+V)^2/(U-K)$. The virtual interatomic hopping processes leading to the strong kinetic exchange are the source of the singlet nature of the H_2 ground state. The H_2^- ground state is unstable with respect to the dissociation into H_2 and e^-, contrary to the H^- case. However, the energetics of such state is important when calculating

[4]For H_2^- one should calculate the optimal α with 1 orbital per atom like it was done for He at the end of Subsection 2.3.2, that is equal to $\frac{11}{16}$, instead of taking the value from Table 3.1, obtained for an enlarged basis.

Table 4.4. The ground state energy E_G, bond length R and the inverse optimal orbital size α for H_2 and H_2^-. The reference value of the energy is from [39]. The experimental value of the bond length is from [40].

	E_G[Ry]	$R[a_0]$	$\alpha_{opt}a_0$	E_G^{ref} [Ry]	$R^{exp}[a_0]$
H_2	-2.29587	1.43042	1.19379	-2.296	1.40963
H_2^-	-1.89215	3.5651	0.78597		instable

e.g. the metallization of molecular hydrogen or determining the tunnelling conductivity through H_2 molecule, as shown schematically in Fig. 4.9. This last Fig. illustrates the method of determining the energetics of excited states of H_2 by measuring e.g. the tunnelling conductivity (i.e. via H_2^- intermediate state).

4.3 Mobile orbitals for H_2

In all calculations so far, we have made an assumption that the wave function is centered around the nuclei. For atoms it could be justified by the symmetry. But for molecules, this may not be certain. We may allow for a displacement d between the center of orbital and its parent nucleus. This approach is similar to the approach utilizing sums of orbitals to express more complicated wave functions in electronic calculations, e.g. to form two displaced s orbitals to simulate a p orbital.

The new idea is illustrated in Fig. 4.11. The distance between the orbitals is reduced to $R - 2d$. The two-electron parameters do not depend on the nucleus position. So, their values calculated already may be used again with changed R. Similarly, the overlap integral does only depend on the interorbital distance, so in effect we can make the list

$$\left.\begin{array}{c} U'(\cdot,\alpha) \\ K'(R,\alpha) \\ V'(R,\alpha) \\ J'(R,\alpha) \\ S(R,\alpha) \end{array}\right\} \rightarrow \left\{\begin{array}{c} U'(\cdot,\alpha) \\ K'(R-2d,\alpha) \\ V'(R-2d,\alpha) \\ J'(R-2d,\alpha) \\ S(R-2d,\alpha) \end{array}\right. . \tag{4.43}$$

For the intraatomic Coulomb interaction there is no R dependence.

The situation becomes more complicated for the single electron parameters, as they include the interaction with the nuclei. The atomic energy may be calculated according to Eq. (4.3), with the exception that we have twice the expression for the 2^{nd} nucleus contribution, calculated in Eq. (4.4), instead of the interaction with the not displaced nucleus. The distances to put

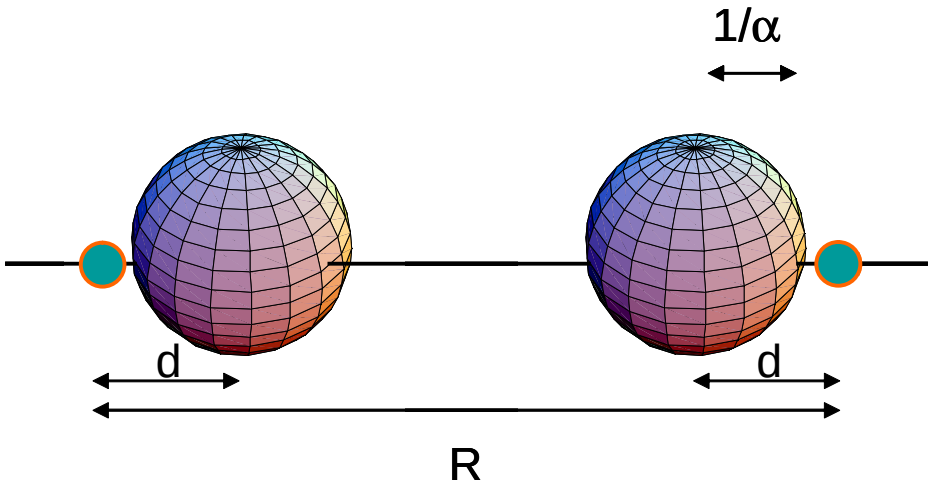

Figure 4.11. Model of a H_2 molecule with additional parameter d - the displacement between the nuclei and the corresponding centers of the orbitals.

in this formula are respectively d and $R-d$. In effect we have

$$\varepsilon' = \alpha^2 + \frac{2\,\alpha\,\left(e^{4\,\alpha\,d}+e^{2\,\alpha\,R}\right)}{e^{2\,\alpha\,(d+R)}} + \frac{2\,\left(\frac{d-d\,e^{4\,\alpha\,d-2\,\alpha\,R}-R}{e^{2\,\alpha\,d}}+R\right)}{d\,(d-R)}. \tag{4.44}$$

The calculation of the hopping integral is more tricky here. The integral can be divided into three parts: the kinetic energy, and the interactions with both Coulomb wells. The kinetic energy was already calculated in Eq. 4.8, and we only need to substitute $R \to R-2d$. The interaction with the Coulomb well is in fact a three-center integral, because we have two orbitals and one well, and in general none of them coincide. We need an integral of type

$$\tau_{ijk} = \frac{\alpha^3}{\pi}\int d^3\mathbf{r}\frac{e^{-\alpha(r_i+r_j)}}{r_k}, \tag{4.45}$$

where r_i, r_j and r_k are the distances from three different points. Luckily, they are located on a straight line, so this calculation can be performed analytically in Appendix G. We parameterize the geometry of the system by $a = R-2d$, the distance between origins of r_i and r_j, and by $h = R/2$, the distance of the origin of r_k from the middle point of the segment a. The hopping integral in atomic representation is

$$t' = \frac{\alpha^2 e^{-\alpha(R-2d)}}{3}(-\alpha^2(R-2d)^2+3\alpha(R-2d)+3)+2\tau_{ijk}(\alpha, R-2d, \frac{R}{2}). \tag{4.46}$$

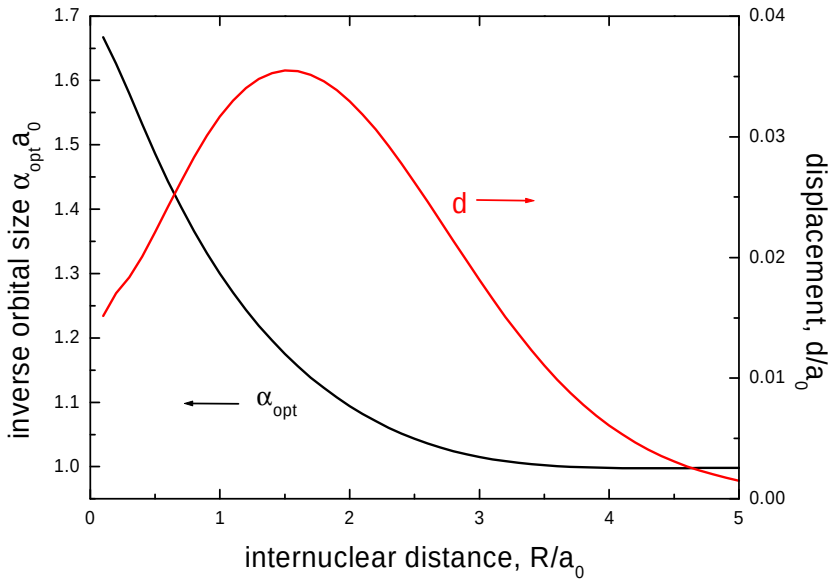

Figure 4.12. The results for the H_2 molecule with mobile orbitals. The optimal inverse size of the orbital α_{opt} has not changed significantly compared to the case with fixed orbital centers at the nuclei positions.

The subsequent calculations are identical as for the molecules with fixed orbital centers $d = 0$. The only difference is the existence of the additional optimization parameter d. We obtain the following values for the H_2 molecule: ground state energy $E_G = -2.3003Ry$, the inverse orbital size $\alpha = 1.19001a_0^{-1}$, the internuclear distance $R = 1.4285a_0$. If we compare this to the results with fixed orbitals in Table 4.4 we see a slight improvement in the energy of the order of 0.2% of the initial value, which is reproduced for $d = 0$. The orbitals are also a little bit larger, the bond is shorter and the electrons moved to the middle of the molecule. The optimal inverse orbital size α_{opt} and the displacement d are shown in Fig. 4.12. The displacement d reaches its maximal value a the internuclear distance corresponding to the lowest ground state energy.

Concluding this Chapter one may say that although it does not provide essentially new values for E_G in H_2 and H_2^- cases, the method is very transparent, allows for a definition of many-body covalency factors, as well for an introduction of the so-called mobile orbitals. The amazing feature of the results for those mobile orbitals is that the nuclei repel each other further

apart, while the electrons come closer (d is positive). This feature shows the truly quantum-mechanical nature of the covalent bond. Obviously, the zero point motion of the nuclei has not been discussed here as our main purpose was to test the EDABI method in the simplest two-site cases.

4.4 Li_2 molecule: role of 2s atomic-like state

The complexity of the calculation in the EDABI method rises quite rapidly with increasing number of electrons. Also, the calculation of microscopic parameters, for wave functions more complicated than 1s functions, is not a simple task. To illustrate the impact of these problems we have chosen a more complicated system, namely the Li_2 molecule. Such molecule has six electrons so we decided to introduce some simplifications.

The major new approximation is considering the two inner ($1s^2$) electrons of each Li atom as core electrons. They are located mostly on the 1s shell. We have chosen to disregard their dynamics and to include them as renormalizing the nucleus charge only, i.e. in subsequent calculations we set the effective charge of the nucleus to $Z = 1$. This corresponds to 1s orbitals, having point size, which means that the inverse size parameter $\alpha_{1s} = \infty$, located at the nucleus. Inserting this value into the atomic energy ϵ' Eq. (4.3) and to the atomic Coulomb interaction U' Eq. (4.15) we get infinite values. Of course, this is a very crude approximation. One should rather use an effective potential, and calculate the single particle parameters with it. But this topic is out of the scope of this Thesis, and the approximation chosen enables us to demonstrate the impact of more complicated wave functions on the results.

Summarizing, our model is identical to the H_2 molecule model, described at the beginning of this Chapter, with the difference that we use 2s atomic-like orbitals of the form

$$\phi_1(\mathbf{r};\alpha) = \sqrt{\frac{\alpha^3}{\pi}}(1-\alpha|\mathbf{r}-\mathbf{R}/2|)\exp(-\alpha|\mathbf{r}-\mathbf{R}/2|)$$
$$\phi_2(\mathbf{r};\alpha) = \sqrt{\frac{\alpha^3}{\pi}}(1-\alpha|\mathbf{r}+\mathbf{R}/2|)\exp(-\alpha|\mathbf{r}+\mathbf{R}/2|). \qquad (4.47)$$

The calculation of the parameters is basically the same as for 1s orbitals, but much more complicated. Some intermediate results for the most complicated exchange integral J' have the size of several pages in printing. The two-electron microscopic parameters for 2s orbitals are shown in Fig. 4.13. Of course in the case of 2s orbitals we also have to go over to Wannier basis. The corresponding parameters in the Wannier basis are shown in Fig. 4.14. Comparing with the 1s situation, displayed in Figs. 4.4 and 4.7, we see that

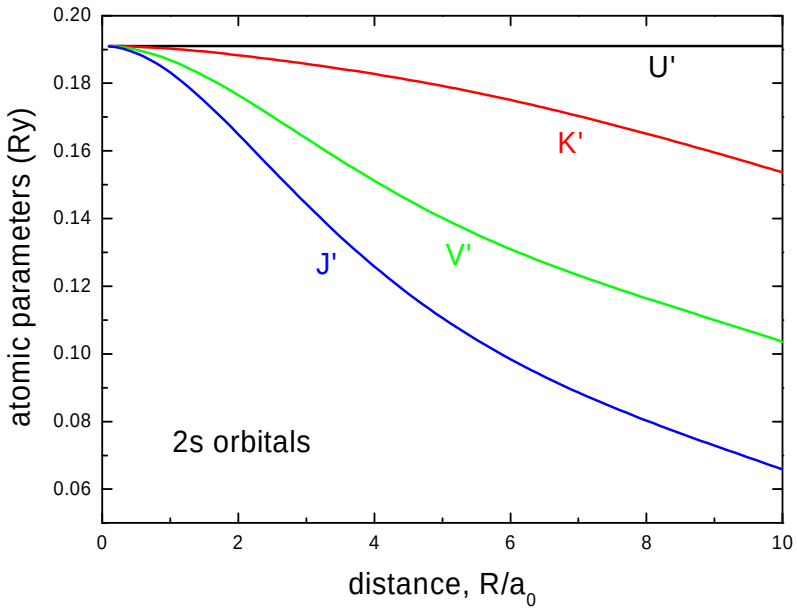

Figure 4.13. Two electron atomic microscopic parameters as a function of interatomic distance R for 2s atomic-like orbitals. The values are in Ry.

the values are lower, and the decay is much slower. This is caused by the increased size of the 2s atomic-like orbital when compared with the 1s orbital.

The diagonalization process does not differ at all from the H_2 case, because the Li_2 model has the same formulation in the Fock space. Only the parameter values differ. The results, consisting of the ground state energy E_G, the bond length R and the optimal value of the inverse size parameter α_{opt}, are shown in the first row of Table 4.5.

Because of the problems appearing in the calculation of the parameters in the atomic basis, one may try to simplify this task. The first possibility is to ignore the integrals which are difficult to evaluate. In our case, we may set the exchange integral $J' = 0$. This approximation turns out to be too radical. After the transformation to the Wannier basis we obtain divergent results. Namely, the ground state energy is divergent in the small R limit, which makes an optimization of the parameter α impossible.

Another possibility is to take the value calculated for a simpler orbital. We may reuse the values for 1s orbitals. They have the correct limits, hence we can get a bound for the ground-state energy. Unfortunately, the nature

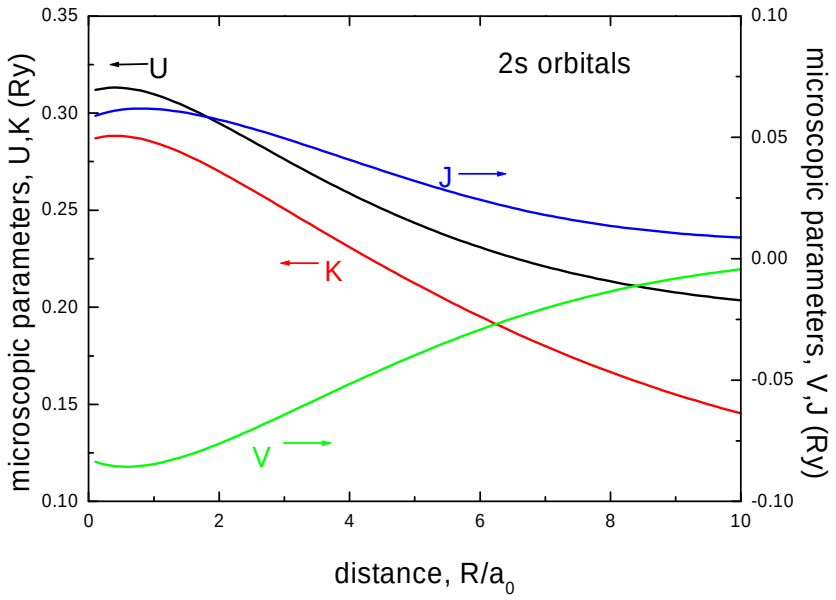

Figure 4.14. Two-electron microscopic parameters for the orthogonalized 2s Wannier basis as a function of the interatomic distance R. The values are in Ry. Compare with Fig. 4.13 to see the influence of the orthogonalization. The left axis is for the intraatomic and interatomic Coulomb interaction U and K. The right axis is for the hybrid and exchange interaction V and J.

Table 4.5. The results for Li_2 molecule with different approximation, regarding the parameters, applied on top of the EDABI method.

approximation	E_G/N (Ry)	$R(a_0)$	$\alpha_{opt}a_0$
exact	-0.89875	4.4534	0.31755
$J'=0$	divergent	divergent	–
$J'=$ 1s value	-0.79627	3.88506	0.4114
$J=0$	-0.93613	4.30151	0.32152
no Wannier basis	-0.714045	5.2331	0.57511

of the ground state is different, the state with the lowest energy is not the same as for the complete calculation.

Still another possibility is to set the value $J = 0$ in the Wannier basis. This is not really a simplification, as far as we still need the atomic value, which is difficult to obtain, but it justifies an approach of obtaining the atomic values from approximated values in the Wannier basis [18]. Within this approach we get the correct ground state, but the calculated values of the ground state energy E_G, the bond length R, and the optimal value of the inverse size parameter α_{opt}, are not in a very good agreement with complete results. Such method yields only qualitative results.

The last approximation,the lowest row in Table 4.5, examined here is of a different nature. We disregard the need to work in an orthogonal basis. The theoretical aspects of this were discussed in Section 3.1. The practical impact is shown in this calculation. We simply assume that the overlap integral $S = 0$. Thus all the parameters in the Wannier basis are identical to that in the atomic basis. This impairs the quality of the results. The nature of the ground state is correct, but the quantitative results are of comparable quality to the approximation $J = 0$, i.e. not very good. Note also that neglecting $1s^2$ electrons the ground state energy is only a fraction of the total atomic energy obtained in the preceding Chapter. The Li_2 example shows explicitly that the extension of EDABI method to more involved molecular systems is associated with additional complications, which should be dealt with separately.

Chapter 5

Crystal field levels from EDABI method

In solid state physics one is usually concerned with systems with a large number of atoms. In a crystal the local electronic properties are influenced by all neighboring atoms. If we consider a single atom in a such structure, we have to include in some way this interaction.

The simplest approximation consists of regarding the neighboring atoms, or rather atomic ions, as simple charged points, without taking in account their electronic structure. In this manner, we may extend the calculations done for atoms in Chapter 3. Namely, in addition to the central nucleus we add several point charges, placed according to the symmetry of the system we want to describe. Obviously such calculation provides realistic results *only* when the states are strictly localized, quasiatomic.

These additional charges change the total charge of the system. A crystal can be imagined as being built of many such blocks. To make it neutral, the total charge of a single block consisting of the central nucleus, its electrons and the auxiliary charges, has to be equal to zero. As a rule, these neighboring ions are shared by several cells. So, we have to use an effective charge Z^{ext} for them as it is partially neutralized by electrons from other blocks. The simplest choice is to take only $\frac{1}{n}$-th of the charge of an atomic ion if it is shared across n cells. The equation for the charge balance can be written down in form

$$Ze + Ne + \sum_{i=1}^{z} Z_i^{ext} e = 0, \tag{5.1}$$

where Ze is the charge of the central nucleus, N is the number of electrons taken into account in the calculation, e is the electron charge, and z is the number of crystal field sources.

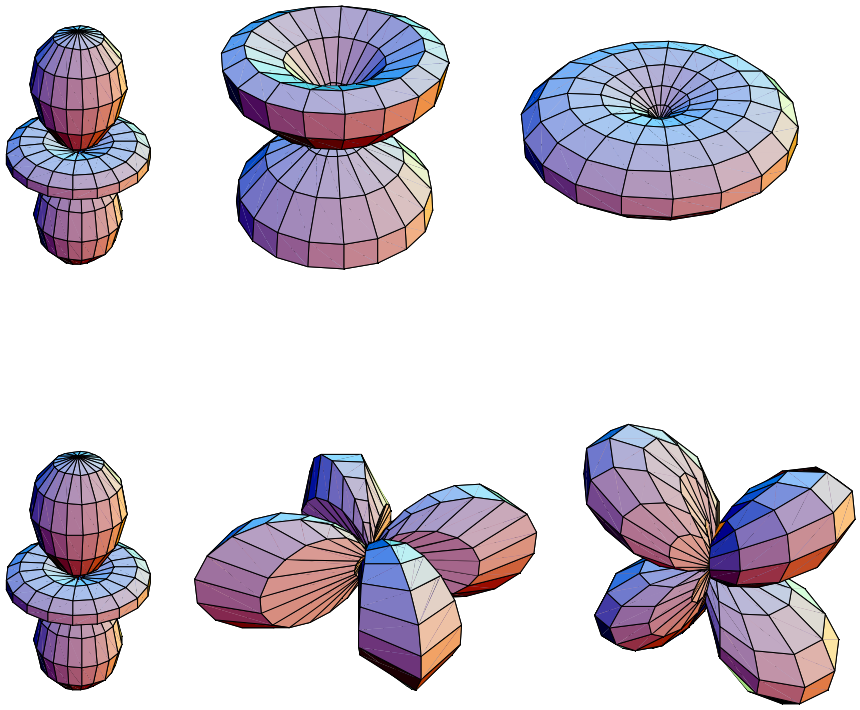

Figure 5.1. The shape of complex (upper row $m = 0, \pm 1, \pm 2$ respectively) and real (lower row) 3d wave functions. For the complex valued wave functions we show the absolute value only, thus the shape of functions with opposite signs of m is identical here. All real wave function, except the first one, can be transformed into each other by a three dimensional rotation. This is the reason why only 3 functions are displayed.

Because the central atom can have many electrons, what increases the difficulty of the calculation, the inner ones may be regarded as composing the atomic core. They just lower the charge of the central atom and do not appear anywhere else in the calculation. An extension of this approach would be the replacement of the Coulomb potential of the central nucleus by an effective potential do describe the contribution of the core electrons in a more precise manner.

The starting point is the choice of the basis wave functions. The crystal field effects are important, for example, in d-shell ions embedded in the chaleogenide matrix. So we can choose for our calculation the 3d wave functions

of adjustable size. Their radial dependence is

$$R_{3d}(r;\alpha) = \sqrt{\frac{8}{45}}\alpha^{7/2} r^2 \exp(-\alpha r). \tag{5.2}$$

The complete wave functions are obtained by multiplying the radial parts by the standard spherical dependence represented by spherical harmonics Y_{lm}, i.e.[1]

$$\phi_{3dm}(r,\theta,\phi;\alpha) = R_{3d}(r;\alpha) Y_{2m}(\theta,\phi). \tag{5.3}$$

But it is not the only choice for the 3d functions. They often appear as real functions. The real functions are defined as follows

$$\phi_{3z^2-r^2}(\mathbf{r};\alpha) = \phi_{3d0}(\mathbf{r};\alpha) \tag{5.4}$$

$$\phi_{yz}(\mathbf{r};\alpha) = -\frac{\imath}{\sqrt{2}}\left(\phi_{3d1}(\mathbf{r};\alpha) + \phi_{3d-1}(\mathbf{r};\alpha)\right) \tag{5.5}$$

$$\phi_{xz}(\mathbf{r};\alpha) = \frac{1}{\sqrt{2}}\left(\phi_{3d1}(\mathbf{r};\alpha) - \phi_{3d-1}(\mathbf{r};\alpha)\right) \tag{5.6}$$

$$\phi_{x^2-y^2}(\mathbf{r};\alpha) = \frac{1}{\sqrt{2}}\left(\phi_{3d2}(\mathbf{r};\alpha) + \phi_{3d-2}(\mathbf{r};\alpha)\right) \tag{5.7}$$

$$\phi_{xy}(\mathbf{r};\alpha) = -\frac{\imath}{\sqrt{2}}\left(\phi_{3d2}(\mathbf{r};\alpha) - \phi_{3d-2}(\mathbf{r};\alpha)\right). \tag{5.8}$$

The indices of the real wave functions represent the shape of the function in the Cartesian coordinate system. The shape of both kinds of 3d functions is depicted schematically in Fig. 5.1. Both choices are equivalent, in the sense that they can be transformed into each other by a unitary transformation, as long as there is only one α. In our calculations we allow each wave function to have an independent inverse size parameter, so the results for both sets may be different.

The five 3d functions, both real and complex, are orthogonal, their overlap integral is $S = 0$. This is because of the different angular dependence of each of these functions. The variation of the inverse size parameter does not break down this orthogonality. This presents itself an advantage because the atomic functions are already the orthogonalized Wannier functions. So, we do not need to transform the parameters calculated in the atomic basis. The Eqs.(3.13, 3.14) are not necessary in this case.

The introduction of the crystal field changes only the potential of the nucleus. The electron-electron interaction $H_2(\mathbf{r},\mathbf{r}')$ has still the form from Eq. (3.20). So, if we want to perform the calculations for two or more electrons, we can calculate the 2 particle microscopic parameters in advance, without

[1] For the definitions and conventions, see Appendix A.

the knowledge about the symmetry of additional charges in our system. We can use the same expressions for calculations for any crystal field arrangement, also for simple atoms and molecular ions. So, if we would have used also the 3d functions in our calculations in Chapter 3, we could reuse these results here. The method of calculation of two-particle microscopic parameters is described in Section 3.2.2. There are 120 nonequivalent integrals for five 3d states. Only 16 of them are nonzero for complex-function basis. In the progress of carrying out the calculations for this Thesis all two-particle integrals involving 1s, 2s, 2p ,3s ,3p and 3d functions with a common origin were calculated. For 14 wave functions we have 5565 nonequivalent integrals, out of which 561 of them are nonzero.

We can transform the parameters from complex-function into real-function single-particle basis using the transformation matrix

$$A = \begin{pmatrix} 1 & 0 & 0 & 0 & 0 \\ 0 & \frac{-\imath}{\sqrt{2}} & \frac{-\imath}{\sqrt{2}} & 0 & 0 \\ 0 & \frac{1}{\sqrt{2}} & -\frac{1}{\sqrt{2}} & 0 & 0 \\ 0 & 0 & 0 & \frac{-\imath}{\sqrt{2}} & \frac{\imath}{\sqrt{2}} \\ 0 & 0 & 0 & \frac{1}{\sqrt{2}} & \frac{1}{\sqrt{2}} \end{pmatrix}, \tag{5.9}$$

and the transformation rule is

$$V'^{real}_{ijkl} = \sum_{i'j'k'l'=1}^{5} A_{ii'} A_{jj'} A_{kk'} A_{ll'} V'^{compl}_{i'j'k'l'} \begin{cases} \alpha_{i'} \rightarrow \alpha_i \\ \alpha_{j'} \rightarrow \alpha_j \\ \alpha_{k'} \rightarrow \alpha_k \\ \alpha_{l'} \rightarrow \alpha_l \end{cases}, \tag{5.10}$$

where the bracket on the right represents the various substitutions of α parameters to be done in each component of the sum. In the real basis, there are 34 nonzero integrals.

5.1 Octahedral surrounding

The model we choose for the examination of the electron states in the crystal field is the octahedral surrounding model. It is shown in Fig. 5.2. On every axis, x, y and z, there is located a charge Z^{ext} in equal distance R from the origin, which contains charge Z. The number of crystal-field charges is thus $z = 6$. We are going to discuss two cases. First, one electron case, $N = 1$. According to charge balance Eq. (5.1), we may choose $Z = 4$ and $Z^{ext} = -1/2$. Z^{ext} may represent an oxygen ion O^{2-} charge shared between four neighboring cells. In the one electron case the two-particle integrals are

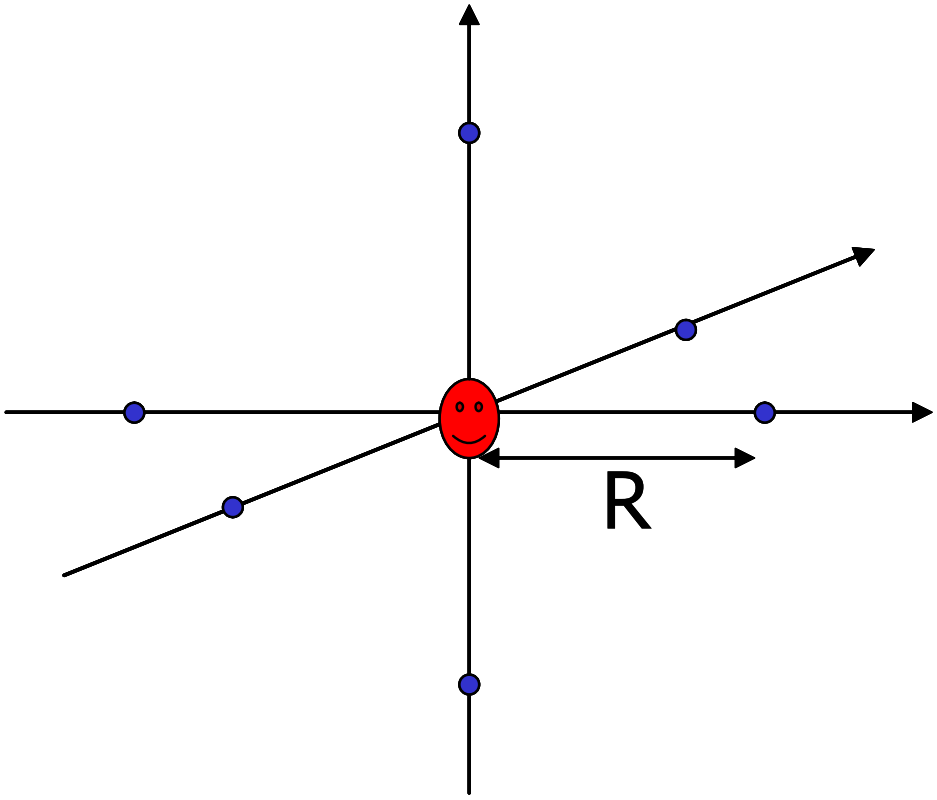

Figure 5.2. Model of the system in octahedral crystal field. The additional charges are located on x, y and z axes in the distance R from the center.

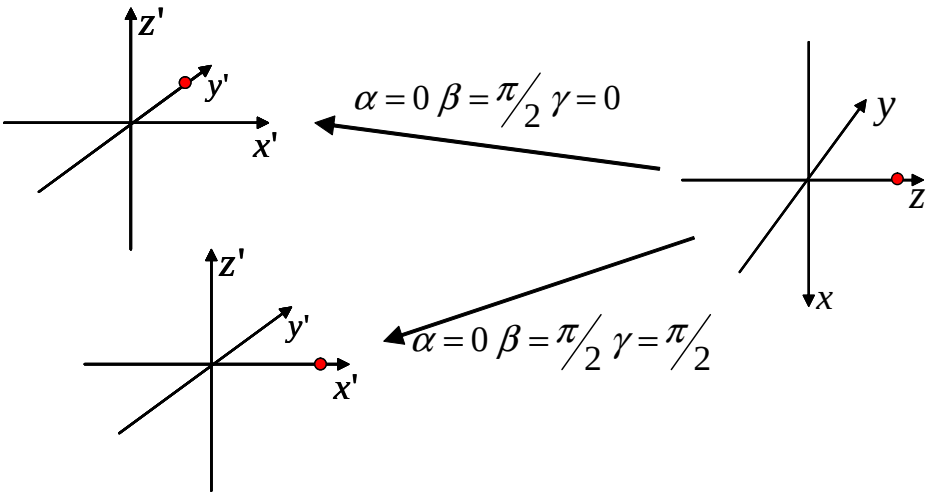

Figure 5.3. Rotation of coordinate system to express the crystal field from charges on x and y axes via the values for the charges located on z axis.

not needed. But because of Z^{ext}, the 3d wave functions are not the eigenfunctions of single-electron Hamiltonian. So in this case the size optimization makes sense even for the single electron. Second case is that with two electrons, $N = 2$. In this situation we need the two electron integrals and the charges are respectively $Z = 5$ and $Z^{ext} = -1/2$.

In both cases we need to calculate the single-electron microscopic parameters according to prescription (2.12). The Hamiltonian changes with respect to the atomic case in Eq. (3.16)

$$H_1(\mathbf{r}) = -\nabla^2 - \frac{2Z}{|\mathbf{r}|} - \sum_{\eta=\pm x,\pm y,\pm z} \frac{2Z^{ext}}{|\mathbf{r} - \mathbf{r}_\eta|}, \tag{5.11}$$

where $\mathbf{r}_\eta$ is the position of the additional charge. The values of η represent the axis and whether the charge is located on positive or negative part of this axis. The first two terms yield the atomic values. For 3d wave functions the parameters are equal to

$$t'_{ij} = \alpha_i(\alpha_i - \frac{2Z}{3}) + \sum_{\eta=\pm x,\pm y,\pm z} \delta t_{ij\eta}, \tag{5.12}$$

where $\delta t_{ij\eta}$ is the crystal field correction from charge η.

This correction can be easily calculated for $\eta = z$. The calculation is done in spherical coordinates, using the inverse distance series expansion given by Eq. (C.3) described in detail in Appendix C. Analyzing the properties of the Legendre functions one sees that the infinite series has only few nonzero terms. The results have the form of finite power functions of α and R multiplied by $\exp(-2\alpha R)$, are diagonal in wave function indices $\delta t_{ijz} \sim \delta_{ij}$ and are even with respect to the transformation $\eta \to -\eta$.

The values for $\eta = \pm x$, and $\pm y$ can be obtained by the rotation of initial wave functions. A rotation can be described by Euler angles α, β and γ, which correspond to rotation axes z, y and again z, every time with respect to actual coordinate system. The values $\alpha = 0, \beta = \pi/2, \gamma = 0$ and $\alpha = 0, \beta = \pi/2, \gamma = \pi/2$ map the $\eta = z$ case respectively on the $\eta = x$ and $\eta = y$ cases. The radial part of the wave functions is invariant under the rotations. The spherical harmonics transform in the following way

$$Y_{lm}(\theta', \phi') = \sum_{\mu=-l}^{l} e^{-\imath(m\gamma+\mu\alpha)} d^l_{m\mu}(\beta) Y_{l\mu}(\theta, \phi), \tag{5.13}$$

where $d^l_{m\mu}(\beta)$ are transformation coefficients, representing the y-axis rotation, described in detail in Appendix H. Because $\delta t_{ijz} \sim \delta_{ij}$, we can compute

δt_{ijx} and δt_{ijy} as

$$\delta t_{ij\{x,y\}} = \sum_{i'=1}^{5} e^{-\imath(m(j)-m(i))\{0,\frac{\pi}{2}\}} d^2_{ji'} d^2_{ii'} \delta t_{ijz}, \tag{5.14}$$

where $m(i)$ is the z-axis component of angular momentum of i-th wave function[2].

How does the Hamiltonian matrix look like? For one electron it is identical with the "hopping" matrix $H_{ij} = t_{ij}$. Without the crystal field it is diagonal because 3d atomic wave functions are eigenfunctions to the one electron Hamiltonian. The introduction of the crystal field does not change the picture. The real wave functions have a symmetry consistent with the octahedral surrounding. Thus the Hamiltonian is still diagonal, and we do not need any diagonalization procedure. The complex functions do not fully agree with the octahedral symmetry, but there is only one off-diagonal element: the state with $m = 2$ is coupled with the state with $m = -2$. The diagonalization yields the real functions $\phi_{x^2-y^2}$ and ϕ_{xy}. For two electrons we have a clear division of the Hamiltonian matrix into blocks corresponding to the values of total spin, and z-component of the total spin. The situation is similar to that for the case of the helium atom discussed in Section 3.3. States belonging to these classes do not mix. Even inside the blocks not all states are interconnected. This allows for an analytic expression of all energy eigenvalues, what makes the optimization process easier.

The resultant ground state energy and the inverse size parameter α_{opt} corresponding to it is shown for one electron in Fig. 5.4 as a function of the distance R. For small R, the ground state energy is slightly decreasing. In the region $3a_0 \leq R \leq 4a_0$ the optimal inverse size changes its value quite rapidly. The step is continuous. We can state it because we know the analytic expression for the ground state energy. In this region E_{GS} starts decreasing more rapidly. The reason for this behavior is clearly seen when we look at Fig. 5.5. In it, there is the complete one electron spectrum for optimized α_{opt} for each value of R, and for fixed values $\alpha = 1/3$ and $\alpha = 4/3$. These fixed values correspond to an electron on 3d orbital without crystal field, when the central charge is equal respectively to $+1$ and $+4$. In the limit of small R the ionic charges combine with that of the nucleus and effectively compensate its charge so the resultant charge is $Z - 6Z^{ext} = +1$. The orbitals are larger, because α is smaller, and all the charges are inside the orbitals. On the contrary, for large R the influence of additional charges is less important and we have only the central charge $Z = +4$. We see that the change in α_{opt}

[2]For $\phi_i = \phi_{3dm}$ we have that $m(i) = m$.

Table 5.1. The results for *one electron*($3d^1$ configuration) in the crystal field of octahedral symmetry. The optimized ground state energy E_G and the inverse size parameter α_{opt} is displayed. The real basis wave functions are used and make the Hamiltonian matrix diagonal. The excited states can be optimized independently providing its own inver size parameter α_+. The values ΔE_G show the crystal field splitting with this independent optimization (own α_+ for excited states), and a single α_{opt} (global α_{opt} determined for E_G only) for all states.

R	E_G(Ry)	$\alpha_{opt}a_0$	α_+a_0	ΔE (mRy) own α	ΔE (mRy) global α
1	-0.111226	0.332265	0.334177	0.2671	0.2708
2	-0.11282	0.323959	0.345815	3.2749	3.7916
3	-0.121248	0.311986	0.42216	14.5495	27.2750
4	-0.345316	1.33679	1.22587	111.0107	120.4242
5	-0.599606	1.35637	1.29966	46.2369	49.4961
6	-0.786454	1.34823	1.32008	20.4196	21.2435
7	-0.924621	1.34148	1.32729	9.7515	9.9586
8	-1.02981	1.33776	1.33026	5.0481	5.1052
9	-1.11224	1.33583	1.33163	2.8086	2.8264
10	-1.17844	1.33482	1.33233	1.6598	1.6660
11	-1.23274	1.33426	1.33271	1.0309	1.0333
12	-1.27804	1.33393	1.33293	0.6674	0.6684
13	-1.31642	1.33374	1.33306	0.4473	0.4478
14	-1.34933	1.33361	1.33315	0.3088	0.3090
15	-1.37787	1.33353	1.3332	0.2187	0.2188

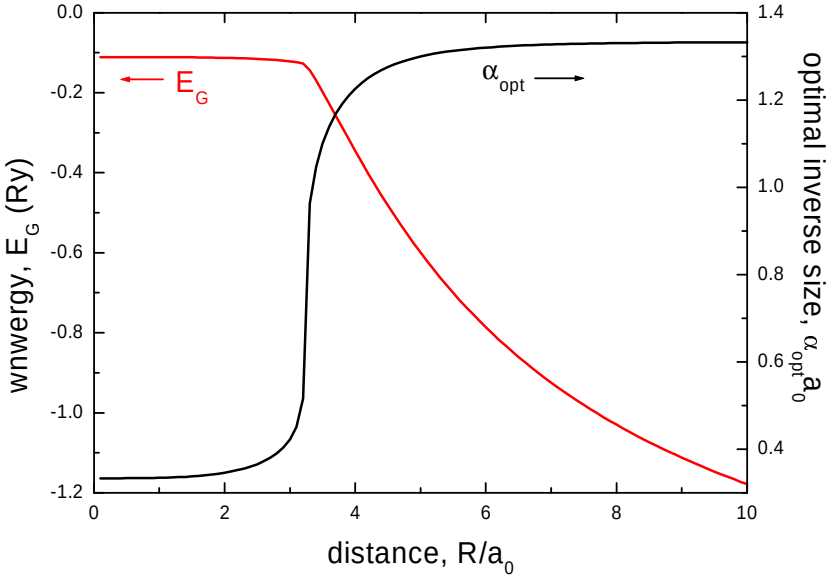

Figure 5.4. The optimized ground state energy E_G and the optimal value of the inverse size α_{opt} for one electron in the case of crystal field of octahedral symmetry.

corresponds to the crossover between the two limiting cases. Because of the increased effective charge, the orbitals are much more compact around the nucleus.

There are only two states visible in the spectrum in Fig. 5.5. This is because the spectrum is degenerate. The ground state is triple degenerate whereas the excited one is double degenerate. Of course if we flip the spin of the electron the picture does not change. So in this case we have to double the multiplicity. This result corresponds to the usual division into t_{2g} and e_g states [47].

Because for one-electron case the initial states are decoupled from the beginning, we can optimize the size of orbital for each state independently. The change of α for the excited state does not affect the ground state energy E_G. The optimal inverse size as a function of R for the excited state[3] α_+ is compared with that for the ground state, in Fig. 5.6. The limits are identical, i.e. 1/3 and 4/3. The behavior in the crossover regime is slightly

[3]The optimization of degenerate excited states yield the same value of α_+ for all of them.

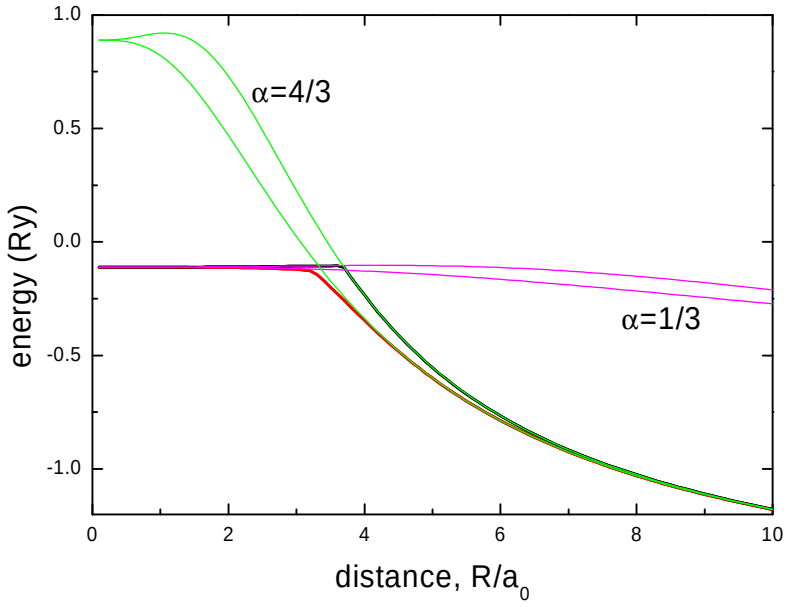

Figure 5.5. The energy spectrum with optimization, and with fixed α. The values $\alpha = 1/3$ and $\alpha = 4/3$ represent the limits with nuclear charge $Z = 1$ and $Z = 4$ respectively. It correspond to the crystal field charges being either included as an effective charge of nucleus or at infinite distance from it. The ground state is three fold degenerate whereas the excited is two fold degenerate. Including the two possible spin values the degeneracy doubles.

different, namely, we do not have a smooth dependence, but a discontinuity at $R \simeq 3.65a_0$. We find thus the exact border between the two limiting regimes. The numerical values of α_{opt} and α_+ are listed in Table 5.1.

Another interesting point is the value of the crystal field splitting. It is shown in Fig. 5.7, together with the values for fixed $\alpha = 1/3$ or $4/3$. One sees that in general the values for the fixed α are valid in the corresponding region. The maximal splitting is observed in the crossover between the regimes. Just after the crossover we see that the splitting for optimal α_{opt} value is slightly larger than that for $\alpha = 4/3$. This is because the optimized ground state energy is always lower than the ground state energy for fixed α, and the crossover of the ground state energy is smoother than the corresponding behavior for the excited state. Numerical values of the splitting are listed explicitly in Table 5.1.

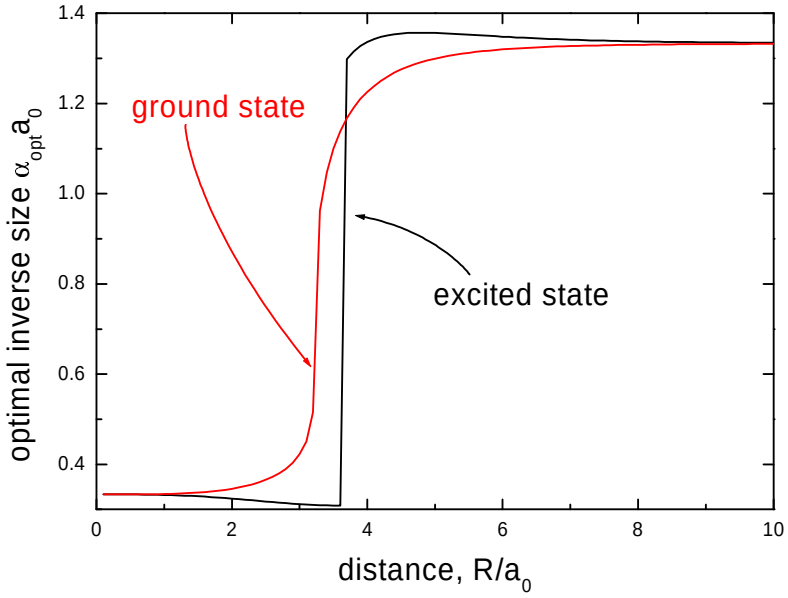

Figure 5.6. The optimal values of the inverse size parameter α for the ground and the excited states vs. interionic distance R. The excited state plot has a discontinuity, whereas the ground state dependence is smooth.

The results for two electrons ($3d^2$ configuration) are shown in Fig. 5.8. There are 45 states displayed as a function of the distance R. The general shape of the ground state is similar to the one electron case. Because of the electron-electron interaction, the orbitals are *smaller*. This is because the electrons try to regain the energy by increasing the attraction to the nucleus. This can be seen in numerical values presented in Table 5.2. Because of the smaller size of the orbitals, the crossover takes also place for smaller R. The new feature is presence of the kink for the excited states in the crossover region. Despite the increasing distance of the additional negative charges, the energy also rises.

Two electron states can be classified in terms of the total spin and its z-component. They are good quantum numbers for this system, if the spin-orbit interaction is ignored, as it is the case so far. High spin states with $S = 1$ are lower. The ground state falls into this class. They have three possible values of $S_z = 0, \pm 1$. For each of them there are three degenerate lowest states. The complete spectrum for each S_z is identical. So the ground state

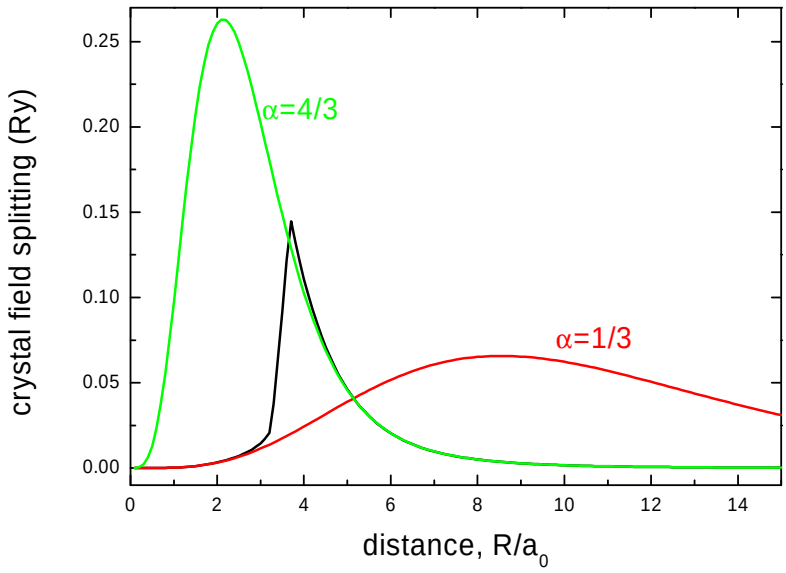

Figure 5.7. The crystal field splitting for one electron in an octahedral crystal field vs. distance R. This corresponds to the energy spectrum shown in Fig. 5.5. For the sake of completeness, we include the corresponding splittings for the α values specified.

is ninefold degenerate.

Another value used to classification of the states is the angular momentum. Unfortunately it is not a good quantum number for crystal field systems. The states obtained in the above procedure are not eigenstates of $\mathbf{L}^2$ operator. The only thing that can be done is the calculation of the expectation values of the angular momentum operator. Depending on the ground state selected, since they are ninefold degenerate, we get values in the in the interval from 7 to 9, what corresponds to angular momentum between 2 and 3. The exact size of the interval depends on R.

5.2 Spin-orbit interaction

So far our calculation included all non-relativistic interactions in the Fock space spanned by the class of 3d wave functions. An extension of this model is the inclusion of some relativistic effects. The contribution we want to include

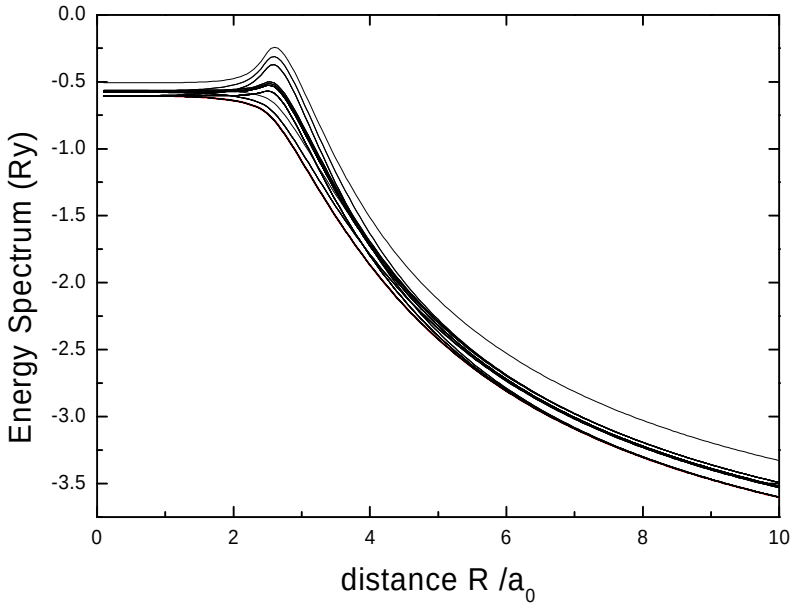

Figure 5.8. Energy spectrum for two electrons in the octahedral crystal field with optimized inverse size parameter α. The results are identical whether we use real or complex 3d states. All electron-electron interactions and the spin-orbit interaction were included (see the discussion of the last interaction below). The spin-orbit correction shown in Fig. 5.10 does not qualitatively change this picture, because of its magnitude.

is the spin-orbit coupling. All the calculations up to this point started with the Schrödinger equation. Because there is no many-particle Dirac equation, we have to continue the way already chosen. The spin-orbit interaction is to be included as a correction to Hamiltonian (2.1). This correction involves only the single electron term, because it originates from a single-particle formalism. It is calculated in Appendix I. It is of the form

$$H'(\mathbf{r}) = \alpha^2 \frac{1}{r}\frac{\partial V^{sph}}{\partial r}\mathbf{L}\cdot\mathbf{S} + \alpha^2 \int d^3\mathbf{r}' \frac{2\rho(\mathbf{r}')\mathbf{S}\cdot((\mathbf{r}-\mathbf{r}')\times\mathbf{p})}{|\mathbf{r}-\mathbf{r}'|^3}, \qquad (5.15)$$

where $\alpha = \frac{e^2}{\hbar c} \simeq \frac{1}{137}$ is the fine structure constant[4]. V^{sph} is the spherically symmetric part of the electrostatic potential, $\mathbf{S}$ is the spin operator, $\mathbf{L}$ is

[4]In atomic units the inverse of the fine structure constant is the speed of light c.

the angular momentum operator and $\mathbf{p}$ is the momentum operator. $\rho(\mathbf{r}')$ is residual charge distribution of the part not included in the potential V^{sph}. As can be seen from Eq. (5.15), the spin-orbit interaction term separates into two parts: the spherical part which gives the name to the interaction, and a non-spherical contribution, which may be of comparable magnitude to the first term, and thus cannot be ignored.

The one-electron microscopic parameters t_{ij}, defined by Eq. (2.12), calculated in Section 5.1, can be used also here. We have to add to each of them the corresponding corrections defined by

$$H'^{s}_{ij} =< i|H'^{s}|j > \quad H'^{ns}_{ij} =< i|H'^{ns}|j >, \tag{5.16}$$

where the superscripts s and ns, denote respectively the spherical and the non-spherical parts. Because of their different nature, they have to be calculated separately.

Another important point to note is that the corrections do not conserve the spin. Hence the Hamiltonian is not spin-rotation invariant any more. From this point we use the *spin-orbitals instead of* the *orbitals*. This increases the variation range of indices i and j, as from now on they include also spin $|i >\equiv |i\sigma >$. The simplifying assumption from Section 2.1 is not longer in use.

The spherically symmetric part is relatively easy to calculate. We may write the initial integral (5.16) as

$$H'^{s}_{s\sigma t\tau} = \int d^3\mathbf{r}(\phi_s\xi_\sigma)^\star H'^{s}(\phi_t\xi_\tau), \tag{5.17}$$

where the spin functions are

$$\xi_\sigma = \begin{cases} \binom{1}{0} & :\sigma =\uparrow \\ \binom{0}{1} & :\sigma =\downarrow \end{cases} . \tag{5.18}$$

Let us define the radial part of the parameters as

$$\zeta(r) = \alpha^2 \frac{1}{r}\frac{\partial V^{sph}}{\partial r}. \tag{5.19}$$

The components of the spin operator are expressed by the Pauli matrices $S^\eta = \tau^\eta/2$. The components of the angular momentum operator can be expressed in a simple form in spherical coordinates

$$L_x = \imath\left(\sin\phi\frac{\partial}{\partial\theta} + \frac{\cos\phi}{\tan\theta}\frac{\partial}{\partial\phi}\right) \tag{5.20}$$

$$L_y = \imath\left(-\cos\phi\frac{\partial}{\partial\theta} + \frac{\sin\phi}{\tan\theta}\frac{\partial}{\partial\phi}\right) \tag{5.21}$$

$$L_z = -\imath\frac{\partial}{\partial\phi}. \tag{5.22}$$

Using the above definitions the value of H'^s can be expressed as

$$H'^s_{s\sigma t\tau} = \Xi(\alpha_s, \alpha_t) \sum_{\eta=x,y,z} S^\eta_{\sigma\tau} L^\eta_{st}. \tag{5.23}$$

The spin part is just a triple product of two spinors and a matrix

$$S^\eta_{\sigma\tau} = \xi^\star_\sigma S^\eta \xi_\tau. \tag{5.24}$$

The angular part is the expectation value of the angular momentum for given orbitals

$$L^\eta_{st} = \int \sin\theta d\theta d\phi Y^\star_{2s}(\theta,\phi) L_\eta Y_{2t}(\theta,\phi), \tag{5.25}$$

and thus, the radial part is

$$\Xi(\alpha_s,\alpha_t) = \int r^2 dr \zeta(r) R_{3d}(r;\alpha_s) R_{3d}(r;\alpha_t) = -\frac{32}{15}\alpha^2 Z \frac{\alpha_s^{7/2}\alpha_t^{7/2}}{(\alpha_s+\alpha_t)^4}. \tag{5.26}$$

The last result was obtained under the assumption that the Coulomb potential $V^{sph}(\mathbf{r})$ originates from charge $+Z$. All the above expressions can be computed in a straightforward manner. The calculation of the non-spherical part is more cumbersome. In our model depicted in Fig. 5.2 all charges except that of the central nucleus are included in the charge distribution $\rho(\mathbf{r}')$. Because we are dealing with the point charges the distribution is a sum of Dirac delta functions, i.e.

$$\rho(\mathbf{r}') = \sum_{i=\pm x,\pm y,\pm z} Z^{ext}\delta(\mathbf{r}' - \mathbf{r}_i). \tag{5.27}$$

The calculation can be separated into two parts in a manner similar to the spherical case

$$H'^{ns}_{s\sigma t\tau} = \alpha^2 \sum_{\eta=x,y,z} S^\eta_{\sigma\tau} \sum_{i=\pm x,\pm y,\pm z} (\mathbf{I}_i)_\eta, \tag{5.28}$$

where i indicates the charge in the octahedra surrounding we are dealing with, and η the components of vector variables. The vector $\mathbf{I}_i$ can be evaluated for $i = +z$, which means the charge lying on the z axis in the distance R from origin in the positive direction,

$$\mathbf{I}_{+z} = \int d^3\mathbf{r}\phi^\star_s(\mathbf{r}) \frac{2Z}{|\mathbf{r}-\mathbf{r}_{+z}|^3} \left((\mathbf{r}-\mathbf{r}_{+z})\times\mathbf{p}\right)\phi_t(\mathbf{r}), \tag{5.29}$$

where $\mathbf{r}_{+z} = (0,0,R)$. The momentum operator in the spherical coordinates has the form ($\hbar = 1$)

$$\mathbf{p} = -\imath \begin{pmatrix} \sin\theta\cos\phi\frac{\partial}{\partial r} + \frac{\cos\theta\cos\phi}{r}\frac{\partial}{\partial\theta} - \frac{\sin\phi}{r\sin\theta}\frac{\partial}{\partial\phi} \\ \sin\theta\sin\phi\frac{\partial}{\partial r} + \frac{\cos\theta\sin\phi}{r}\frac{\partial}{\partial\theta} - \frac{\cos\phi}{r\sin\theta}\frac{\partial}{\partial\phi} \\ \cos\theta\frac{\partial}{\partial r} - \frac{\sin\theta}{r}\frac{\partial}{\partial\theta} \end{pmatrix}. \tag{5.30}$$

The most difficult point of the whole calculation is the expansion for the inverse of $|\mathbf{r} - \mathbf{r}_{+z}|^3$. We use the spherical coordinates where $\mathbf{r} = (r, \theta, \phi)$. The inverse-distance expansions are described in Appendix C. The usual expansion defined by Eq. (C.3) does not work, since we have the third power here. One could try to use expression (C.4) but, unfortunately, it yields during the calculation infinite series, which are difficult to deal with. In effect, one has to use the expression

$$\frac{1}{|\mathbf{r} - \mathbf{r}_{+z}|^3} = \sum_{l=0}^{\infty} R_{-3,l}(r, R) P_l(\cos\theta), \tag{5.31}$$

which is the special case of Eq. (C.5). The $R_{-3,l}$ is a rational function of its arguments. P_l is the Legendre polynomial. In connection with the Legendre polynomials included in the wave functions, the integration over θ cancels all terms with $l > 5$. Because of this cancellation, we can compute the values of $\mathbf{I}_{+z}$.

To get the values for the additional charges located in places other than $+z$, we have to rotate the spherical harmonics in a manner similar to the calculation of the crystal field. The rotation of spherical harmonics is described in Appendix H. Nevertheless, one has to be very careful while executing this procedure, as it also mixes the angular momentum components. For each rotation, the initial angular momentum components have to be swapped in such way that after the rotation they are in the correct order.

For both spherical and non-spherical part of the spin-orbit interaction we obtain exact analytic formulas. In the limit $R \to 0$ the non-spherical part goes over into the spherical one. As it is proportional to the charge Z, we obtain a contribution of the order of $(\sum Z^{ext})/Z$, which in case of one and two electrons is respectively 75% and 80% percent. The R dependence of the non-spherical part is an exponential decay multiplied by a rational function. For R in the interval between $3a_0$ and $4a_0$ the magnitude of the non-spherical part is approximately the same for inverse size equal to $\alpha = 1/3$ and 5% of the initial value for $\alpha = 4/3$.

The form of the Hamiltonian matrices for this calculation is much more complicated. For one electron case, it is still possible to obtain analytic expressions for the eigenenergies. For two electrons, it is not possible any more and one has to resort to a numerical diagonalization.

The general form of the results, after including the spin orbit interaction does not change significantly. The difference between these two cases for a single electron is shown in Fig. 5.9. The spin-orbit interaction shifts the ground state by a value of order of 10^{-4} of the initial value. The change in optimal α_{opt} also is not significant. The main is difference is the lifting of the

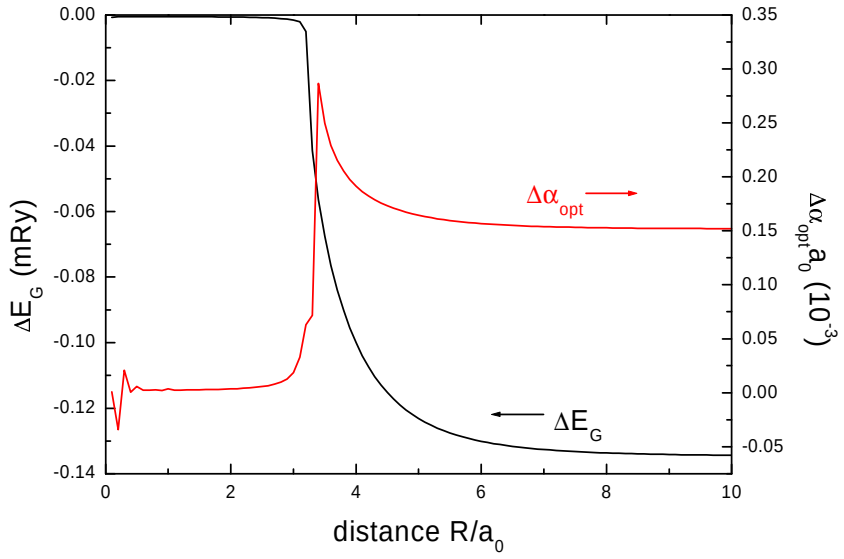

Figure 5.9. Change in the ground-state energy in the octahedral crystal field for a single electron in $3d^1$ configuration under the influence of the spin-orbit coupling. The difference in the optimized ground-state energy and in the optimization parameter α is shown.

ground state degeneracy. The initial 6-fold degenerate state splits up into two lower-laying states and four higher-laying states.

For the two-electron case the results are shown in Fig. 5.10. They show that the change in energy for all 45 states due to the introduction of the spin-orbit interaction as a function of R. One sees that the contribution is larger for larger R when the electrons are located closer to the center. The numerical values of the calculation are shown in Table 5.2. The introduction of the spin-orbit interaction lifts the degeneracy also in this case. This is because in the crystal-field presence the angular momentum is not a good quantum number. The behavior of the spin-orbit splitting for the two-electron case is generally similar to the one-electron case, just analogically, as it was without the spin-orbit interaction (cf. Section 5.1).

Concluding briefly this Chapter one may say that we have shown the EDABI method feasibility in the situation when we consider an atom in an effective potential of the surrounding atoms at nanoscale. The evolution is provided as a function of interatomic distance. Also, the same method can be applied to the arbitrary $3d^n$ configuration with $n > 2$, but the correspond-

Table 5.2. The results for *two electrons* in the crystal field. The optimized ground state energy E_G and the inverse size parameter α_{opt} is displayed. Electron - electron and the spin-orbit interactions are included. The values ΔE_G and $\Delta\alpha_{opt}$ show the difference between the displayed values and the case without the spin-orbit interaction.

R	E_G (Ry)	ΔE_G (mRy)	$\alpha_{opt}a_0$	$\Delta\alpha_{opt}a_0$ (10^{-3})
1	-0.606257	-0.00393101	0.554265	0.00552596
2	-0.640402	-0.00696643	0.636646	0.0172102
3	-1.09376	-0.135879	1.34359	0.142002
4	-1.86717	-0.178994	1.50346	0.0971859
5	-2.42211	-0.192729	1.53612	0.109143
6	-2.81023	-0.208104	1.54477	0.116282
7	-3.09194	-0.220503	1.54756	0.124974
8	-3.30461	-0.233996	1.54867	0.140295
9	-3.47054	-0.25149	1.54919	0.162035
10	-3.60352	-0.273405	1.54946	0.185649

ing Hamiltonian matrices in the Fock space will be of higher dimension. For example, for $N = 3$ electrons we will have $\binom{10}{3} = 120$ three electron states in our Fock subspace. Also, the results can be applied to two concrete situations. First, we can compare the present results with measured crystal field splitting for the Mott insulators containing $3d^n$ configurations. But to perform that fully, we should repeat our calculations also for slightly distorted octahedra because not only the numbers matter, but also the trends of the data, which make the whole picture coherent. This is still before us. Second, we should extend our method to a truly nanoscopic cluster, for example to the nanowire Na_4 or Na_6 or to the cluster e.g. V_4O_9, both measured experimentally and containing correlated electronic states.

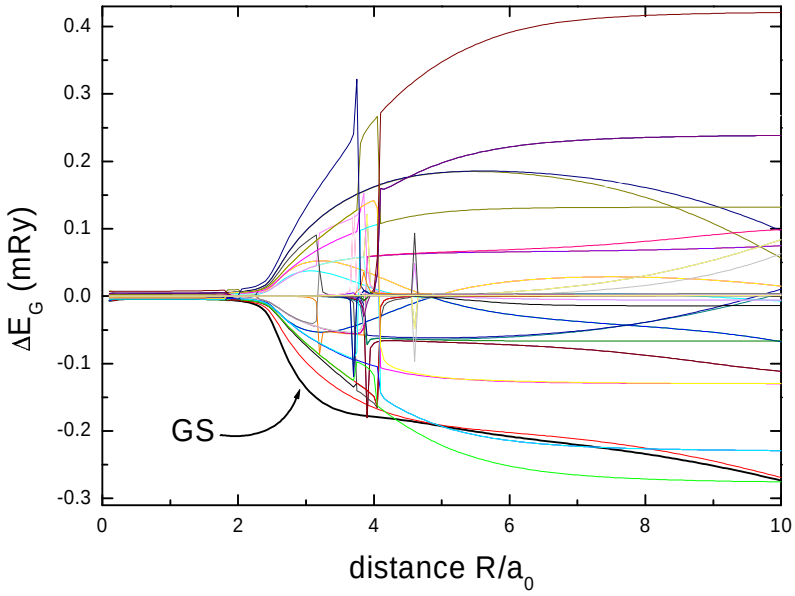

Figure 5.10. The spin-orbit interaction correction (difference between the energy of a state with and without the LS terms in the Hamiltonian) for two electrons in octahedral crystal field for all 45 states. The lines are plotted as a function of the distance R of the crystal-field charges from the center. The peaks are a numerical artifact in the crossover regime, when the parameter α is changing rapidly. The thicker black line shows the corresponding dependence for the ground state.

Chapter 6

Summary and conclusions

In this Thesis we have introduced the formal aspects (cf. Chapter 2) of the original method (EDABI) of calculating the many-electron states microscopically, as well have tested it on the simple examples from atomic (cf. Chapter 3), molecular (cf. Chapter 4), and cluster (cf. 5) quantum physics. Together with the Appendices (A-I), the present Thesis can be seen as a basis to concrete application in nanophysics calculations, though it stops short of providing them. Concrete applications will require additional time, as the formulation of the method to this stage required an extensive reevaluation of the past atomic and molecular approaches to quantum physics. In this reformulation both wave- and particle (matrix)- aspects of quantum theory are intertwined.

Let us summarize briefly the principal original results of the Thesis. In Chapter 2 we extend the equivalence between 1^{st} and 2^{nd} quantization schemes to the formal expressions for the corresponding wave functions in the Hilbert and Fock spaces. One should underline that it follows that to define the quantum state $|\Psi>$ (in the Dirac sense) in the Fock space we need to know the many-particle wave function $\Psi(\mathbf{r}_1, \ldots, \mathbf{r}_N)$ in the Hilbert space, and vice versa. Therefore, the two representations (Fock and Hilbert) are complementary, as is the physical picture of the particles. This formal relation between the representations allowed us, among others, to define the many-body covalency for H_2 molecule. We are not aware of that definition being used in the literature. The truly fundamental feature there is the self-adjusted wave equation, which we are not able so far to solve exactly in any realistic situation.

In Chapter 3 we essentially reproduce the results for simplest two- and three- electron atoms and ions. The method provides rapidly converging results with the enlargement of quantum-mechanical basis for the Fock space, although the extension to including $n = 3$ orbitals would be required to reach

truly quantitative results comparable with the best variational estimates.

In Chapter 4 we study H_2 molecule and H_2^- ion and relate the determination of the ground state and the first excited states to the many-body models of correlated electrons, with explicit calculation of the corresponding microscopic parameters. We also analyze there the situation with the so-called *mobile orbitals*, which decrease the energy of the ground state by about 0.2%. Such displacement of the centers of orbitals with respect to those of their parent nuclei introduces compensating electric dipole moment, which are often present in the solid-state systems, although this topic is beyond the scope of the Thesis.

In Chapter 5 we consider a cluster composed of a central atom with well localized quasiatomic $3d^n$ states ($n = 1, 2$), in the Coulomb field of anions arranged in the octahedral configuration. This calculation is only the first step in truly first-principle crystal-field calculations of nanoclusters. The nontrivial result here is a quantum "phase transition" characterized by an orbital-size jump, here obtained as a function of the distance between the central atom and the surrounding anions. The calculations performed in Chapter 5 show clearly what sort of mixture of analytic and numerical skills we should acquire before approaching the *exact* calculations of both multiple-electron configurations and the single-particle wave function simultaneously.

A separate project resulting from this Thesis should involve creation of a code for calculating the properties of nanoclusters rigorously for any space configuration of atoms.

Appendix A

Spherical harmonics

There are many possible definitions of the Legendre polynomials. They can be defined in terms of a generating function

$$\frac{1}{\sqrt{1-2xt+t^2}} = \sum_{l=0}^{\infty} P_l(x)t^n, \quad |t| < 1. \tag{A.1}$$

They appear in the inverse distance expansion, i.e. in the multipole expansion and in many other physical systems, e.g. the expressions for hydrogen- and hydrogenic- like wave functions. The associated Legendre functions[1] P_l^m are connected to the Legendre polynomials by

$$P_l^m(\mu) = (-1)^m(1-\mu^2)^{m/2}\frac{d^m}{d\mu^m}P_l(\mu), \quad m > 0, \tag{A.2}$$

and for negative m by

$$P_l^{-m}(\mu) = (-1)^m\frac{(l-m)!}{(l+m)!}P_l^m(\mu). \tag{A.3}$$

The orthogonality and the normalization criteria, widely used in this Thesis as a tool of reducing the infinite series, is

$$\int_{-1}^{1} P_l^m(\mu)P_k^m(\mu)d\mu = \frac{2}{2l+1}\frac{(l+m)!}{(l-m)!}\delta_{lk} \tag{A.4}$$

The complex spherical harmonics $Y_{lm}(\theta,\phi)$ can be expressed in terms of the associated Legendre functions $P_l^m(x)$ as follows

$$Y_{lm}(\theta,\phi) = \beta_{lm}P_l^m(\cos\theta)\exp(\imath m\phi), \tag{A.5}$$

[1] They are the solutions of one of the separated parts of Helmholtz equation in spherical coordinates.

where β_{lm} is a normalization constant. In the case we want them to fulfil the normalization criterion

$$\int_{\sigma} Y_{lm}(\mathbf{r}) Y^{\star}_{l'm'}(\mathbf{r}) d\mathbf{r} = \delta_{ll'}\delta_{mm'}, \tag{A.6}$$

we have to set them as

$$\beta_{lm} = \sqrt{\frac{(2l+1)(l-m)!}{4\pi(l+m)!}}.$$

From the definitions it is easily to derive, that the following symmetry relations hold:

$$\begin{aligned} Y^{\star}_{lm} &= (-1)^m Y_{l-m}, \\ Y^{unorm\star}_{lm} &= (-1)^m \frac{(l+m)!}{(l-m)!} Y^{unorm}_{l-m} \\ Y_{lm}(\mathbf{r}) &= (-1)^l Y_{lm}(-\mathbf{r}). \end{aligned} \tag{A.7}$$

Y^{unorm}_{lm} stands here for the not normalized spherical harmonics with $\beta_{lm} = 1$. For further details regarding the Legendre functions and the spherical harmonics, see [45, 46].

Appendix B

Löwdin method of wave-function orthogonalization

There is no unique way to orthogonalize a set of functions. The transformation from a non-orthogonal to an orthogonal set of functions can be achieved to an accuracy, at least of a unitary transformation.

One of the method of orthogonalization is the Löwdin method, which yields symmetrical results. For normalized atomic wave functions the overlap matrix has the diagonal elements equal to unity and off-diagonal, we want to get rid off, equal to S_{ij}. We diagonalize the overlap matrix by a unitary transformation matrix O, such that $O^{\dagger}SO$ is diagonal. Next, we square root and invert the obtained diagonal elements, and then do the inverse O transformation. In this way we define

$$S^{-1/2} = O(O^{\dagger}SO)^{-1/2}O^{\dagger}. \tag{B.1}$$

If we apply this matrix to a vector composed of atomic functions, we get a vector of orthogonal Wannier functions. For infinite systems this may require some refinement [12]. The method of orthogonalization does not change the result, as long as we do not do any subsequent approximations. It helps to simplify the calculations. For spatially extended centers of wave functions we may define the level of orthogonality as a number n, which says that $(n+1)$-th and further neighbor overlaps have been set to zero by hand. This simplifies the orthogonalization process.

Appendix C

Inverse distance expansions

In this Thesis we often use expressions involving powers of the inverse distance between two points. In spherical coordinates, let us define two points $\mathbf{r} = (r, \theta, \phi)$ and $\mathbf{r}' = (r', \theta', \phi')$, with a reference point at a common origin. The inverse distance between $\mathbf{r}$ and $\mathbf{r}'$ is given by the well-known Legendre expansion, which originates directly from the generating function (A.1) of the Legendre polynomials, namely

$$\frac{1}{|\mathbf{r} - \mathbf{r}'|} = r_>^{-1} \sum_{l=0}^{\infty} \left(\frac{r_<}{r_>} \right)^l P_l(\cos \sphericalangle(\mathbf{r}, \mathbf{r}')), \tag{C.1}$$

where $r_<$ and $r_>$ are the minimum and maximum of r and r'. The angle between the vectors $\mathbf{r}$ and $\mathbf{r}'$ is often not very convenient in the calculations, but it can be expressed by the coordinates of each vector using the trigonometric identity

$$\cos \sphericalangle(\mathbf{r}, \mathbf{r}') = \cos\theta \cos\theta' + \sin\theta \sin\theta' \cos(\phi - \phi'). \tag{C.2}$$

Combining this equation with Eq. (C.1) we obtain on the basis of the addition theorem for Legendre functions

$$\frac{1}{|\mathbf{r} - \mathbf{r}'|} = \sum_{l=0}^{\infty} \sum_{m=-l}^{l} \frac{(l - |m|)!}{(l + |m|)!} \left(\frac{r_<}{r_>} \right)^l P_l^{|m|}(\cos\theta) P_l^{|m|}(\cos\theta') e^{\imath m(\phi - \phi')}. \tag{C.3}$$

This expansion is widely used in the determination of the microscopic parameters in this Thesis.

Sometimes, there is a necessity to expand other powers of the inverse distance. There exists a formula [48], which preserves the expansion in powers of $r_</r_>$

$$|\mathbf{r} - \mathbf{r}'|^{-2\nu} = r_>^{-2\nu} \sum_{l=0}^{\infty} \left(\frac{r_<}{r_>} \right)^l C_l^{\nu}(\cos \sphericalangle(\mathbf{r}, \mathbf{r}')), \tag{C.4}$$

where C_l^ν are the Gegenbauer polynomials[1]. Sometimes it is more convenient to preserve the angular dependence expressed through the Legendre polynomials. This is particularly useful when subsequent angular integrations can make all the terms with l larger than a certain value, vanish. There exists such expansion [49]

$$|\mathbf{r}-\mathbf{r}'|^n = \sum_l R_{nl}(r,r')P_l(\cos\sphericalangle(\mathbf{r},\mathbf{r}')). \tag{C.5}$$

The whole expansion is hidden inside the $R_{nl}(r,r')$ functions. To define them we need some preliminary definitions. First,

$$(\alpha)_s = \alpha(\alpha+1)\cdots(\alpha+s-1) = \frac{\Gamma(\alpha+s)}{\Gamma(\alpha)} \tag{C.6}$$

is the Pochhammer symbol, where Γ is the Euler Gamma function. Second, the Gauss' hypergeometric function is defined as

$${}_2F_1(\alpha,\beta;\gamma;x) = \sum_{s=0}^{\infty}\frac{(\alpha)_s(\beta)_s}{(\gamma)_s s!}x^s. \tag{C.7}$$

If the arguments α or β are non-positive integers, then the hypergeometric function is a finite series, i.e. a polynomial in argument x. With the help of above expressions we can write down the formula

$$R_{nl}(r,r') = \frac{(-\frac{1}{2}n)_l}{(\frac{1}{2})_l}r_>^n\left(\frac{r_<}{r_>}\right)^l {}_2F_1(l-\frac{1}{2}n,-\frac{1}{2}(n+1);l+\frac{3}{2};\frac{r_<^2}{r_>^2}). \tag{C.8}$$

In the case, we are interested in in Section 5.2, we have $n=-3$. The first two arguments of the hypergeometric function are positive, which yields an infinite series

$${}_2F_1(l+\frac{3}{2},1;l+\frac{3}{2};\frac{r_<^2}{r_>^2}) = \sum_{s=0}^{\infty}\left(\frac{r_<^2}{r_>^2}\right)^s = \frac{1}{1-\frac{r_<^2}{r_>^2}}, \tag{C.9}$$

which fortunately is a geometric series, and can be recast into a closed form.

There exists also a symmetric definition of R_{nl}, in the sense that there are r' and r instead of $r_<$ and $r_>$ in it. The formula is more complicated, so the splitting of integrals involving this expansion according to Eq. (3.25) is more advisable. For details of the symmetric case, see [49].

[1]They can be regarded as an extension of the Legendre polynomials, their generating function is equal to Formula (A.1) raised to the power 2ν. For $\nu = 1/2$ they are the same.

Appendix D

Analytic formulas for the two-particle interaction parameters

The interaction integrals between two electrons located on atomic hydrogenic-like orbitals centered at the same origin can be evaluated analytically, as described in Section 3.2.2. The orbitals numbered $1 \ldots 5$ are respectively 1s, 2s, 2p0, 2p1, and 2p-1. Each orbital has its own inverse size parameter $\alpha_1 \ldots \alpha_5$. The interaction is defined by Eqs. (3.20) and (3.21). Not all nonzero elements are independent, some permutations of $ijkl$ indices lead to the same parameters. All nonequivalent nonzero V_{ijkl} elements are listed below:

$$V_{1111} = \frac{5\,\alpha_1}{4},$$

$$V_{1112} = \frac{16\,\alpha_1\,(\alpha_1\,\alpha_2)^{\frac{3}{2}}\,(33\,{\alpha_1}^4 - 7\,{\alpha_1}^3\,\alpha_2 - 43\,{\alpha_1}^2\,{\alpha_2}^2 - 21\,\alpha_1\,{\alpha_2}^3 - 2\,{\alpha_2}^4)}{(\alpha_1 + \alpha_2)^3\,(3\,\alpha_1 + \alpha_2)^4},$$

$$V_{1212} = \frac{\alpha_1\,\alpha_2\,({\alpha_1}^4 + 5\,{\alpha_1}^3\,\alpha_2 + 6\,{\alpha_1}^2\,{\alpha_2}^2 + 10\,\alpha_1\,{\alpha_2}^3 + 2\,{\alpha_2}^4)}{(\alpha_1 + \alpha_2)^5},$$

$$V_{1313} = {\alpha_3}^5\left({\alpha_3}^{-4} - \frac{3\,\alpha_1 + \alpha_3}{(\alpha_1 + \alpha_3)^5}\right),$$

$$V_{1515} = 16\,(\alpha_4\,\alpha_5)^{\frac{5}{2}}\left((\alpha_4 + \alpha_5)^{-4} - \frac{6\,\alpha_1 + \alpha_4 + \alpha_5}{(2\,\alpha_1 + \alpha_4 + \alpha_5)^5}\right),$$

$$V_{1122} = \frac{8\,{\alpha_1}^3\,{\alpha_2}^3\,(5\,{\alpha_1}^2 - 15\,\alpha_1\,\alpha_2 + 13\,{\alpha_2}^2)}{(\alpha_1 + \alpha_2)^7},$$

$$V_{1222} = \frac{8\,\alpha_2\,(\alpha_1\,\alpha_2)^{\frac{3}{2}}}{(\alpha_1 + \alpha_2)^3\,(\alpha_1 + 3\,\alpha_2)^6} \times$$

$$\times \left({\alpha_1}^6 + 15\,{\alpha_1}^5\,\alpha_2 + 68\,{\alpha_1}^4\,{\alpha_2}^2 + 170\,{\alpha_1}^3\,{\alpha_2}^3 - 51\,{\alpha_1}^2\,{\alpha_2}^4 - 729\,\alpha_1\,{\alpha_2}^5 - 690\,{\alpha_2}^6\right),$$

$$V_{1323} = \frac{8\,(\alpha_1\,\alpha_2)^{\frac{3}{2}}\,\alpha_3}{(\alpha_1+\alpha_2+2\,\alpha_3)^6} \times$$

$$\left((\alpha_1 - 2\,\alpha_2)\,\left((\alpha_1+\alpha_2)^2 + 12\,(\alpha_1+\alpha_2)\,\alpha_3 + 60\,{\alpha_3}^2 + \frac{160\,{\alpha_3}^3}{\alpha_1+\alpha_2}\right) +\right.$$

$$\left. + (\alpha_1 - \alpha_2)\,\left(\frac{192\,{\alpha_3}^4}{(\alpha_1+\alpha_2)^2} + \frac{64\,{\alpha_3}^5}{(\alpha_1+\alpha_2)^3}\right)\right),$$

$$V_{1525} = \frac{128\,\alpha_4\,\alpha_5\,\sqrt{{\alpha_1}^3\,{\alpha_2}^3\,{\alpha_4}^3\,{\alpha_5}^3}}{(\alpha_1+\alpha_2)^4} \times$$

$$\times \left(\frac{\alpha_1 - 2\,\alpha_2}{(\alpha_4+\alpha_5)^4} + \frac{10\,\alpha_2\,(\alpha_1+\alpha_2)^2}{(\alpha_1+\alpha_2+\alpha_4+\alpha_5)^6} - \frac{2\,(\alpha_1 - 3\,\alpha_2)\,(\alpha_1+\alpha_2)}{(\alpha_1+\alpha_2+\alpha_4+\alpha_5)^5}\right.$$

$$\left. - \frac{\alpha_1 - 2\,\alpha_2}{(\alpha_1+\alpha_2+\alpha_4+\alpha_5)^4}\right),$$

$$V_{1133} = \frac{56\,{\alpha_1}^3\,{\alpha_3}^5}{3\,(\alpha_1+\alpha_3)^7},$$

$$V_{1233} = \frac{-256\,(\alpha_1\,\alpha_2)^{\frac{3}{2}}\,{\alpha_3}^5}{3\,(\alpha_1+\alpha_3)^2\,(\alpha_2+\alpha_3)^3\,(\alpha_1+\alpha_2+2\,\alpha_3)^6} \times$$

$$\times \left(4\,{\alpha_2}^4 + {\alpha_1}^3\,(\alpha_2 - \alpha_3) + 35\,{\alpha_2}^3\,\alpha_3 + 57\,{\alpha_2}^2\,{\alpha_3}^2 + 14\,\alpha_2\,{\alpha_3}^3 - 14\,{\alpha_3}^4 +\right.$$

$$\left. + 3\,{\alpha_1}^2\,(\alpha_2 - \alpha_3)\,(2\,\alpha_2 + 3\,\alpha_3) + 3\,\alpha_1\,\left(8\,{\alpha_2}^3 + 18\,{\alpha_2}^2\,\alpha_3 + 5\,\alpha_2\,{\alpha_3}^2 - 7\,{\alpha_3}^3\right)\right),$$

$$V_{1145} = \frac{256\,{\alpha_1}^3\,(\alpha_4\,\alpha_5)^{\frac{5}{2}}\,\left(7\,{\alpha_1}^2 + {\alpha_4}^2 + 5\,\alpha_4\,\alpha_5 + {\alpha_5}^2 + 7\,\alpha_1\,(\alpha_4+\alpha_5)\right)}{3\,(\alpha_1+\alpha_4)^2\,(\alpha_1+\alpha_5)^2\,(2\,\alpha_1+\alpha_4+\alpha_5)^5},$$

$$V_{1245} = \frac{256\,\alpha_4\,\alpha_5\,\sqrt{{\alpha_1}^3\,{\alpha_2}^3\,{\alpha_4}^3\,{\alpha_5}^3}}{3\,(\alpha_1+\alpha_4)^2\,(\alpha_2+\alpha_5)^3\,(\alpha_1+\alpha_2+\alpha_4+\alpha_5)^6} \times$$

$$\times \left(-\left({\alpha_1}^3\,\alpha_2\right) - 6\,{\alpha_1}^2\,{\alpha_2}^2 - 24\,\alpha_1\,{\alpha_2}^3 - 4\,{\alpha_2}^4 - 3\,{\alpha_1}^2\,\alpha_2\,\alpha_4 - 12\,\alpha_1\,{\alpha_2}^2\,\alpha_4 - 24\,{\alpha_2}^3\,\alpha_4 -\right.$$

$$-3\,\alpha_1\,\alpha_2\,{\alpha_4}^2 - 6\,{\alpha_2}^2\,{\alpha_4}^2 - \alpha_2\,{\alpha_4}^3 + {\alpha_1}^3\,\alpha_5 - 42\,\alpha_1\,{\alpha_2}^2\,\alpha_5 - 11\,{\alpha_2}^3\,\alpha_5 +$$

$$+3\,{\alpha_1}^2\,\alpha_4\,\alpha_5 - 42\,{\alpha_2}^2\,\alpha_4\,\alpha_5 + 3\,\alpha_1\,{\alpha_4}^2\,\alpha_5 + {\alpha_4}^3\,\alpha_5 + 6\,{\alpha_1}^2\,{\alpha_5}^2 - 12\,\alpha_1\,\alpha_2\,{\alpha_5}^2 -$$

$$-9\,{\alpha_2}^2\,{\alpha_5}^2 + 12\,\alpha_1\,\alpha_4\,{\alpha_5}^2 - 12\,\alpha_2\,\alpha_4\,{\alpha_5}^2 + 6\,{\alpha_4}^2\,{\alpha_5}^2 + 6\,\alpha_1\,{\alpha_5}^3$$

$$\left. -\alpha_2\,{\alpha_5}^3 + 6\,\alpha_4\,{\alpha_5}^3 + {\alpha_5}^4\right),$$

$$V_{1254} = \frac{256\,\alpha_4\,\alpha_5\,\sqrt{{\alpha_1}^3\,{\alpha_2}^3\,{\alpha_4}^3\,{\alpha_5}^3}}{3\,(\alpha_1+\alpha_4)^2\,(\alpha_2+\alpha_5)^3\,(\alpha_1+\alpha_2+\alpha_4+\alpha_5)^6} \times$$

$$\times \left(-\left({\alpha_1}^3\,\alpha_2\right) - 6\,{\alpha_1}^2\,{\alpha_2}^2 - 24\,\alpha_1\,{\alpha_2}^3 - 4\,{\alpha_2}^4 + {\alpha_1}^3\,\alpha_4 - 42\,\alpha_1\,{\alpha_2}^2\,\alpha_4 - 11\,{\alpha_2}^3\,\alpha_4 +\right.$$

$$+6\,{\alpha_1}^2\,{\alpha_4}^2 - 12\,\alpha_1\,\alpha_2\,{\alpha_4}^2 - 9\,{\alpha_2}^2\,{\alpha_4}^2 + 6\,\alpha_1\,{\alpha_4}^3 - \alpha_2\,{\alpha_4}^3 + {\alpha_4}^4 - 3\,{\alpha_1}^2\,\alpha_2\,\alpha_5 -$$

$$-12\,\alpha_1\,{\alpha_2}^2\,\alpha_5 - 24\,{\alpha_2}^3\,\alpha_5 + 3\,{\alpha_1}^2\,\alpha_4\,\alpha_5 - 42\,{\alpha_2}^2\,\alpha_4\,\alpha_5 + 12\,\alpha_1\,{\alpha_4}^2\,\alpha_5 - 12\,\alpha_2\,{\alpha_4}^2\,\alpha_5 +$$

$$+ 6\,{\alpha_4}^3\,\alpha_5 - 3\,\alpha_1\,\alpha_2\,{\alpha_5}^2 - 6\,{\alpha_2}^2\,{\alpha_5}^2 + 3\,\alpha_1\,\alpha_4\,{\alpha_5}^2 + 6\,{\alpha_4}^2\,{\alpha_5}^2 - \alpha_2\,{\alpha_5}^3 + \alpha_4\,{\alpha_5}^3\big),$$

$$V_{2222} = \frac{77\,\alpha_2}{128},$$

$$V_{2323} = \frac{\alpha_2\,\alpha_3\,\left({\alpha_2}^6 + 7\,{\alpha_2}^5\,\alpha_3 + 21\,{\alpha_2}^4\,{\alpha_3}^2 + 35\,{\alpha_2}^3\,{\alpha_3}^3 + 11\,{\alpha_2}^2\,{\alpha_3}^4 + 7\,\alpha_2\,{\alpha_3}^5 + {\alpha_3}^6\right)}{\left(\alpha_2 + \alpha_3\right)^7},$$

$$V_{2525} = 16\,\left(\alpha_4\,\alpha_5\right)^{\frac{5}{2}} \times$$

$$\times \left(\left(\alpha_4 + \alpha_5\right)^{-4} - \frac{\left(8\,\alpha_2 + \alpha_4 + \alpha_5\right)\,\left(24\,{\alpha_2}^2 + 4\,\alpha_2\,\left(\alpha_4 + \alpha_5\right) + \left(\alpha_4 + \alpha_5\right)^2\right)}{\left(2\,\alpha_2 + \alpha_4 + \alpha_5\right)^7}\right),$$

$$V_{2233} = \frac{4\,{\alpha_2}^3\,{\alpha_3}^5\,\left(101\,{\alpha_2}^2 - 70\,\alpha_2\,\alpha_3 + 14\,{\alpha_3}^2\right)}{3\,\left(\alpha_2 + \alpha_3\right)^9},$$

$$V_{2245} = \frac{256\,{\alpha_2}^3\,\left(\alpha_4\,\alpha_5\right)^{\frac{5}{2}}}{3\,\left(\alpha_2 + \alpha_4\right)^3\,\left(\alpha_2 + \alpha_5\right)^3\,\left(2\,\alpha_2 + \alpha_4 + \alpha_5\right)^7} \times$$

$$\times \big(202\,{\alpha_2}^6 + 334\,{\alpha_2}^5\,\alpha_4 + 133\,{\alpha_2}^4\,{\alpha_4}^2 - 13\,{\alpha_2}^3\,{\alpha_4}^3 - 7\,{\alpha_2}^2\,{\alpha_4}^4 - \alpha_2\,{\alpha_4}^5 + 334\,{\alpha_2}^5\,\alpha_5 +$$

$$+414\,{\alpha_2}^4\,\alpha_4\,\alpha_5 + 53\,{\alpha_2}^3\,{\alpha_4}^2\,\alpha_5 - 58\,{\alpha_2}^2\,{\alpha_4}^3\,\alpha_5 + {\alpha_4}^5\,\alpha_5 + 133\,{\alpha_2}^4\,{\alpha_5}^2 + 53\,{\alpha_2}^3\,\alpha_4\,{\alpha_5}^2 -$$

$$-60\,{\alpha_2}^2\,{\alpha_4}^2\,{\alpha_5}^2 - 13\,\alpha_2\,{\alpha_4}^3\,{\alpha_5}^2 + 7\,{\alpha_4}^4\,{\alpha_5}^2 - 13\,{\alpha_2}^3\,{\alpha_5}^3 - 58\,{\alpha_2}^2\,\alpha_4\,{\alpha_5}^3 -$$

$$+13\,\alpha_2\,{\alpha_4}^2\,{\alpha_5}^3 + 12\,{\alpha_4}^3\,{\alpha_5}^3 - 7\,{\alpha_2}^2\,{\alpha_5}^4 + 7\,{\alpha_4}^2\,{\alpha_5}^4 - \alpha_2\,{\alpha_5}^5 + \alpha_4\,{\alpha_5}^5\big),$$

$$V_{3333} = \frac{501\,\alpha_3}{640},$$

$$V_{3535} = \frac{16\,\left(\alpha_4\,\alpha_5\right)^{\frac{5}{2}}}{\left(2\,\alpha_3 + \alpha_4 + \alpha_5\right)^7} \times$$

$$\times \left(\frac{824\,{\alpha_3}^3}{5} + \frac{128\,{\alpha_3}^7}{\left(\alpha_4 + \alpha_5\right)^4} + \frac{448\,{\alpha_3}^6}{\left(\alpha_4 + \alpha_5\right)^3} + \frac{3296\,{\alpha_3}^5}{5\,\left(\alpha_4 + \alpha_5\right)^2} +\right.$$

$$\left. + \frac{2576\,{\alpha_3}^4}{5\,\left(\alpha_4 + \alpha_5\right)} + 28\,{\alpha_3}^2\,\left(\alpha_4 + \alpha_5\right) + 2\,\alpha_3\,\left(\alpha_4 + \alpha_5\right)^2\right),$$

$$V_{3345} = \frac{1536\,{\alpha_3}^5\,\left(\alpha_4\,\alpha_5\right)^{\frac{5}{2}}\,\left(9\,{\alpha_3}^2 + {\alpha_4}^2 + 7\,\alpha_4\,\alpha_5 + {\alpha_5}^2 + 9\,\alpha_3\,\left(\alpha_4 + \alpha_5\right)\right)}{5\,\left(\alpha_3 + \alpha_4\right)^2\,\left(\alpha_3 + \alpha_5\right)^2\,\left(2\,\alpha_3 + \alpha_4 + \alpha_5\right)^7},$$

$$V_{5445} = \frac{6\,{\alpha_4}^3\,{\alpha_5}^3\,\left({\alpha_4}^2 + 7\,\alpha_4\,\alpha_5 + {\alpha_5}^2\right)}{5\,\left(\alpha_4 + \alpha_5\right)^7},$$

$$V_{5555} = \frac{1896\,{\alpha_4}^5\,{\alpha_5}^5}{5\,\left(\alpha_4 + \alpha_5\right)^9}.$$

Appendix E

Fock space states for He.

The complete spectrum of states for the He atom for the case with 5 orbitals. All 45 energy levels together with the corresponding multiparticle states are shown. The creation operators $\tilde{a}^{\dagger}$ correspond to the atomic orbitals not the Wannier functions.

$E_1 = -5.79404,$
$|1> = -0.82274\,\tilde{a}^{\dagger}_{1s\downarrow}\,\tilde{a}^{\dagger}_{1s\uparrow} - 0.404512\,\tilde{a}^{\dagger}_{1s\uparrow}\,\tilde{a}^{\dagger}_{2s\downarrow} + 0.309636\,\tilde{a}^{\dagger}_{1s\downarrow}\,\tilde{a}^{\dagger}_{2s\uparrow}$
$-0.021729\,\tilde{a}^{\dagger}_{2s\downarrow}\,\tilde{a}^{\dagger}_{2s\uparrow} + 0.0357708\,\tilde{a}^{\dagger}_{2p0\downarrow}\,\tilde{a}^{\dagger}_{2p0\uparrow} - 0.0357641\,\tilde{a}^{\dagger}_{2p1\uparrow}\,\tilde{a}^{\dagger}_{2p-1\downarrow}$
$+0.0357641\,\tilde{a}^{\dagger}_{2p1\downarrow}\,\tilde{a}^{\dagger}_{2p-1\uparrow}|0>,$
$E_2 = -2.36898,$
$|2> = -0.727924\,\tilde{a}^{\dagger}_{1s\uparrow}\,\tilde{a}^{\dagger}_{2s\downarrow} - 0.727924\,\tilde{a}^{\dagger}_{1s\downarrow}\,\tilde{a}^{\dagger}_{2s\uparrow} - 1.53385\,10^{-6}\,\tilde{a}^{\dagger}_{2p1\uparrow}\,\tilde{a}^{\dagger}_{2p-1\downarrow}$
$-1.53385\,10^{-6}\,\tilde{a}^{\dagger}_{2p1\downarrow}\,\tilde{a}^{\dagger}_{2p-1\uparrow}|0>,$
$E_3 = -2.36898,$
$|3> = 1.02944\,\tilde{a}^{\dagger}_{1s\uparrow}\,\tilde{a}^{\dagger}_{2s\uparrow} + 2.16919\,10^{-6}\,\tilde{a}^{\dagger}_{2p1\uparrow}\,\tilde{a}^{\dagger}_{2p-1\uparrow}|0>,$
$E_4 = -2.36898,$
$|4> = -1.02944\,\tilde{a}^{\dagger}_{1s\downarrow}\,\tilde{a}^{\dagger}_{2s\downarrow} + 8.76031\,10^{-18}\,\tilde{a}^{\dagger}_{1s\uparrow}\,\tilde{a}^{\dagger}_{2p-1\downarrow} + 1.21637\,10^{-18}\,\tilde{a}^{\dagger}_{2s\uparrow}\,\tilde{a}^{\dagger}_{2p-1\downarrow}$
$-2.16919\,10^{-6}\,\tilde{a}^{\dagger}_{2p1\downarrow}\,\tilde{a}^{\dagger}_{2p-1\downarrow} + 8.76031\,10^{-18}\,\tilde{a}^{\dagger}_{1s\downarrow}\,\tilde{a}^{\dagger}_{2p-1\uparrow}$
$+1.21637\,10^{-18}\,\tilde{a}^{\dagger}_{2s\downarrow}\,\tilde{a}^{\dagger}_{2p-1\uparrow}|0>,$
$E_5 = -1.37035,$
$|5> = 0.567495\,\tilde{a}^{\dagger}_{1s\downarrow}\,\tilde{a}^{\dagger}_{1s\uparrow} - 0.381789\,\tilde{a}^{\dagger}_{1s\uparrow}\,\tilde{a}^{\dagger}_{2s\downarrow} + 0.53849\,\tilde{a}^{\dagger}_{1s\downarrow}\,\tilde{a}^{\dagger}_{2s\uparrow}$
$-0.433411\,\tilde{a}^{\dagger}_{2s\downarrow}\,\tilde{a}^{\dagger}_{2s\uparrow} - 0.00910772\,\tilde{a}^{\dagger}_{2p0\downarrow}\,\tilde{a}^{\dagger}_{2p0\uparrow} + 0.00912602\,\tilde{a}^{\dagger}_{2p1\uparrow}\,\tilde{a}^{\dagger}_{2p-1\downarrow}$
$-0.00912602\,\tilde{a}^{\dagger}_{2p1\downarrow}\,\tilde{a}^{\dagger}_{2p-1\uparrow}|0>,$
$E_6 = -1.26427,$

$$|6>= -0.895812\,\tilde{a}^{\dagger}_{1s\downarrow}\,\tilde{a}^{\dagger}_{2p0\downarrow} + 0.262975\,\tilde{a}^{\dagger}_{2s\downarrow}\,\tilde{a}^{\dagger}_{2p0\downarrow} - 1.47163\,10^{-17}\,\tilde{a}^{\dagger}_{1s\uparrow}\,\tilde{a}^{\dagger}_{2p-1\downarrow}$$
$$-2.04336\,10^{-18}\,\tilde{a}^{\dagger}_{2s\uparrow}\,\tilde{a}^{\dagger}_{2p-1\downarrow} + 1.47163\,10^{-17}\,\tilde{a}^{\dagger}_{1s\downarrow}\,\tilde{a}^{\dagger}_{2p-1\uparrow}$$
$$+2.04336\,10^{-18}\,\tilde{a}^{\dagger}_{2s\downarrow}\,\tilde{a}^{\dagger}_{2p-1\uparrow}|0>,$$
$$E_7 = -1.26427,$$
$$|7>= -0.633435\,\tilde{a}^{\dagger}_{1s\uparrow}\,\tilde{a}^{\dagger}_{2p0\downarrow} + 0.185951\,\tilde{a}^{\dagger}_{2s\uparrow}\,\tilde{a}^{\dagger}_{2p0\downarrow} - 0.633435\,\tilde{a}^{\dagger}_{1s\downarrow}\,\tilde{a}^{\dagger}_{2p0\uparrow}$$
$$+0.185951\,\tilde{a}^{\dagger}_{2s\downarrow}\,\tilde{a}^{\dagger}_{2p0\uparrow}|0>,$$
$$E_8 = -1.26427,$$
$$|8>= -0.895812\,\tilde{a}^{\dagger}_{1s\uparrow}\,\tilde{a}^{\dagger}_{2p0\uparrow} + 0.262975\,\tilde{a}^{\dagger}_{2s\uparrow}\,\tilde{a}^{\dagger}_{2p0\uparrow}|0>,$$
$$E_9 = -1.26273,$$
$$|9>= 1.14407\,10^{-17}\,\tilde{a}^{\dagger}_{1s\downarrow}\,\tilde{a}^{\dagger}_{2s\downarrow} - 7.06025\,10^{-17}\,\tilde{a}^{\dagger}_{1s\downarrow}\,\tilde{a}^{\dagger}_{2p-1\downarrow} - 0.633428\,\tilde{a}^{\dagger}_{1s\uparrow}\,\tilde{a}^{\dagger}_{2p-1\downarrow}$$
$$-9.80316\,10^{-18}\,\tilde{a}^{\dagger}_{2s\downarrow}\,\tilde{a}^{\dagger}_{2p-1\downarrow} + 0.185964\,\tilde{a}^{\dagger}_{2s\uparrow}\,\tilde{a}^{\dagger}_{2p-1\downarrow} - 0.633428\,\tilde{a}^{\dagger}_{1s\downarrow}\,\tilde{a}^{\dagger}_{2p-1\uparrow}$$
$$+0.185964\,\tilde{a}^{\dagger}_{2s\downarrow}\,\tilde{a}^{\dagger}_{2p-1\uparrow}|0>,$$
$$E_{10} = -1.26273,$$
$$|10>= 4.97198\,10^{-33}\,\tilde{a}^{\dagger}_{1s\downarrow}\,\tilde{a}^{\dagger}_{2s\downarrow} - 0.895803\,\tilde{a}^{\dagger}_{1s\downarrow}\,\tilde{a}^{\dagger}_{2p-1\downarrow} - 4.99235\,10^{-17}\,\tilde{a}^{\dagger}_{1s\uparrow}\,\tilde{a}^{\dagger}_{2p-1\downarrow}$$
$$+0.262993\,\tilde{a}^{\dagger}_{2s\downarrow}\,\tilde{a}^{\dagger}_{2p-1\downarrow} - 6.93188\,10^{-18}\,\tilde{a}^{\dagger}_{2s\uparrow}\,\tilde{a}^{\dagger}_{2p-1\downarrow} - 4.99235\,10^{-17}\,\tilde{a}^{\dagger}_{1s\downarrow}\,\tilde{a}^{\dagger}_{2p-1\uparrow}$$
$$-7.06025\,10^{-17}\,\tilde{a}^{\dagger}_{1s\uparrow}\,\tilde{a}^{\dagger}_{2p-1\uparrow} - 6.93188\,10^{-18}\,\tilde{a}^{\dagger}_{2s\downarrow}\,\tilde{a}^{\dagger}_{2p-1\uparrow} - 9.80316\,10^{-18}\,\tilde{a}^{\dagger}_{2s\uparrow}\,\tilde{a}^{\dagger}_{2p-1\uparrow}|0>,$$
$$E_{11} = -1.26273,$$
$$|11>= 1.21485\,10^{-49}\,\tilde{a}^{\dagger}_{1s\downarrow}\,\tilde{a}^{\dagger}_{2s\downarrow} - 1.40484\,10^{-16}\,\tilde{a}^{\dagger}_{1s\downarrow}\,\tilde{a}^{\dagger}_{2p-1\downarrow} - 1.05189\,10^{-33}\,\tilde{a}^{\dagger}_{1s\uparrow}\,\tilde{a}^{\dagger}_{2p-1\downarrow}$$
$$-1.95061\,10^{-17}\,\tilde{a}^{\dagger}_{2s\downarrow}\,\tilde{a}^{\dagger}_{2p-1\downarrow} - 1.46054\,10^{-34}\,\tilde{a}^{\dagger}_{2s\uparrow}\,\tilde{a}^{\dagger}_{2p-1\downarrow} - 1.05189\,10^{-33}\,\tilde{a}^{\dagger}_{1s\downarrow}\,\tilde{a}^{\dagger}_{2p-1\uparrow}$$
$$+0.895803\,\tilde{a}^{\dagger}_{1s\uparrow}\,\tilde{a}^{\dagger}_{2p-1\uparrow} - 1.46054\,10^{-34}\,\tilde{a}^{\dagger}_{2s\downarrow}\,\tilde{a}^{\dagger}_{2p-1\uparrow} - 0.262993\,\tilde{a}^{\dagger}_{2s\uparrow}\,\tilde{a}^{\dagger}_{2p-1\uparrow}|0>,$$
$$E_{12} = -1.26214,$$
$$|12>= -0.633427\,\tilde{a}^{\dagger}_{1s\uparrow}\,\tilde{a}^{\dagger}_{2p1\downarrow} + 0.185967\,\tilde{a}^{\dagger}_{2s\uparrow}\,\tilde{a}^{\dagger}_{2p1\downarrow} - 0.633427\,\tilde{a}^{\dagger}_{1s\downarrow}\,\tilde{a}^{\dagger}_{2p1\uparrow}$$
$$+0.185967\,\tilde{a}^{\dagger}_{2s\downarrow}\,\tilde{a}^{\dagger}_{2p1\uparrow}|0>,$$
$$E_{13} = -1.26214,$$
$$|13>= -0.895801\,\tilde{a}^{\dagger}_{1s\uparrow}\,\tilde{a}^{\dagger}_{2p1\uparrow} + 0.262996\,\tilde{a}^{\dagger}_{2s\uparrow}\,\tilde{a}^{\dagger}_{2p1\uparrow}|0>,$$
$$E_{14} = -1.26214,$$
$$|14>= -0.895801\,\tilde{a}^{\dagger}_{1s\downarrow}\,\tilde{a}^{\dagger}_{2p1\downarrow} + 0.262996\,\tilde{a}^{\dagger}_{2s\downarrow}\,\tilde{a}^{\dagger}_{2p1\downarrow}|0>,$$
$$E_{15} = -0.516353,$$
$$|15>= -0.628776\,\tilde{a}^{\dagger}_{1s\uparrow}\,\tilde{a}^{\dagger}_{2p0\downarrow} + 0.194735\,\tilde{a}^{\dagger}_{2s\uparrow}\,\tilde{a}^{\dagger}_{2p0\downarrow} + 0.628776\,\tilde{a}^{\dagger}_{1s\downarrow}\,\tilde{a}^{\dagger}_{2p0\uparrow}$$
$$-0.194735\,\tilde{a}^{\dagger}_{2s\downarrow}\,\tilde{a}^{\dagger}_{2p0\uparrow}|0>,$$
$$E_{16} = -0.514665,$$
$$|16>= -6.91877\,10^{-18}\,\tilde{a}^{\dagger}_{1s\downarrow}\,\tilde{a}^{\dagger}_{2p0\downarrow} - 4.98291\,10^{-17}\,\tilde{a}^{\dagger}_{2s\downarrow}\,\tilde{a}^{\dagger}_{2p0\downarrow} + 0.628746\,\tilde{a}^{\dagger}_{1s\uparrow}\,\tilde{a}^{\dagger}_{2p-1\downarrow}$$

$-0.194789\,\tilde{a}^{\dagger}_{2s\uparrow}\,\tilde{a}^{\dagger}_{2p-1\downarrow} - 0.628746\,\tilde{a}^{\dagger}_{1s\downarrow}\,\tilde{a}^{\dagger}_{2p-1\uparrow} + 0.194789\,\tilde{a}^{\dagger}_{2s\downarrow}\,\tilde{a}^{\dagger}_{2p-1\uparrow}|0>,$

$E_{17} = -0.514078,$

$|17> = -0.628748\,\tilde{a}^{\dagger}_{1s\uparrow}\,\tilde{a}^{\dagger}_{2p1\downarrow} + 0.194787\,\tilde{a}^{\dagger}_{2s\uparrow}\,\tilde{a}^{\dagger}_{2p1\downarrow} + 0.628748\,\tilde{a}^{\dagger}_{1s\downarrow}\,\tilde{a}^{\dagger}_{2p1\uparrow}$
$-0.194787\,\tilde{a}^{\dagger}_{2s\downarrow}\,\tilde{a}^{\dagger}_{2p1\uparrow}|0>,$

$E_{18} = 2.15918,$

$|18> = -0.23304\,\tilde{a}^{\dagger}_{1s\downarrow}\,\tilde{a}^{\dagger}_{1s\uparrow} + 0.490265\,\tilde{a}^{\dagger}_{1s\uparrow}\,\tilde{a}^{\dagger}_{2s\downarrow} - 0.404797\,\tilde{a}^{\dagger}_{1s\downarrow}\,\tilde{a}^{\dagger}_{2s\uparrow}$
$-0.952009\,\tilde{a}^{\dagger}_{2s\downarrow}\,\tilde{a}^{\dagger}_{2s\uparrow} + 0.0499905\,\tilde{a}^{\dagger}_{2p0\downarrow}\,\tilde{a}^{\dagger}_{2p0\uparrow} - 0.0499032\,\tilde{a}^{\dagger}_{2p1\uparrow}\,\tilde{a}^{\dagger}_{2p-1\downarrow}$
$+0.0499032\,\tilde{a}^{\dagger}_{2p1\downarrow}\,\tilde{a}^{\dagger}_{2p-1\uparrow}|0>,$

$E_{19} = 2.85271,$

$|19> = 0.526972\,\tilde{a}^{\dagger}_{1s\downarrow}\,\tilde{a}^{\dagger}_{2p0\downarrow} + 1.0055\,\tilde{a}^{\dagger}_{2s\downarrow}\,\tilde{a}^{\dagger}_{2p0\downarrow} - 3.54205\,10^{-17}\,\tilde{a}^{\dagger}_{1s\uparrow}\,\tilde{a}^{\dagger}_{2p-1\downarrow}$
$-4.91813\,10^{-18}\,\tilde{a}^{\dagger}_{2s\uparrow}\,\tilde{a}^{\dagger}_{2p-1\downarrow} + 3.54205\,10^{-17}\,\tilde{a}^{\dagger}_{1s\downarrow}\,\tilde{a}^{\dagger}_{2p-1\uparrow}$
$+4.91813\,10^{-18}\,\tilde{a}^{\dagger}_{2s\downarrow}\,\tilde{a}^{\dagger}_{2p-1\uparrow}|0>,$

$E_{20} = 2.85271,$

$|20> = 0.526972\,\tilde{a}^{\dagger}_{1s\uparrow}\,\tilde{a}^{\dagger}_{2p0\uparrow} + 1.0055\,\tilde{a}^{\dagger}_{2s\uparrow}\,\tilde{a}^{\dagger}_{2p0\uparrow}|0>,$

$E_{21} = 2.85271,$

$|21> = 0.372625\,\tilde{a}^{\dagger}_{1s\uparrow}\,\tilde{a}^{\dagger}_{2p0\downarrow} + 0.710993\,\tilde{a}^{\dagger}_{2s\uparrow}\,\tilde{a}^{\dagger}_{2p0\downarrow} + 0.372625\,\tilde{a}^{\dagger}_{1s\downarrow}\,\tilde{a}^{\dagger}_{2p0\uparrow}$
$+0.710993\,\tilde{a}^{\dagger}_{2s\downarrow}\,\tilde{a}^{\dagger}_{2p0\uparrow}|0>,$

$E_{22} = 2.85425,$

$|22> = 5.04768\,10^{-50}\,\tilde{a}^{\dagger}_{1s\downarrow}\,\tilde{a}^{\dagger}_{2s\downarrow} - 5.83709\,10^{-17}\,\tilde{a}^{\dagger}_{1s\downarrow}\,\tilde{a}^{\dagger}_{2p-1\downarrow} - 4.37058\,10^{-34}\,\tilde{a}^{\dagger}_{1s\uparrow}\,\tilde{a}^{\dagger}_{2p-1\downarrow}$
$-8.10479\,10^{-18}\,\tilde{a}^{\dagger}_{2s\downarrow}\,\tilde{a}^{\dagger}_{2p-1\downarrow} - 6.06855\,10^{-35}\,\tilde{a}^{\dagger}_{2s\uparrow}\,\tilde{a}^{\dagger}_{2p-1\downarrow} - 4.37058\,10^{-34}\,\tilde{a}^{\dagger}_{1s\downarrow}\,\tilde{a}^{\dagger}_{2p-1\uparrow}$
$+0.526991\,\tilde{a}^{\dagger}_{1s\uparrow}\,\tilde{a}^{\dagger}_{2p-1\uparrow} - 6.06855\,10^{-35}\,\tilde{a}^{\dagger}_{2s\downarrow}\,\tilde{a}^{\dagger}_{2p-1\uparrow} + 1.00549\,\tilde{a}^{\dagger}_{2s\uparrow}\,\tilde{a}^{\dagger}_{2p-1\uparrow}|0>,$

$E_{23} = 2.85425,$

$|23> = -2.06586\,10^{-33}\,\tilde{a}^{\dagger}_{1s\downarrow}\,\tilde{a}^{\dagger}_{2s\downarrow} + 0.526991\,\tilde{a}^{\dagger}_{1s\downarrow}\,\tilde{a}^{\dagger}_{2p-1\downarrow} + 2.07432\,10^{-17}\,\tilde{a}^{\dagger}_{1s\uparrow}\,\tilde{a}^{\dagger}_{2p-1\downarrow}$
$+1.00549\,\tilde{a}^{\dagger}_{2s\downarrow}\,\tilde{a}^{\dagger}_{2p-1\downarrow} + 2.88019\,10^{-18}\,\tilde{a}^{\dagger}_{2s\uparrow}\,\tilde{a}^{\dagger}_{2p-1\downarrow} + 2.07432\,10^{-17}\,\tilde{a}^{\dagger}_{1s\downarrow}\,\tilde{a}^{\dagger}_{2p-1\uparrow}$
$+2.93353\,10^{-17}\,\tilde{a}^{\dagger}_{1s\uparrow}\,\tilde{a}^{\dagger}_{2p-1\uparrow} + 2.88019\,10^{-18}\,\tilde{a}^{\dagger}_{2s\downarrow}\,\tilde{a}^{\dagger}_{2p-1\uparrow} + 4.07321\,10^{-18}\,\tilde{a}^{\dagger}_{2s\uparrow}\,\tilde{a}^{\dagger}_{2p-1\uparrow}|0>,$

$E_{24} = 2.85425,$

$|24> = -4.75361\,10^{-18}\,\tilde{a}^{\dagger}_{1s\downarrow}\,\tilde{a}^{\dagger}_{2s\downarrow} + 2.93353\,10^{-17}\,\tilde{a}^{\dagger}_{1s\downarrow}\,\tilde{a}^{\dagger}_{2p-1\downarrow} + 0.372639\,\tilde{a}^{\dagger}_{1s\uparrow}\,\tilde{a}^{\dagger}_{2p-1\downarrow}$
$+4.07321\,10^{-18}\,\tilde{a}^{\dagger}_{2s\downarrow}\,\tilde{a}^{\dagger}_{2p-1\downarrow} + 0.710989\,\tilde{a}^{\dagger}_{2s\uparrow}\,\tilde{a}^{\dagger}_{2p-1\downarrow} + 0.372639\,\tilde{a}^{\dagger}_{1s\downarrow}\,\tilde{a}^{\dagger}_{2p-1\uparrow}$
$+0.710989\,\tilde{a}^{\dagger}_{2s\downarrow}\,\tilde{a}^{\dagger}_{2p-1\uparrow}|0>,$

$E_{25} = 2.85483,$

$|25> = 0.526988\,\tilde{a}^{\dagger}_{1s\downarrow}\,\tilde{a}^{\dagger}_{2p1\downarrow} + 1.00549\,\tilde{a}^{\dagger}_{2s\downarrow}\,\tilde{a}^{\dagger}_{2p1\downarrow}|0>,$

$E_{26} = 2.85483,$

$$|26>= 0.526988\,\tilde{a}^{\dagger}_{1s\uparrow}\,\tilde{a}^{\dagger}_{2p1\uparrow} + 1.00549\,\tilde{a}^{\dagger}_{2s\uparrow}\,\tilde{a}^{\dagger}_{2p1\uparrow}|0>,$$
$$E_{27} = 2.85483,$$
$$|27>= 0.372637\,\tilde{a}^{\dagger}_{1s\uparrow}\,\tilde{a}^{\dagger}_{2p1\downarrow} + 0.71099\,\tilde{a}^{\dagger}_{2s\uparrow}\,\tilde{a}^{\dagger}_{2p1\downarrow} + 0.372637\,\tilde{a}^{\dagger}_{1s\downarrow}\,\tilde{a}^{\dagger}_{2p1\uparrow}$$
$$+0.71099\,\tilde{a}^{\dagger}_{2s\downarrow}\,\tilde{a}^{\dagger}_{2p1\uparrow}|0>,$$
$$E_{28} = 3.02981,$$
$$|28>= 0.380435\,\tilde{a}^{\dagger}_{1s\uparrow}\,\tilde{a}^{\dagger}_{2p0\downarrow} + 0.708638\,\tilde{a}^{\dagger}_{2s\uparrow}\,\tilde{a}^{\dagger}_{2p0\downarrow} - 0.380435\,\tilde{a}^{\dagger}_{1s\downarrow}\,\tilde{a}^{\dagger}_{2p0\uparrow}$$
$$-0.708638\,\tilde{a}^{\dagger}_{2s\downarrow}\,\tilde{a}^{\dagger}_{2p0\uparrow}|0>,$$
$$E_{29} = 3.03136,$$
$$|29>= -2.9761\,10^{-18}\,\tilde{a}^{\dagger}_{1s\downarrow}\,\tilde{a}^{\dagger}_{2p0\downarrow} - 2.14339\,10^{-17}\,\tilde{a}^{\dagger}_{2s\downarrow}\,\tilde{a}^{\dagger}_{2p0\downarrow} + 0.380481\,\tilde{a}^{\dagger}_{1s\uparrow}\,\tilde{a}^{\dagger}_{2p-1\downarrow}$$
$$+0.708624\,\tilde{a}^{\dagger}_{2s\uparrow}\,\tilde{a}^{\dagger}_{2p-1\downarrow} - 0.380481\,\tilde{a}^{\dagger}_{1s\downarrow}\,\tilde{a}^{\dagger}_{2p-1\uparrow}$$
$$-0.708624\,\tilde{a}^{\dagger}_{2s\downarrow}\,\tilde{a}^{\dagger}_{2p-1\uparrow}|0>,$$
$$E_{30} = 3.03195,$$
$$|30>= 0.380483\,\tilde{a}^{\dagger}_{1s\uparrow}\,\tilde{a}^{\dagger}_{2p1\downarrow} + 0.708623\,\tilde{a}^{\dagger}_{2s\uparrow}\,\tilde{a}^{\dagger}_{2p1\downarrow} - 0.380483\,\tilde{a}^{\dagger}_{1s\downarrow}\,\tilde{a}^{\dagger}_{2p1\uparrow}$$
$$-0.708623\,\tilde{a}^{\dagger}_{2s\downarrow}\,\tilde{a}^{\dagger}_{2p1\uparrow}|0>,$$
$$E_{31} = 3.86792,$$
$$|31>= 1.\,\tilde{a}^{\dagger}_{2p0\downarrow}\,\tilde{a}^{\dagger}_{2p-1\downarrow}|0>,$$
$$E_{32} = 3.86792,$$
$$|32>= 1.\,\tilde{a}^{\dagger}_{2p0\uparrow}\,\tilde{a}^{\dagger}_{2p-1\uparrow}|0>,$$
$$E_{33} = 3.86792,$$
$$|33>= 0.707107\,\tilde{a}^{\dagger}_{2p0\uparrow}\,\tilde{a}^{\dagger}_{2p-1\downarrow} + 0.707107\,\tilde{a}^{\dagger}_{2p0\downarrow}\,\tilde{a}^{\dagger}_{2p-1\uparrow}|0>,$$
$$E_{34} = 3.86851,$$
$$|34>= 1.\,\tilde{a}^{\dagger}_{2p0\downarrow}\,\tilde{a}^{\dagger}_{2p1\downarrow}|0>,$$
$$E_{35} = 3.86851,$$
$$|35>= 1.\,\tilde{a}^{\dagger}_{2p0\uparrow}\,\tilde{a}^{\dagger}_{2p1\uparrow}|0>,$$
$$E_{36} = 3.86851,$$
$$|36>= 0.707107\,\tilde{a}^{\dagger}_{2p0\uparrow}\,\tilde{a}^{\dagger}_{2p1\downarrow} + 0.707107\,\tilde{a}^{\dagger}_{2p0\downarrow}\,\tilde{a}^{\dagger}_{2p1\uparrow}|0>,$$
$$E_{37} = 3.87003,$$
$$|37>= 2.23305\,10^{-6}\,\tilde{a}^{\dagger}_{1s\downarrow}\,\tilde{a}^{\dagger}_{2s\downarrow} - 1.90028\,10^{-23}\,\tilde{a}^{\dagger}_{1s\uparrow}\,\tilde{a}^{\dagger}_{2p-1\downarrow} - 2.63853\,10^{-24}\,\tilde{a}^{\dagger}_{2s\uparrow}\,\tilde{a}^{\dagger}_{2p-1\downarrow}$$
$$+1.\,\tilde{a}^{\dagger}_{2p1\downarrow}\,\tilde{a}^{\dagger}_{2p-1\downarrow} - 1.90028\,10^{-23}\,\tilde{a}^{\dagger}_{1s\downarrow}\,\tilde{a}^{\dagger}_{2p-1\uparrow}$$
$$-2.63853\,10^{-24}\,\tilde{a}^{\dagger}_{2s\downarrow}\,\tilde{a}^{\dagger}_{2p-1\uparrow}|0>,$$
$$E_{38} = 3.87003,$$
$$|38>= 2.23305\,10^{-6}\,\tilde{a}^{\dagger}_{1s\uparrow}\,\tilde{a}^{\dagger}_{2s\uparrow} + 1.\,\tilde{a}^{\dagger}_{2p1\uparrow}\,\tilde{a}^{\dagger}_{2p-1\uparrow}|0>,$$
$$E_{39} = 3.87003,$$

$$
\begin{aligned}
&|39>= 1.579\,10^{-6}\,\tilde{a}^{\dagger}_{1s\uparrow}\,\tilde{a}^{\dagger}_{2s\downarrow} + 1.579\,10^{-6}\,\tilde{a}^{\dagger}_{1s\downarrow}\,\tilde{a}^{\dagger}_{2s\uparrow} + 0.707107\,\tilde{a}^{\dagger}_{2p1\uparrow}\,\tilde{a}^{\dagger}_{2p-1\downarrow}\\
&+0.707107\,\tilde{a}^{\dagger}_{2p1\downarrow}\,\tilde{a}^{\dagger}_{2p-1\uparrow}|0>,\\
&E_{40} = 4.07503,\\
&|40>= 0.000393282\,\tilde{a}^{\dagger}_{1s\downarrow}\,\tilde{a}^{\dagger}_{1s\uparrow} - 0.000138099\,\tilde{a}^{\dagger}_{1s\uparrow}\,\tilde{a}^{\dagger}_{2s\downarrow} + 0.000134757\,\tilde{a}^{\dagger}_{1s\downarrow}\,\tilde{a}^{\dagger}_{2s\uparrow}\\
&+0.000439612\,\tilde{a}^{\dagger}_{2s\downarrow}\,\tilde{a}^{\dagger}_{2s\uparrow} + 0.819196\,\tilde{a}^{\dagger}_{2p0\downarrow}\,\tilde{a}^{\dagger}_{2p0\uparrow} + 0.405535\,\tilde{a}^{\dagger}_{2p1\uparrow}\,\tilde{a}^{\dagger}_{2p-1\downarrow}\\
&-0.405535\,\tilde{a}^{\dagger}_{2p1\downarrow}\,\tilde{a}^{\dagger}_{2p-1\uparrow}|0>,\\
&E_{41} = 4.07536,\\
&|41>= 0.707107\,\tilde{a}^{\dagger}_{2p0\uparrow}\,\tilde{a}^{\dagger}_{2p-1\downarrow} - 0.707107\,\tilde{a}^{\dagger}_{2p0\downarrow}\,\tilde{a}^{\dagger}_{2p-1\uparrow}|0>,\\
&E_{42} = 4.07595,\\
&|42>= 0.707107\,\tilde{a}^{\dagger}_{2p0\uparrow}\,\tilde{a}^{\dagger}_{2p1\downarrow} - 0.707107\,\tilde{a}^{\dagger}_{2p0\downarrow}\,\tilde{a}^{\dagger}_{2p1\uparrow}|0>,\\
&E_{43} = 4.07691,\\
&|43>= -1.\,\tilde{a}^{\dagger}_{2p-1\downarrow}\,\tilde{a}^{\dagger}_{2p-1\uparrow}|0>,\\
&E_{44} = 4.07808,\\
&|44>= -1.\,\tilde{a}^{\dagger}_{2p1\downarrow}\,\tilde{a}^{\dagger}_{2p1\uparrow}|0>,\\
&E_{45} = 4.4453,\\
&|45>= 0.080553\,\tilde{a}^{\dagger}_{1s\downarrow}\,\tilde{a}^{\dagger}_{1s\uparrow} - 0.0235083\,\tilde{a}^{\dagger}_{1s\uparrow}\,\tilde{a}^{\dagger}_{2s\downarrow} + 0.024475\,\tilde{a}^{\dagger}_{1s\downarrow}\,\tilde{a}^{\dagger}_{2s\uparrow}\\
&+0.0772817\,\tilde{a}^{\dagger}_{2s\downarrow}\,\tilde{a}^{\dagger}_{2s\uparrow} + 0.570136\,\tilde{a}^{\dagger}_{2p0\downarrow}\,\tilde{a}^{\dagger}_{2p0\uparrow} - 0.575924\,\tilde{a}^{\dagger}_{2p1\uparrow}\,\tilde{a}^{\dagger}_{2p-1\downarrow}\\
&+0.575924\,\tilde{a}^{\dagger}_{2p1\downarrow}\,\tilde{a}^{\dagger}_{2p-1\uparrow}|0>\,.
\end{aligned}
\tag{E.1}
$$

Appendix F

Spheroidal coordinates

There is a convenient coordinate system necessary for calculations of two center integrals. Such integrals contain expressions depending on the distance from two different points separated by a distance R. The spheroidal coordinate system is very useful here [44]. In two dimensions one can define the elliptical coordinates and then easily extend them to three dimensions.

All the following definitions are illustrated in Fig. F.1. Let r_a and r_b be the distances from two points A and B. Point O is the origin of the Cartesian coordinate system. The z axis is also shown. Let us define new coordinates as

$$\lambda = \frac{r_a + r_b}{R} \quad \mu = \frac{r_a - r_b}{R}. \tag{F.1}$$

r_a and r_b can be interpreted as the distances to the foci of a family of confocal ellipses and hyperbolas, where R is the distance between foci. The parameters of such ellipses can be expressed by the new coordinates in the form

$$a = \frac{R}{2}\lambda, \quad b = \frac{R}{2}\sqrt{\lambda^2 - 1}, \quad e = \frac{R}{2a} = \frac{1}{\lambda}, \tag{F.2}$$

where a is the semi-major axis, b is the semi-minor axis and e is the eccentricity. From Eq. (F.1) we see that $1 \leq \lambda < \infty$ and $-1 \leq \mu \leq 1$. One can write down the equation for confocal ellipses mentioned before in the Cartesian coordinates [1] as

$$\frac{z^2}{\lambda^2} - \frac{y^2}{\lambda^2 - 1} = \left(\frac{R}{2}\right)^2. \quad (1 \leq \lambda < \infty) \tag{F.3}$$

Analogously, for the hyperbolas

$$\frac{z^2}{\mu^2} - \frac{y^2}{1 - \mu^2} = \left(\frac{R}{2}\right)^2. \quad (-1 \leq \mu \leq 1) \tag{F.4}$$

[1] Let us denote here in two dimensions one axis as z the second one as y.

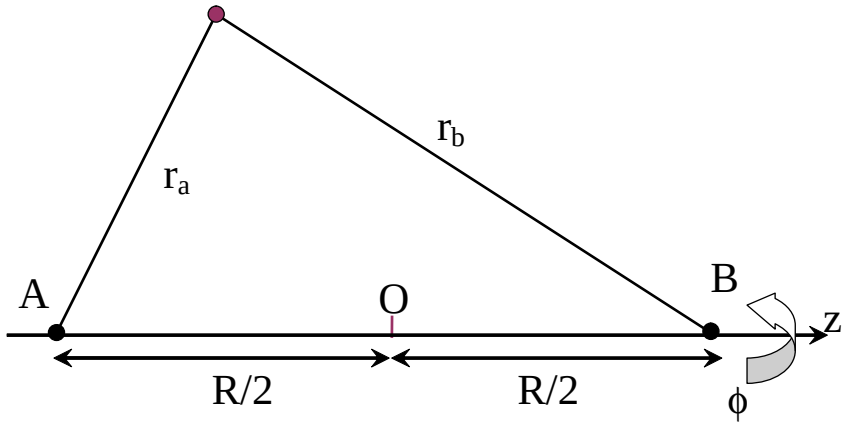

Figure F.1. The prolate spheroidal coordinates system. If we disregard the rotation around the z axis is disregarded we get the elliptical coordinate system.

The relations between Cartesian and elliptical coordinates are

$$z = \frac{R\lambda\mu}{2}, \quad y = \frac{R}{2}\sqrt{(\lambda^2-1)(1-\mu^2)} \tag{F.5}$$

We may get to three dimensions if the system of confocal ellipses and hyperbolas referred to in Eqs. (F.3,F.4) revolves around the major axis[2], which is the z axis in this case. The z coordinate does not change whereas the former y coordinate defines together with the rotation angle ϕ, which takes values in the range $0 \leq \phi < 2\pi$, the values of the Cartesian x and y coordinates

$$z = \frac{R\lambda\mu}{2}, \quad x = \frac{R}{2}\sqrt{(\lambda^2-1)(1-\mu^2)}\cos\phi \quad x = \frac{R}{2}\sqrt{(\lambda^2-1)(1-\mu^2)}\sin\phi. \tag{F.6}$$

The Jacobian, which defines the volume element is

$$d^3\mathbf{r} = \frac{R^3}{8}\left(\lambda^2-\mu^2\right)d\lambda d\mu d\phi. \tag{F.7}$$

The expression for Laplacian is

$$\nabla^2 = \frac{4}{R^2}\left(\frac{1}{\lambda^2-\mu^2}\frac{\partial}{\partial\lambda}\left((\lambda^2-1)\frac{\partial}{\partial\lambda}\right) + \frac{1}{\lambda^2-\mu^2}\frac{\partial}{\partial\mu}\left((1-\mu^2)\frac{\partial}{\partial\mu}\right) + \right.$$
$$\left. + \frac{1}{(\lambda^2-1)(1-\mu^2)}\frac{\partial^2}{\partial\phi^2}\right). \tag{F.8}$$

[2]The rotation around the minor axis gives the so called oblate spheroidal coordinates.

Sometimes there is also an alternate definition [43] of prolate spheroidal coordinates used which is related to this one by

$$\lambda = \cosh\xi, \quad \mu = \cos\eta, \quad \phi = \phi. \tag{F.9}$$

The Cartesian coordinates are then expressed via

$$\begin{aligned} x &= \frac{R}{2}\sinh\xi\sin\eta\cos\phi, \\ y &= \frac{R}{2}\sinh\xi\sin\eta\sin\phi, \\ z &= \frac{R}{2}\cosh\xi\cos\eta. \end{aligned} \tag{F.10}$$

Appendix G

The three-center element τ_{ijk} of the hopping integral t'

In this Appendix we evaluate the following integral

$$\tau_{ijk}(\alpha, a, h) = \frac{\alpha^3}{\pi} \int d^3\mathbf{r} \frac{e^{-\alpha(r_i + r_j)}}{r_k}, \tag{G.1}$$

where α is a parameter and h and a define the geometry of the system as shown in Fig. G.1. We should express the value of r_k with the help of other parameters and then go over to the spheroidal coordinates. From basic triangular geometry we know

$$\begin{cases} r_i^2 = r_j^2 + a^2 - 2ar_j \cos\theta \\ r_k = r_j + (\frac{a}{2} + h)^2 - 2(\frac{a}{2} + h) r_j \cos\theta \end{cases} \tag{G.2}$$

We use prolate spheroidal coordinates with foci in the origins of r_i and r_j

$$r_i + r_j = a\lambda \quad r_i - r_j = a\mu. \tag{G.3}$$

Solving the system of Eqs. (G.2) we get the value

$$r_k = \sqrt{\frac{a^2}{4}\left(\lambda^2 - 1\right)\left(1 - \mu^2\right) + \left(\lambda\mu\frac{a}{2} - h\right)^2}. \tag{G.4}$$

We may insert it into Eq. (G.1) and integrate over the variables ϕ and μ without any major difficulties obtaining

$$\tau_{ijk} = \int_1^\infty d\lambda \Big(\frac{\alpha^3 e^{-a\alpha\lambda}}{4}\Big(\sqrt{(2h + a\lambda)^2}(6h\lambda - a) - \sqrt{(a\lambda - 2h)^2}(6h\lambda + a) \\ (a^2 - 4h^2)(3\lambda^2 - 1) \ln \frac{2h\lambda - a + \sqrt{(\alpha\lambda - 2h)^2}}{2h\lambda + a + \sqrt{(\alpha\lambda + 2h)^2}}\Big)\Big). \tag{G.5}$$

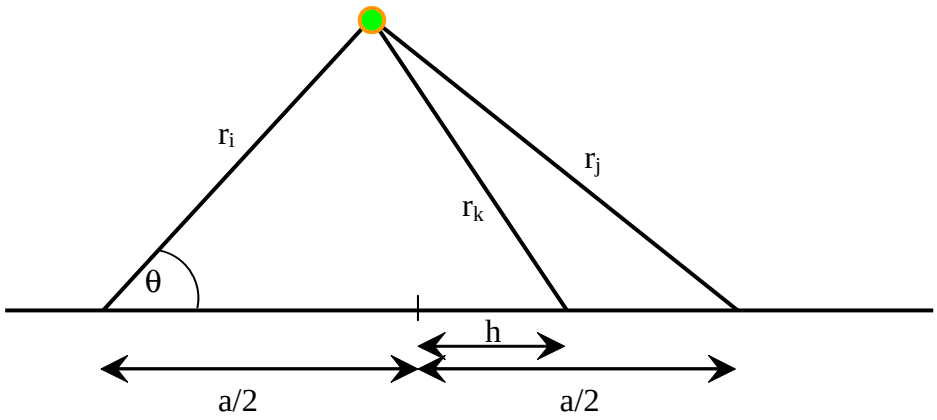

Figure G.1. The geometry of the system used to calculate the three center integral.

In this expression, there are many square roots of a value squared. It may be greatly simplified, enabling further computation, by splitting it up in different h regions. These regions are (i) $h > a/2$, (i) $a/2 > h > -a/2$ and (iii) $-a/2 > h$. Because of the symmetry one might also add the assumption $h > 0$ but it is not necessary. In various regions we split up the integration over λ into two parts simplifying the expressions according to the chosen region. Finally we obtain two different results

$$A = \frac{1}{2a^3}(e^{-a\alpha}((a^2-4h^2)(3+3a\alpha+a^2\alpha^2)(\gamma_{Euler}+\ln 2+\ln(a\alpha)) \\ -a\alpha(4a^2-24h^2+a^3\alpha-12ah^2\alpha))+ \\ e^{a\alpha}(a^2-4h^2)(3-3a\alpha+a^2\alpha^2)\Gamma(0,2a\alpha)), \quad \text{(G.6)}$$

where $\Gamma(a,z)$ is the incomplete gamma function $\Gamma(a,z) = \int_z^\infty t^{a-1}e^{-t}dt$ and $\gamma_{Euler} \simeq 0.5772$ is the Euler's constant, and

$$B = \frac{1}{2a^3}\left(4a\left(e^{-a\alpha}h(3+3a\alpha+a^2\alpha^2) - e^{-2h\alpha}(3h+a^2\alpha)\right)+ \right. \\ +(a^2-4h^2)(e^{a\alpha}(3-3a\alpha+a^2\alpha^2)\Gamma(0,(2h+a)\alpha) - \\ \left. -e^{-a\alpha}(3+3a\alpha+a^2\alpha^2)(\Gamma(0,(2h-a)\alpha)+\ln\left(\frac{2h-a}{2h+a}\right)\right)). \quad \text{(G.7)}$$

They are valid respectively

$$\tau_{ijk}(\alpha,a,h) = \begin{cases} B & h \in (i) \\ A & h \in (ii) \\ B: h \to -h & h \in (iii) \end{cases}. \quad \text{(G.8)}$$

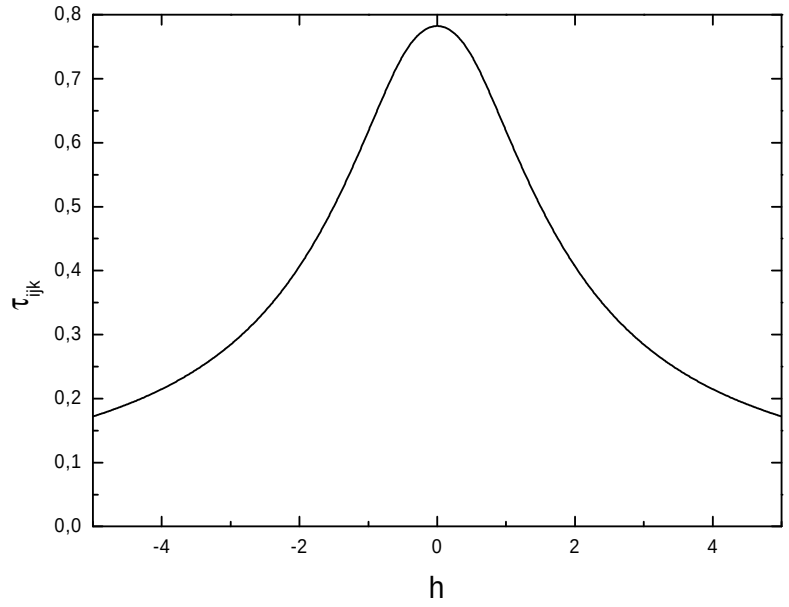

Figure G.2. The three center integral $\tau_{ijk}(\alpha, a, h)$. For this plot we set $\alpha = a = 1$.

A the region borders the function is continuous. The results for the three center integrals are exact, and could be obtained because the origins of r_i, r_j and r_k were located collinear. The function is plotted in Fig. G.2.

Appendix H

Rotation of spherical harmonics

Performing a rotation of the spherical harmonics is sometimes useful. It allows to express some parameters by their values calculated for a simpler geometry of the system. We want to get form a coordinate system $\mathbf{r} = (r, \theta, \phi)$ to a rotated $\mathbf{r}' = (r', \theta', \phi')$. The procedure is described in detail in [45]. It can be done by a consecutive rotation about angle α around z axis, then about angle β around the y axis and finally about γ around the z axis. The angular momentum operator $\mathbf{L} = (L_x, L_y, L_z)$ act as the rotation operator generators on the spherical harmonics. We can describe such rotation as

$$Y_{lm}(\theta', \phi') = e^{-\imath\alpha L_z} e^{-\imath\alpha L_z} e^{-\imath\alpha L_z} Y_{lm}(\theta, \phi) = \sum_{\mu=-l}^{l} D^l_{m\mu}(\alpha, \beta, \gamma) Y_{l\mu}(\theta, \phi). \tag{H.1}$$

The angular momentum operators do not lead us outside the subspace with a fixed l, hence we can write the second equality. Because the spherical harmonics are eigenfunctions of the L_z operator we can write

$$D^l_{m\mu}(\alpha, \beta, \gamma) = e^{-\imath m\gamma} d^l_{m\mu}(\beta) e^{-\imath\mu\alpha}. \tag{H.2}$$

The coefficients $d^l m\mu(\beta)$ can be systematically computed using the formula

$$e^{-\imath\beta L_y} \begin{pmatrix} x \\ y \\ z \end{pmatrix} = \begin{pmatrix} x\cos\beta - z\sin\beta \\ y \\ x\sin\beta + z\cos\beta \end{pmatrix}. \tag{H.3}$$

They have the form polynomials of $\sin\frac{\beta}{2}$ and $\cos\frac{\beta}{2}$. There is a recursion relation which simplifies the calculation

$$\frac{1}{2}(a_{l,m+1} d^l_{m+1,\mu}(\beta) - a_{l,m} d^l_{m-1,\mu}(\beta)) = \frac{d}{d\beta} d^l_{m\mu}(\beta), \tag{H.4}$$

where $a_{l,m+1} = \sqrt{l(l+1) - m(m+1)}$. For details see [45].

Appendix I

Spin-orbit coupling term

The spin-orbit coupling follows naturally from the Dirac equation.Since we are dealing with interacting electrons, and there is no Dirac equation for the many-particle case, we need to obtain the non-relativistic limit of this equation [50]. It can be achieved by means of the Pauli approximation. We will now derive a wave equation for a two-component function similar to the Schrödinger equation that contains relativistic corrections to the order $(1/c)^2$. The present treatment closely follows Landau and Lifschitz [51].

The time independent Dirac equation can be written in the matrix form

$$\begin{pmatrix} eV + mc^2 - E & c\sigma \cdot \mathbf{p} \\ c\sigma \cdot \mathbf{p} & eV + mc^2 - E \end{pmatrix} \begin{pmatrix} \xi \\ \phi \end{pmatrix} = 0, \tag{I.1}$$

where eV is the electron potential energy, m is the electron mass, $\mathbf{p} = -\imath\hbar\frac{\partial}{\partial \mathbf{r}}$, ξ and ϕ are the components of the wave function, and σ are the Pauli matrices. To get to the energy scale of the Schrödinger equation we have to subtract the rest energy of the electron $E_S = E - mc^2$. The formula for the component ξ can be extracted from the above matrix equation

$$\left(eV - E_S + c^2(\sigma \cdot \mathbf{p})(-eV + 2mc^2 + E_S)^{-1}(\sigma \cdot \mathbf{p})\right)\xi = 0. \tag{I.2}$$

Now we do the following expansion in terms of inverse c, leaving only the leading terms, which is the non-relativistic limit,

$$\frac{c^2}{-eV + 2mc^2 + E_S} \simeq \frac{1}{2m}\left(1 - \frac{E_S - eV}{2mc^2}\right). \tag{I.3}$$

Applying this expansion to Eq. (I.2) one can write down the terms which are included in E_S

$$E_S\xi = \left(\frac{p^2}{2m} + eV - \frac{p^4}{8m^3c^2} - \underbrace{\frac{\imath\sigma \cdot \mathbf{p} \times [\mathbf{p}, eV]}{4m^2c^2}}_{H'} - \frac{\mathbf{p} \cdot [\mathbf{p}, eV]}{4m^2c^2}\right)\xi. \tag{I.4}$$

The first two terms are the Hamiltonian for the Schrödinger equation. The third term is the relativistic kinetic energy correction. The fourth is the spin-orbit coupling H'. The fifth term is another relativistic correction.

The term H' can be written as

$$H' = \frac{e\hbar}{m^2c^2}\sigma \cdot \left(\frac{\partial V}{\partial \mathbf{r}} \times \mathbf{p}\right) \overset{a.u.}{\equiv} \alpha^2 \sigma \cdot \left(\frac{\partial V}{\partial \mathbf{r}} \times \mathbf{p}\right), \tag{I.5}$$

with the corresponding definitions in atomic units (a.u.) after the second equality sign. $\alpha \simeq \frac{1}{137}$ is the fine structure constant. The above expression takes the known form of spin-orbit coupling for spherically symmetric potential only. We can separate the potential into the spherically symmetric and the remaining part $V = V^{sph} + V'$, where V' can be originating from Coulomb interaction

$$V'(\mathbf{r}) = \int d^3\mathbf{r}' \frac{\rho(\mathbf{r}')}{|\mathbf{r} - \mathbf{r}'|}. \tag{I.6}$$

Inserting it into the formula for H' we get the following two terms

$$H'(\mathbf{r}) = \alpha^2 \frac{1}{r}\frac{\partial V}{\partial r}\mathbf{L} \cdot \mathbf{S} + \alpha^2 \int d^3\mathbf{r}' \frac{2\rho(\mathbf{r}')\mathbf{S} \cdot ((\mathbf{r} - \mathbf{r}') \times \mathbf{p})}{|\mathbf{r} - \mathbf{r}'|^3}. \tag{I.7}$$

The first is a special case of the second term, and gives the name to the spin-orbit interaction. The second is the general formula for an arbitrary location of charges producing the potential, and is more difficult to calculate due to the third power in the inverse $|\mathbf{r} - \mathbf{r}'|$ dependence.

Bibliography

[1] J. C. Slater, *Quantum Theory of Atomic Structure Vol.2*, McGraw-Hill, New York, 1960.

[2] see e.g. W. Jones and N.H. March, *Theoretical Solid State Physics*, vol. 1, Dover Publ., New York, 1973

[3] S. Hüffner, *Photoelectron Spectroscopy*, Springer Verlag, Berlin, 2003.

[4] V.I. Anisimov, J. Zaanen, O.K. Andersen, Phys Rev. B **44**, 943 (1991); P. Wei, Z.Q. Qi, *ibid.* **49**, 10864 (1994).

[5] S.Y. Ezhov, V.I. Anisimov, D.I Khomskii, G.A. Sawatzky, Phys. Rev. Lett. **83**, 4136(1999); K. Held, G. Keller, V. Eyert, D. Vollhardt, V. I. Anisimov, *ibid.* **86**, 5345 (2001).

[6] A. Rycerz, Ph. D. Thesis, Jagiellonian University, Kraków, 2003.

[7] R. Zahorbeński, Ph. D. Thesis, Jagiellonian University, Kraków, 2004.

[8] V.A. Fock, Zs.f.Phys. **75**, 622 (1932); V.A. Fock, *Raboty po kvantovoi teorii pola*, Leningrad University, Leningrad, 1957.

[9] A. L. Fetter, J. D. Walecka, *Kwantowa Teoria Układów Wielu Cząstek*, Państwowe Wydawnictwo Naukowe, Warszawa, 1982.

[10] S. Schweber, *An introduction to relativistic quantum field theory*, Row, Peterson and Co., Evanston, 1961.

[11] B. Robertson, Am. J. Phys. **41**, 678 (1973).

[12] J. Spalek, E. M. Görlich, A. Rycerz, R. Zahorbenski *A combined second- and first- quantization approach to the nanoscopic systems of interacting fermions. Revisited*, submitted to Phys. Rev. B.

[13] Spałek J. et al., Acta Phys. Polonica B**31**, 2879 (2000); *ibid.***32**, 3189 (2001).

[14] A. Szabo and N.S. Ostlund, *Quantum Chemistry* (Dover, Mineola, 1996).

[15] R. A. Shavitt, in *Methods of Electronic Structure Theory*, edited by H. Schaeffer (Plenum Press, New York, 1977), pp. 189-275.

[16] E.M. Görlich, J. Kurzyk, A. Rycerz, R. Zahorbeński, R. Podsiadły, W. Wójcik, J. Spałek, "Electronic states of nanoscopic chains and rings from first principles: EDABI method", in *Proc. of the NATO: Advanced Research Workshop: Concepts in Electron Correlations*, ed. A.S. Alexandrov et al., Kluwer Academic Publisher, Dordrecht 2004, pp. 355-375.

[17] J. Spa-ek, E.M. Görlich, A. Rycerz, R. Zahorbeński, and R. Podsiadły, "Properties of correlated nanoscopic systems from the combined exact diagonalization - *ab initio* method", in: *Concepts in Electron Correlation*, ed. A.C. Hewson, V. Zlatic, Kluwer Academic Publisher, Dordrecht 2003, pp. 257-268.

[18] E.M. Görlich, R. Zahorbeński, and J. Spałek, "Correlated states for atoms and atomic clusters: a combined exact diagonalization - *ab initio* approach", Acta Phys. Polonica B **34**/2, pp. 645-649, 2003.

[19] J. Spałek, A. Rycerz, E.M. Görlich, and R. Zahorbeński, "Electron correlation at nanoscale", in: *Highlights in Condensed Matter Physics*, ed. A. Avella et al., American Institute of Physics, New York 2003, pp. 291-303.

[20] A. Rycerz, J. Spalek, Phys. Rev. B **63**, 073101 (2001); A. Rycerz, J. Spalek, *ibid.* **65**, 035110 (2002).

[21] J.A. Pople, W.J. Hehre, J. Comput. Phys. **27**, 161 (1978).

[22] P.M.W. Gill, M. Head-Gordon, J.A. Pople, J. Phys. Chem. **94**, 5564 (1990).

[23] P.M.W. Gill, J.A. Pople, Int. J. Quantum Chem. **40**, 753 (1991).

[24] P.M.W. Gill, Adv. Quantum Chem. **25**, 141 (1994).

[25] B.I. Dunlap, Int. J. Quantum Chem. **81**, 373 (2001).

[26] R. P. Feynman, *Statistical Mechanics*, W.A. Benjamin, Inc., Reading Massachusetts 1972.

[27] H.A. Bethe, E.E.Salpeter, *Quantum Mechanics of One and Two- Electron Systems*, Springer Verlag, Berlin, 1957.

[28] E.E. Schrödinger, Ann. Phys. **79**, 1 (1926).

[29] S. Brzezowski, *Wstęp do mechaniki kwantowej*, Jagiellonian University, Kraków, 1997.

[30] National Institute of Standards and Technology web page http://physics.nist.gov/cgi-bin/AtData/main_asd

[31] L.M. Delves, Proc. Phys. Soc. **92**,55 (1967).

[32] V.I. Korobov, Phys. Rev. A **61**, 064503 (2000).

[33] J.S. Sims, S.A. Hagstrom, J. Phys. B: At. Mol. Opt. Phys **37**, 1519 (2004).

[34] C. L. Pekeris, Phys. Rev. **126**, 1470 (1962).

[35] C.D. Lin, Phys. Rev. A **12**, 493 (1975).

[36] T. Sako, G.H.F. Diercksen, J. Phys. B: At. Mol. Opt. Phys. **36**, 1681(2003).

[37] R.N. Hill, Phys. Rev. Lett. **38**, 643(1977).

[38] J.Spałek, A.M. Oleś, Chao, Phys. Stat. Sol. (b) **108**, 329 (1981).

[39] W. Kołos, L. Wolniewicz, J. Chem. Phys. **49**, 404 (1968).

[40] G. Herzberg, *Molecular Spectra and Molecular Structure. 1. Spectra of Diatomic Molecules*, Van Nostrand, Princeton, 1950.

[41] J. Spałek, R. Podsiadły, W. Wójcik, A Rycerz, Phys. Rev. B **61**, 15676 (2000).

[42] J. C. Slater, *Quantum Theory of Molecules and Solids*, McGraw-Hill, New York, 1963.

[43] Eric W. Weisstein "Prolate Spheroidal Coordinates." From MathWorld–A Wolfram Web Resource. http://mathworld.wolfram.com/ProlateSpheroidalCoordinates.html

[44] M. Abramowitz and I. A. Stegun(Eds.). "Definition of Prolate Spheroidal Coordinates." §21.2 in *Handbook of Mathematical Functions with Formulas, Graphs, and Mathematical Tables*, 9th printing. Dover, New York, p. 752, 1972.

[45] S. Flügge, *Mathematische Methoden der Physik*, Springer-Verlag, Berlin, 1979.

[46] G. Arfken, *Mathematical Methods for Physicists*, Academic Press, San Diego, 1985.

[47] A. Gołębiewski, *Chemia kwantowa związków nieorganicznych*, PWN, Warszawa, 1969.

[48] L. Gegenbauer, Wien. Sitzung. **70**, 434 (1874); **75**, 891 (1877).

[49] R.A. Sack, J. Math. Phys. **5**, 245 (1964)

[50] J. Avery, *Creation and Annihilation Operators*, McGraw-Hill, New York, 1976, p. 160.

[51] W. B. Bierestecki, E. M. Lifszyc, L. P. Pitajewski, *Relatywistyczna teoria kwantów. Cz. 1*, PWN, Warszawa 1972.

List of Figures

List of Tables